AD NUMBER

AD819967

NEW LIMITATION CHANGE

TO

Approved for public release, distribution unlimited

FROM

Distribution authorized to U.S. Gov't. agencies and their contractors; Administrative/Operational use; 31 Aug 1967. Other requests shall be referred to AFAPL, Research and Technology Division, AFSC, Wright-Patterson AFB, OH 45433.

AUTHORITY

AFAPL ltr, 12 Apr 1972

AFAPL-TR-67-107

SILVER-ZINC ELECTRODES and SEPARATOR RESEARCH

J.J. Lander and J.A. Keralla

Delco-Remy Division, General Motors Corporation

TECHNICAL REPORT AFAPL-67-107

31 August 1967

NOTICE

When Government drawings, specifications, or other data are used for any purpose other than in connection with a definitely related Government procurement operation, the United States Government thereby incurs no responsibility nor any obligation whatsoever; and the fact that the Government may have formulated, furnished, or in any way supplied the said drawings, specifications, or other data, is not to be regarded by implication or otherwise as in any manner licensing the holder or any other person or corporation, or conveying any rights or permission to manufacture, use, or sell any patented invention that may in any way be related thereto.

Copies of this report should not be returned unless return is required by security considerations, contractual obligations, or notice on a specific document.

FOREWORD

This report was prepared by Delco-Remy Division of General Motors Corporation, Anderson, Indiana, on Air Force Contract Nr. AF33(615)-3487, under Task Nr. 314522 of Project Nr. 3145, "Silver-Zinc Electrodes and Separator Research". The work was administered under the direction of the Static Energy Conversion Section, Flight Vehicle Power Branch, Aero Space Power Division, Aero Propulsion Laboratory; Mr. J. E. Cooper was task engineer for the laboratory.

The assistance of Dr. T. P. Dirkse, Professor of Chemistry, Calvin College, Grand Rapids, Michigan, as consultant on this project is greatly appreciated.

This report was submitted by the authors on 31 August 1967.

Publication of this report does not constitute Air Force approval of the report's findings or conclusions. It is published only for the exchange and stimulation of ideas.

J. J. Lander

J. J. Lander, Director
Electrochemical Research Department

J. A. Kerailla, Project Leader
Electrochemical Research Department

ABSTRACT

Additions of 1.2% to 2% lignosulfonic acid in the negative mix is helpful to negative plate cycle life. The use of cotton fibers helps to maintain the negative plate active material in place during cycle life. The surfactant BC-610 is the best choice for use in the zinc negative material found to date. However, at cold temperatures, surfactants appear to inhibit cycle life. The use of .1% Ethanol in the negative material helps cell cycle life as well as surfactant FC-95. Small percentages of acicular ZnO mixed with Kadox-15 appear to help negative plate cycle life. The use of 3% to 5% $ZnSO_4$ aids the negative plate cycle life at room temperature but is detrimental to cold (30-40°F) operation. The best electrolyte to date at 60% depth-of-discharge is 50% KOH yielding 220 cycles.

TABLE OF CONTENTS

TABLE OF CONTENTS (CONTINUED)

LIST OF FIGURES

LIST OF FIGURES (CONTINUED)

LIST OF TABLES

I. Introduction

The objectives of this program are to provide design criteria for long life (5,000 cycles), light weight (25 wh/#) silver-zinc batteries for military aerospace applications. Effort will be concentrated on the zinc electrode and separator since these are recognized as the major causes of premature failure of the silver-zinc battery.

The specific items under study in this contract are:

A. Mechanical Barriers to Zinc Agglomeration
B. Surfactant Additions
C. Fundamental Studies on Surfactants
D. Particle Size and Morphology of Zinc Oxides
E. Zinc Electrode Fabrication Techniques
F. Influence of Membrane Separator Characteristics
G. Sites for Zinc Oxide Overgrowths
H. Development of Failure Analysis Techniques
I. Sizes of Zincate Ion and Soluble Silver Species in KOH
J. Membrane Pore Size Measurements in KOH
K. Stoichiometric Ratio of Formed Zinc
L. Alternate Method of Surface Area Measurement
M. Separator Development
N. Electrolytes
O. Factors Controlling Zinc Particle Size Growth

This report covers the first twelve month's work on most of the above items.

All test cells were cycled at 60% depth-of-discharge at the two-hour cycle program of 35 minutes discharge and 85 minutes charge. Four layers of fibrous sausage casing were used for separation in these cells in order to insure zinc plate failure. That is to say, that in almost no instance was there any evidence of short-circuiting failure on these tests for the standard 15-plate design.

II. Factual Data

A. Mechanical Barriers to Zinc Agglomeration

In an effort to minimize the agglomeration of particles in the negative active material, addition of the following materials to the negative plate mix were tested:

1. shredded fibrous sausage casing
2. shredded asbestos
3. zinc metal
4. lignosulfonic acid
5. cotton fibers
6. Avicel (a finely powdered cellulosic material)

One hundred and ninety-one 25 a.h. cells were constructed utilizing various percentages of the above materials. Table I shows the construction details, initial capacity, cycle data and appearance of cell components of inspected cells after failure. Control cells on this test ran from 84 to 180 cycles, averaging 140 cycles. The major cause of failure was loss of zinc at the tops and edges of the zinc plate and agglomeration of the zinc. Figure 1 shows a typical zinc plate from a control cell after failure at 140 cycles. Control cells on this program are made with negative plates containing 20 g Kadox-15 zinc oxide, 2% HgO, and 0.5% Emulphogene BC-610.

1. Effects of Asbestos

Cells #1 through #27 containing asbestos fibers in the negative plate in quantities 5, 10, and 15% did not increase the cycle life of the zinc plate, yielding 134 cycles. These failed by loss of zinc plate capacity due to washout around the edges and in spite of the fact that the photomicrographs of failed zinc plates (Figures 2, 3 and 4) show reduced agglomeration by comparison with Figure 1. Except for cells #1, 2, 10, 11 and 27, which were opened for examination after the first discharge, all cells had received an accumulated overcharge of 22-24 a.h. (~ 1.14% per

cycle) at the end of life and failure examination disclosed the active material to be in the form of zinc.

Considerable trouble was experienced in getting these cells ready for test. They were given what appeared to be a normal formation charge, based on charge voltage behavior; however, on the first capacity discharge, all cells gave less than one minute capacity. At this point the above-mentioned cells (1, 2, 10, 11 and 27) were opened for examination and it was found that the zinc plates were substantially unformed. The remaining cells were soaked for an additional two weeks (standard procedure is to soak cells one week before giving the formation charge), then they were given an additional charge of 50 hours at one ampere. The initial capacity data shown in Table I was then obtained on a 15 ampere discharge rate.

Subsequently, 3-cell groups containing 0.5, 1.0 and 1.5% asbestos were tested. These failed very suddenly at 74 cycles, even though plates were well-formed and showed relatively little loss of electrolyte around the plate edges. These were, however, 19-plate cells, and it is thought that the additional 8 layers of fibrous sausage casing separation may have dried out the negative plates.

2. Effects of Shredded Fibrous Sausage Casing

Cells 31 through 59 contained 5, 10 and 15% shredded fibrous sausage casing in the negative plates and yielded an average of 146 cycles. The individual groups received a minimum of 16 - 24 a.h. of accumulated overcharge and on teardown the negative plates were substantially 100% metallic zinc. Figures 5, 6 and 7 show representative photomicrographs of failed negative plates. It appears that the fibers have done a good job of keeping the metal dispersed; however, there are many gaping voids and along with the loss of material around the edges, there may have been a good deal of loss in electrical contact from place to place in the active material contributing to loss in negative plate capacity.

This test was repeated with 9-cell groups containing 1, 3 and 5% shredded fibrous sausage casing in 19-plate cells. These all gave 134 cycles or less with some very early failures (v.g. 14 cycles). In spite of the fact that these cells had received an accumulated overcharge of 40 a.h., teardown examination revealed the negative plates to be mostly zinc oxide. It is evident that these plates were not accepting charge for some reason, or either the large quantities of overcharge oxygen was oxidizing the negative plates.

The 19-plate construction was used for some of the cell groups during this phase to determine whether going to more, but thinner, plate construction could improve cycle life. Obviously, it didn't.

3. Effects of Zinc Metal

Cells 60 through 86 contained elongated metallic zinc particles (#1208 zinc powder) to the extent of 5, 10 and 15% by weight. The groups containing 5% and 15% zinc powder averaged very well at 171 and 168 cycles, while the group containing 10% zinc failed at 108 cycles. These groups accumulated 13 to 25 a.h. of overcharge during life and showed substantially 100% zinc metal on teardown. Figures 8, 9 and 10 show photomicrographs of failed zinc plates. That for 5% zinc (Figure 8) is comparable in density to the control (Figure 1). The others exhibit a considerable loss in active material.

4. Effects of Lignosulfonic Acid

Cells 126 to 143 contained lignosulfonic acid in the negative mix in concentrations of 0.2, 1.2 and 2%. These concentrations yielded average cycle lives of 84, 168 and 132 cycles, respectively. It appears that too little of this additive is not enough to be effective, and that an optimum quantity around 1.2% for best life exists. Figures 11, 12 and 13 show photomicrographs of zinc plates from failed cells. Figure 14 shows a photomicrograph of a zinc plate from a failed control cell for

comparison. Apparently, the lignosulfonic acid can have some dispersing effect although comparing the particle sizes in Figures 12 and 14 would lead to the conclusion that this is not the major effect.

5. Effects of Cotton Fibers

Cells 150 through 167 contained concentrations of 5, 3 and 1% of cotton fibers in the negative plate. Control cells (168 through 173) which were run with this group averaged 122 cycles, while those with the fibers averaged 128, 144 and 138 for 5, 3 and 1% respectively. These cells accumulated 37 a.h. of overcharge throughout cell life for 1.7% per cycle and showed substantially 100% metallic zinc in the negative plates on teardown. Figures 15, 16 and 17 show photomicrographs of failed negative plates. This additive appears to aid materially in keeping the metallic zinc dispersed; moreover, it was the only one examined (of the mechanical barrier type) which appeared to have any effect at all in retaining the zinc active material at the tops and edges of the plates.

6. Effects of Avicel*

Avicel is a very finely powdered microcrystalline cellulose (particles in the 10 μ range). Cells 174 through 191 contained concentrations of 5, 10 and 15% of this material and averaged 130, 96 and 72 cycles respectively. These showed substantially 100% metallic zinc on teardown and they had accumulated 24 a.h. overcharge through cycle-life testing. However, their voltage behavior throughout life was very erratic and it is concluded that this material has no merit as an addition agent. Photomicrographs are under preparation.

As a matter of curiosity, three cells (147, 148 and 149) were

---

*FMC Corporation, American Viscose Division, Newark, N. J.

built with 30% by weight shredded fibrous sausage casing and cycled at 40% depth-of-discharge. These gave 300 cycles, which may be compared with the 400-600 cycles obtained with 0.5% Emulphogene BC-610 obtained on the last contract. Figure 18 shows a photomicrograph of a failed zinc plate. It appears that 30% by weight of this low-density material is just too much bulk and it keeps the zinc dispersed so well that the particles fail to maintain contact.

TABLE I

Study: Mechanical Barriers to Zinc Agglomeration

Note: The separation system was one layer of acrylonitrile monomer and four layers of reinforced cellulosic material. The electrolyte amount was 90 c.c. of 50% KOH. Upon cell examination, the separator appearance was good.

Cell Nr.	Cycles	Initial Capacity	Pos. Plate Construction	Neg. Plate Construction	Additive Material	Negative Plate Extent Form.	Treeing	Creeping	Washout
1	0	0 a.h.	Eight plates .020"-.023" 4" x 2.5" 15 g Ag + 1% Pd	Seven plates 20 g Kadox-15 + 2% HgO + .5% BC-610	5% Asbestos fibers	90% Oxide	Unformed		
2	0	0			"	"	"		
3-9	134	36 a.h.				100% Zn	None	Light 1-2 layers	30%
10	0	29			10% "	90% Oxide	Unformed		
11	0	29				"	"		
12-18	134	29 a.h.	"	"	" "	100% Zn	None	"	30-35%
19-26	134	29	"	"	15% "	"	"	"	"
27	0	29	"	"	" "	90% Oxide	Unformed		
28*	156	33 a.h.	"	"	None	100% Zn	None	Light 3 layers	30-45%
29*	144	33	"	"	"	"	"	"	"
30*	180	33	"	"	"	"	"	"	"
31-38	146	32 a.h.	"	"	5% Shredded	"	"	Light 1-2 layers	"
39	132	32	"	"	Cellulosic fibers	"	"	"	"
40-49	146	33 a.h.	"	"	10% "	"	"	"	"
50-59	146	31 a.h.	"	"	15% "	"	"	"	"
60-68	171	31	"	"	5% Zinc Metal fibers (1208)	"	Yes, at top	"	"
69-77	108	31	"	"	10% "	"	"	"	"
78-86	168	34 a.h.	"	"	15% "	"	Very light on edges		"

*Control Cells.

TABLE I (Continued)

Study: Mechanical Barriers to Zinc Agglomeration (Continued) Note: Same as previous Table

Cell No.	Cycles	Initial Capacity	Pos. Plate Construction	Neg. Plate Construction	% Addition Material	Extent Form.	Negative Treeing	Plate Creeping	Washout
87-93	122	25 a.h.	Ten plates	Nine plates	1% Shredded Cellulosic fibers	mostly oxide	None	Light 2 layers	10-20%
94	14	"	.015"-.017"	15 g Kadox-15	"	"	"	"	"
95	98	"			"	"	"	None	None
96	122	"	4" x 2.5"	2% HgO	"	"	"	Light 2 layers	20-25%
97-99	134	"	10 g Ag	+ .5% PC-610	3% "	"	"		"
100	98	"	+ 1% Pd		" "	"	"	"	"
101-104	134	"	"	"	" "	"	"	"	"
105-113	134	"	"	"	5% "	"	"	"	"
114-116	73	"	"	"	.5% Asbestos fibers	90% Zn	"	"	10-15% around 2 layers
117-119	73	"	"	"	1% "	"	"	"	
120-122	73	"	"	"	1.5% "	"	"	"	"
123*	157	24 a.h.	"	"	None	"	"	"	25-35%
124*	157	"	"	"	"	"	"	"	"
125*	157	"	"	"	"	"	"	"	"
126-131	84	22a.h.	Eight plates	Seven plates	.2% LSA	90% ZnO	"	"	10-20%
132	168	21a.h.	.015"-.017"	20 g Kadox-	1.2% "	95% Zn	Light	"	40-50%
133	156	"	4" x 2.5"	15 + 2% HgO	" "	"	"	"	"
134-135	168	20a.h.	10 g Ag	"	" "	"	"	"	"
136-137	168	21a.h.	+ 1% Pd	"	" "	"	"	"	"
138-139	144	20a.h.	"	"	2% "	90% ZnO	None	Light 2 layers	20-25%
140	60	"	"	"	" "	"	"		"
141	144	"	"	"	" "	"	"	"	"
142	132	"	"	"	" "	"	"	"	"
143	168	21a.h.	"	"	" "	"	"	"	"

* Control Cells.

TABLE I (Continued)

Study: Mechanical Barriers to Zinc Agglomeration Note: Same as previous Table

Cell No.	Cycles	Initial Capacity	Pos. Plate Construction	Neg. Plate Construction	% Addition Material	Negative Plate Extent Form.	Treeing	Creeping	Washout
144*	156	33 a.h.	Eight plates	Seven plates	None	90% Zn	None	Light 2	20-25%
145*	144	33	.015"-.017"	20 g Kadox-15	"	"	"	layers	"
146*	180	33	4" x 2.5"	+ 2% HgO	"	"	"	"	"
147	300**	21	10 g Ag +	+ .5% BC-610	30% Cellu-	"	"	"	None
148	300**	21	1% Pd	"	losic	"	"	"	"
149	300**	21	"	"	fibers	"	"	"	"
150	1[illegible]	23	"	"	5% cotton	95% Zn	"	Light 3	20-25%
151	108	"	"	"	fibers	"	"	layers	"
152	144	"	"	"	" "	"	"	"	"
153	108	"	"	"	" "	"	"	"	"
154	144	"	"	"	" "	"	"	"	"
155	124	"	"	"	" "	"	"	"	"
156-161	144	24 a.h.	"	"	3% cotton	"	"	"	"
162	108	23 a.h.	"	"	fibers	"	"	"	"
163-167	144	"	"	"	1% "	"	"	"	"
168*	132	24 a.h.	"	"	None	"	"	"	"
169*	144	"	"	"	"	"	"	"	"
170*	132	"	"	"	"	"	"	"	"
171*	108	"	"	"	"	"	"	"	"
172*	132	"	"	"	"	"	"	"	"
173*	84	"	"	"	"	"	"	"	"
174-177	132	22 a.h.	"	"	5% Avicel	"	"	"	"
178	120	"	"	"	powdered	"	"	"	"
179	132	"	"	"	cellulose	"	"	"	"
180-182	72	"	"	"	10% "	"	"	"	Very slight
183	132	"	"	"	" "	"	"	"	"
184	96	"	"	"	" "	"	"	"	"
185	120	"	"	"	" "	"	"	"	"
186-191	72	21 a.h.	"	"	15% "	"	"	"	"

* Control Cells.
**Cells cycled at 40% depth-of-discharge.

B. Surfactant Additions

The following Emulphogene-type surfactants were tested in order to complete the Emulphogene series, which is characterized by longer and longer polyethylene-oxide chains as the series goes up in number from BC-420 to BC-840; BC-420, BC-720 and BC-840. The increasing chain length of the polyethylene-oxide structure renders the material more and more soluble in water and water solutions. BC-610 in 0.5% concentration was used in the control cells. FC-95, an anionic flurochemical surfactant*, was also tested.

In addition, a group of alcohols were tested to determine whether the alcoholic functional group, in combination with various chain lengths, might function in the same way as the Emulphogene. These were: tridecanol, propanol, ethanol, tertiary amyl alcohol and butanol.

Table II shows the construction features, initial capacities, cycle life data, and appearance of the cell components after failure.

Cells 1 through 91 were constructed with 21 plates and three layers of fibrous sausage casing separation. This was an attempt to ascertain whether thin plate construction with reduced numbers of layers of cellulosic separation might provide longer cycle life for the same internal cell volume. The results speak pretty clearly: the major cause of failure was short-circuiting in combination with a very high degree of washout of the zinc plate active material. Initial capacities and discharge voltage characteristics of these cells were very good, at the expense of cycle life, however. The most noteworthy feature of this group of cells is (although those made with 0.5% BC-610 washed and shorted) like most of the others that it achieved 166 cycles, where other groups were shorting or otherwise failing around 100-120 cycles, or less.

---

*Minnesota Mining and Manufacturing Co., St. Paul, Minnesota.

Because of the short-circuiting failure mode, the thin-plate construction did not allow a good evaluation of the surfactant series in terms of their capability to extend zinc plate life and the test was repeated with the standard 15-plate construction and four layers of fibrous sausage casing using 3-cell groups.

Cells 91 through 120 show the pertinent data. The BC-420 is probably as good as but no better than the standard 0.5% BC-610. The BC-720 and BC-840 show somewhat reduced average cycle life in comparison. Figures 19 through 25 show photomicrographs of the negative material from failing cells for the surfactants. A good deal of loss of active material, or separation of active material from the grid, seems to be involved in this whole series.

Cells 121 through 156 and 157 through 192 contain various concentrations of BC-610 and were life-tested at 40°F. and 100°F. respectively at Dayrad Laboratories, Dayton, Ohio. Cycle life at either temperature was less than that obtained at room temperature. The spread of data at any one temperature is low. If any conclusion can be drawn, it is that for best cycle life at low temperatures a low concentration of surfactant is favored; at the high temperature, a high concentration is favored.

Figures 26, 27 and 28 show photomicrographs of failed negative plates at 40°F. for 0.15, 0.6 and 1.0% BC-610, respectively. They look much like the material when it fails at room temperature around 160 cycles. Figures 29, 30 and 31 show photomicrographs of failed negative plates at 100°F. for the same surfactant concentrations. The low temperature cells failed in spite of the fact that they were given 1-10% overcharge and the negatives appeared to consist mostly of metallic zinc on failure examination. The high temperature cells lost negative plate capacity in spite of 1-2% overcharge per cycle.

Cells 289 through 306 contained FC-95 in concentrations of 0.1, 0.6 and 1%. There was a slight improvement as concentration increased. In fact the 1% solution gave as good cycle life as 0.5% Emulphogene. The photomicrographs are shown in Figures 32, 33 and 34. They look much like the photomicrographs for Emulphogene. The FC-95 test had a total

of 40 a.h. overcharge, which is ample.

Cells 193 through 282 contained various percentages of the alcohols. The control cells for this group (cells 283-288) gave only 104 cycles. Cycle life for these groups ran from 60 to 159 (except for the ethanol) and the zinc plates showed mostly oxide on teardown examination. Integrator readings for these groups showed that they received less than 0.5% overcharge per cycle; consequently, this cannot be considered a good test of the several alcohols and needs to be repeated.

C. Fundamental Studies on Surfactants

The Second Quarterly Report on "Adsorption of Organic Materials on Zinc Electrodes" from the University of Texas is attached.

D. Particle Size and Morphology of Zinc Oxides

In an effort to determine whether the starting zinc oxide has any effect on cycle life, a variety of oxides, embodying variations in preparation process, particle size, crystal morphology, surface area, doping agents to improve oxide conductivity, and impurities have been prepared and tested. Twenty variations have been tested so far with results as shown in Table III. The data to date show nothing of major significance in comparison with the standard oxide, Kadox-15.

Photomicrographs have been prepared for representative zinc plates from failing cells. These are not reproduced herein because all the samples have not yet been submitted. Similarly, analysis of the data will be held until all information is at hand for the preliminary samples. The Second Quarterly Progress Report submitted by the New Jersey Zinc Company is attached.

TABLE II

Study: Surfactants

Note: The separator system for the first 90 cells was one layer acrylonitrile monomer and three layers of reinforced cellulosic material; remaining cells were same but with four layers of reinforced cellulosic material. The electrolyte amount was 90 c.c. of 50% KOH. Accumulated overcharge is 20 ampere-hours.

Cell No.	Cycles	Initial Capacity	Pos. Plate Construction	Neg. Plate Construction	Surfactant	Negative Plate Extent Formed	Treeing	Creeping	Washout
1-9	108	31 a.h.	Eleven	Ten	.15% BC-420	50% Zn	Light	Light	45-50%
10-18	108	30 a.h.	plates	plates	.6%	"	"	2 layer	"
19-27	108	28 a.h.	.015"-.017"	15g Kadox-15	1.0%	"	"	"	"
28-31	114	39 a.h.	10g Ag +	+ 2% HgO	.15% BC-720	90% Zn	Heavy	Heavy	40-50%
32-33	114	"	1% Pd	"	"	Shorted	"	2 layers	"
34-35	114	"	"	"	"	90% Zn	"	"	"
36	84	"	"	"	"	"	"	"	"
37-39	114	37 a.h.	"	"	.6%	Shorted	"	"	"
40-45	114	"	"	"	"	90% Zn	"	"	"
46-50	114	30 a.h.	"	"	1%	Shorted	"	"	"
51-54	114	"	"	"	"	90% Zn	"	"	"
55-57	36	32 a.h.	"	"	.15% BC-240	Shorts	"	"	"
58	116	"	"	"	"	"	"	"	"
59-62	36	"	"	"	"	"	"	"	"
63	116	"	"	"	"	90% Zn	"	"	"
64-66	36	34 a.h.	"	"	.6%	Shorts	"	"	"
67	119	"	"	"	"	"	"	"	"
68	34	"	"	"	"	"	"	"	"
69	100	"	"	"	"	"	"	"	"
70-72	36	"	"	"	"	"	"	"	"
73-80	36	39 a.h.	"	"	1%	Shorted	"	"	"
81	150	"	"	"	"	90% Zn	"	"	"
82*-89*	166	27 a.h.	"	"	.5% BC-610	Shorted	"	"	"
90*	166	"	"	"	"	90% Zn	"	"	"
91	168	25 a.h.	Eight plates	Seven plates	.15% BC-420	Mostly Zn	Medium	Heavy	"
92-93	132	"	.015"-.017"	20g Kadox-15	"	"	sides	4 layers	"
94-96	168	24 a.h.	10g Ag +	+ 2% HgO	.6%	"	and	"	"
97-99	168	"	1% Pd	"	1%	"	bottom	"	"
100-101	168	25 a.h.	"	"	.15% BC-720	"	None	Light 3 layers	35-40%

*Control Cells.

TABLE II (Continued)

Study: Surfactants

Cell No.	Cycles	Initial Capacity	Pos. Plate Construction	Neg. Plate Construction	Surfactant	Negative Plate: Extent Formed	Treeing	Creeping	Washout
102	108	25 a.h.	Eight plates .015"-.017" 10 g Ag + 1% Pd	Seven plates 20g Kadox-15 + 2% HgO	.15% BC-720	Mostly Zn	None	Light 3 layers	35-40%
103	108	"			.6% "	"	"	"	"
104	120	"			"	"	"	"	"
105	108	"			"	"	"	"	"
106-108	108	22 a.h.			1% BC-720	"	"	"	"
109	144	25 a.h.			.15% BC-840	"	"	"	"
110-111	168	"			"	"	"	"	"
112	132	24 a.h.			.6% "	"	"	"	"
113	144	"			"	"	"	"	"
114	132	"			"	"	"	"	"
115-116	144	22 a.h.			1% BC-840	"	"	"	"
117	132	"			"	"	"	"	"
118*-120*	168	"			.5% BC-610	"	"	"	"
121-132	76**	25 a.h.			.15% "	90% ZnO	None	"	30-40%
133-144	52**	"			.6% "	"	"	"	15-25%
145-156	58**	"			1% "	"	"	"	"
157-168	110***	24 a.h.			.15% "	"	"	Light 2 layers	20-30%
169-180	121***	25 a.h.			.5% "	"	"	"	"
181-192	124***	26 a.h.			1% "	"	"	"	"
193-198	120	27 a.h.			.1% Tridecanol		"	"	35-40%
199-204	108	"			.6% "	"	"	"	"
205-210	108	"			1% "	"	"	"	"
211-216	72	26 a.h.			.1% Propanol	"	"	"	20-30%
217-222	72	"			.6% "	"	"	"	"
223-228	60	"			1% "	"	"	"	"
229-234	159	27 a.h.			.1% Ethanol	90% Zn	Light	"	"
235-240	135	25 a.h.			.6% "	"	"	"	"
241-246	111	23 a.h.			1% "	"	"	"	"
247-252	124	26 a.h.			.1% Tert.Amyl	90% ZnO	None	"	35-45%
253-258	130	25 a.h.			.6% "	"	"	"	"
259-264	108	24 a.h.			1% "	"	"	"	"
265-270	92	23 a.h.			.1% Butyl Alco.		"	"	25-30%
271-276	100	"			.6% "	"	"	"	"
277-282	88	"			1% "	"	"	"	"
283*-288*	104	25 a.h.			.5% BC-610	"	"	"	20-30%
289-294	150	23 a.h.			.1% FC-95	"	"	"	"
295-300	152	"			.6% "	"	"	"	"
301-306	168	"			1% "	"	"	"	"

*Control Cells. **At 40°F. ***At 100°F.

TABLE III

Study: Particle Size and Morphology of Zinc Oxides

Note: Same as Table I

Cell Nr.	Cycles	Initial Capacity	Pos. Plate Construction	Neg. Plate Construction	Zinc Oxide Type	Extent Formed	Accumulated Overcharge	Neg. Plate Treeing	Neg. Plate Creeping	Neg. Plate Washout
1-6	108	23 a.h.	Eight plates	Seven plates	243-7-1	90% ZnO	+ 34 a.h.	None	Around	25-35%
7-12	96	25 a.h.	.015"-.017"	20g Test	243-11-1	"	"	"	2 layers	"
13-18	106	24 a.h.	10 g Ag +	Oxide + 2%	243-15-1	"	"	"	"	"
19-24	140	"	1% Pd	HgO + .5%	243-19-1	"	"	"	"	"
25-30	96	26 a.h.	"	BC-610	243-23-1	"	+ 43 a.h.	"	"	"
31-36	80	25 a.h.	"	"	243-27-1	"	"	"	"	"
37-42	130	"	"	"	243-31-1	"	"	"	"	"
43-48	12	23 a.h.	"	"	243-35-1	"	"	"	"	"
49-54	150	24 a.h.	"	"	243-41-1	"	+ 38 a.h.	"	"	"
55-60	135	25 a.h.	"	"	243-45-1	"	"	"	"	"
61-66	148	"	"	"	243-63-1	"	"	"	"	"
67-72	132	22 a.h.	"	"	243-71-1	"	+ 39 a.h.	"	"	30-40%
73-78	126	21 a.h.	"	"	243-75-1	"	"	"	"	"
79-84	122	24 a.h.	"	"	243-79-1	"	"	"	"	"
85*-90*	130	23 a.h.	"	"	Kadox-15	90% Zn	+ 40 a.h.	"	"	50%
91-96	135	24 a.h.	"	"	243-67-2	"	"	"	"	"
97-102	150	27 a.h.	"	"	243-83-1	"	"	"	"	"
103-108	132	26 a.h.	"	"	243-87-1	"	+ 30 a.h.	"	"	"
109-114	120	25 a.h.	"	"	243-91-1	"	"	"	"	"
115-120	132	"	"	"	243-95-1	"	"	"	"	"
121-126	156	26 a.h.	"	"	243-49-4	"	+ 40 a.h.	"	"	"

*Control Cells.

E. Zinc Electrode Fabrication Techniques

In an effort to determine whether negative plate cycle life could be increased by achieving an interlacing network of basic zinc oxides and, subsequently, of zinc crystals by means of wet pasting with $ZnCO_3$ and $ZnSO_4$ additions, the following wet pastes were tested: zinc oxide plus various concentrations of $ZnCO_3$ and zinc oxide plus various concentrations of $ZnSO_4$. In addition, admixtures of the acicular zinc oxides XX601 and XX4 to the Kadox-15 were tested.

After drying plates made with wet pastes of the $ZnSO_4$ additions showed the presence of basic zinc sulfates in the X-ray pattern. Wet-pasted plates made with $ZnCO_3$ additions showed simple mixtures of ZnO and $ZnCO_3$ in their X-ray patterns.

Table IV shows the initial capacity, cycle data, construction and appearance of cell components on failure analysis.

Cells 1 through 18 were fabricated with thin plates and 21-plate construction with the usual four layers of fibrous sausage casing separation. Trouble on cycling was immediately experienced, some cells failing before 20 cycles. These could be brought back by extended overcharges but they wouldn't last long anyway even after the overcharge. This is believed to be an electrolyte starvation situation at the zinc electrode due to the high ratio of separator weight. Control cells (19-27) behaved the same way.

It is interesting and must be significant of something that the 21-plate construction which utilized $ZnCO_3$ and $ZnSO_4$ additions to the negative plates did not experience this difficulty (cells 38-55). These gave respectable cycle lives ranging from 132 to 180 cycles with the cells having $ZnSO_4$-containing negatives showing up a little better. These cells exhibited very heavy zinc mossing around the bottom and edges of the plates, although they did not fail by short-circuiting but by loss of active material.

Cells 28 through 37 contained admixtures of XX4 zinc oxide in 2, 5, and 10% by weight concentrations. These utilized thin-plate, 17-plate construction, so the ratio of plate weight to separator

weight was higher than in the case of the 21-plate construction. These cycled without any problem, but their life of 157 cycles doesn't represent any increase over that obtained with the 15-plate construction and the addition of Emulphogene BC-610.

A repeat test was made with the standard 15-plate construction with negative plates containing $ZnCO_3$ and $ZnSO_4$ (cells 5%-76). Some improvement in cycle life was achieved by cells containing negatives with 5% $ZnSO_4$ and 5% appears to be a near-optimum concentration. The addition of $ZnCO_3$ was definitely harmful on this test. These cells accumulated 14.4 a.h. of overcharge for about 0.6% per cycle and they exhibited a relatively low amount of washout. The negatives showed mixed oxide and metallic zinc on teardown. It seems possible that these cells may have done slightly better if given a little more overcharge.

Cells containing 2 and 5% $ZnSO_4$ admixtures to the negative plate were tested at Dayrad at low temperature. They would not cycle at all at 30°F. or 40°F. and had to be brought back to room temperature before they would cycle.

F. Influence of Membrane Separator Characteristics

The Third Quarterly Report of the NARMCO Division of Whittaker Corporation is attached.

Study: Zinc Electrode Fabrication Techniques

Note: Same as Table I

Cell Nr.	Cycles	Initial Capacity	Pos. Plate Construction	Neg. Plate Construction	Variable Tested	Accumulated Overcharge	Extent Formed	Negative Plate Treeing	Growth	Washout
1	41	24 a.h.	Eleven	Ten	5% XX601	-20 a.h.	90% Zinc	Very	Around	30-40%
2	77	"	.015"-.017"	15g Kadox	Zinc Oxide	"	"	light	4 layers	"
3	26	"	10g Ag +	+ 2% HgO	"	"	"	"	"	"
4	65	"	1% Pd	+ .5%	"	"	"	"	"	"
5	26	"	"	BC-610	"	"	"	"	"	"
6-8	77	"	"	"	"	"	"	"	"	"
9	67	"	"	"	"	"	"	"	"	"
10-12	77	25 a.h.	"	"	10% XX601	"	"	"	"	"
13	65	"	"	"	Zinc Oxide	"	"	"	"	"
14-16	77	"	"	"	"	"	"	"	"	"
17	65	"	"	"	"	"	"	"	"	"
18	77	"	"	"	"	"	"	"	"	"
19*-27*	77	24 a.h.	"	"	None	"	"	"	"	"
28-30	157	19 a.h.	Nine	Eight	2% XX-4	-2 a.h.	"	"	"	40-50%
31-33	157	22 a.h.	.015"-.017"	15g Kadox	5% "	+50 a.h.	"	"	"	"
34-37	157	23 a.h.	10g Ag + 1% Pd	+ 2% HgO + .5% BC-610	10% "	"	"	Heavy	"	"
38-40	157	37 a.h.	Eleven plates	Ten plates	2% $ZnCO_3$	+16 a.h.	"	"	"	"
41-43	156	34 a.h.	.015"-.017"	15g Kadox	5% "	"	"	"	"	"
44-46	132	28 a.h.	10g Ag +	+ 2% HgO	10% "	"	"	"	"	"
47-49	180	38 a.h.	1% Pd	+ .5% BC-610	2% $ZnSO_4$	"	"	"	"	"
50-52	168	33 a.h.	"	"	5% "	"	"	"	"	"
53-55	180	36 a.h.	"	"	10% "	"	"	"	"	"
56*	204	38 a.h.	Eight plates	Seven plates	None	"	"	None	Light	15-25%
57*	96	"	.020"-.023"	20g ZnO	"	"	"	"	2 layers	"
58*	120	"	15g Ag +	+ 2% HgO +	"	"	"	"	"	"
59	156	21 a.h.	1% Pd	.5% BC-610	2% $ZnSO_4$	"	"	"	"	"
60	168	17 a.h.	"	"	"	"	"	"	"	"
61	168	22 a.h.	"	"	"	"	"	"	"	"
62	204	25 a.h.	"	"	5%"	"	"	"	"	"
63	168	"	"	"	"	"	"	"	"	"
64	204	"	"	"	"	"	"	"	"	"
65-67	132	"	"	"	10%"	"	"	"	"	"
68-70	132	24 a.h.	"	"	2% $ZnCO_3$	"	"	"	"	"
71-73	132	25 a.h.	"	"	5% "	"	"	"	"	"
74	24	24 a.h.	"	"	10% "	"	"	"	"	"
75	48	"	"	"	"	"	"	"	"	"
76	120	"	"	"	"	"	"	"	"	"

*Control Cells.

G. Sites for ZnO Overgrowths

The basis for this approach toward extending the capacity and, perhaps, cycle life is to provide crystal sites for precipitation of ZnO within the zinc plate itself, thus discouraging its transport through the separator and to the bottom of the plate. Fast precipitation should tend to increase the zinc plate capacity by slowing down the accumulation of zincate ion in solution, which might be expected in turn to slow down the onset of passivation. Also, if precipitation could be induced at the location where the zinc is going into solution during discharge, on the subsequent charge the formation of metallic zinc might be expected to take place at the same location, thus tending to stabilize the geometrical distribution of zinc on the electrode and so promote longer life.

Russian work (N. Julidov, Author's Certificate No. 116812 of 3/7/58) had shown the possibility of using $Ca(OH)_2$, which is quite insoluble in alkali, to accomplish this purpose in the study of zinc-nickel oxide cells. Based on that work, 18 cells were constructed, 6 cells each containing 1, 3 and 5% by weight of finely divided CaO in the negative plate, initial capacities were checked, and the cells cycle-life tested. The data are shown in Table V.

TABLE V

Initial Capacity and Cycle Life of Cells with Negative Plates Containing Insoluble CaO

No. of Cells	CaO in Negative (% by Weight)	Initial Capacity (A.H.)	Cycle Life
6	1	24.1	156
6	3	24.1	96
6	5	23.8	156

The data show no obvious effects on either initial capacity or cycle life, and it is concluded that the use of CaO does not achieve the

desired result, at least in these small concentrations. This is in sharp contrast to the behavior of $BaSO_4$ in lead-acid cells which has appreciable effects on capacity of lead plates when used in quantities of less than 0.5%.

The reason for the ineffectiveness of CaO additions (which was also found to be true by V. V. Romanov, "On approaches to Extend Service Life of the Nickel-Zinc Battery") was shown by him to be due to the slowness with which $Ca(OH)_2$ induces precipitation of zincate ion from solution. Although substantially complete precipitation could be achieved in a 90-day period, it takes 30 days to reduce the zincate ion concentration by one-half. Romanov used a $Ca(OH)_2$ concentration in the ratio of 1:2.2 to ZnO in his plates, and he abandoned this approach toward extending zinc plate cycle life.

A literature search has been made by Dr. W. VanDoorne (Calvin College, Grand Rapids, Michigan) in order to disclose, if possible, other oxides or hydroxides which might possibly be tried out to achieve the desired effects. This survey is included in this report as Appendix I in order to preserve the referencing system in his report.

The search disclosed the following oxides as possibilities - all of which form solid solutions with ZnO: BeO, MnO, FeO, CoO, NiO, CuO, PdO, MgO, CdO, SnO. In addition it was found that both $Ni(OH)_2$ and $Co(OH)_2$ form solid solutions with $Zn(OH)_2$. Thus, from the point of view of crystal structure, any one or all of these might be tried for their possible effects along the desired lines.

If the slowness of precipitation of zincate ion from solution were to hold, regardless of the nature of the host crystal, then this approach is doomed to failure in any case (for the 2-hour cycle); however, inasmuch as this is not known at this time, such of these materials as meet the criteria described below might be tried out in the next year's work.

The criteria are:

one, the oxide or hydroxide must be insoluble;

two, the oxide or hydroxide must have a reduction potential more negative than that for the ZnO → Zn charging reaction.

The reasons for these criteria are fairly obvious. If the material is soluble, it can't remain in the plate in its crystalline form. If it is reduced to metal at potentials less negative than that for the ZnO → Zn, then on the formation charge it would go to the metallic state and remain that way on the plate. In the latter instance, it would, furthermore, be disastrous to incorporate a substance with a low hydrogen overvoltage, because then hydrogen gas generation rates would be expected to become unbearable for sealed cell operation. FeO is a good example of the latter situation. It is well known that the iron electrode of the Edison cell has a very short charged stand life because of the rate at which it generates hydrogen in the KOH electrolyte environment.

Reference to Latimer, "Oxidation Potentials," 2nd ed., Table 85 (Prentice-Hall, Inc. 1952, Englewood Cliffs, N.J.) gives the line-up in Table VI for the oxidation-reduction potentials of the candidate oxides or hydroxides in alkaline solutions.

TABLE VI

Reduction Potentials

Couple	E°
$Ca + 2\ OH^- = Ca(OH)_2 + 2e$	-3.03
$Mg + 2\ OH^- = Mg(OH)_2 + 2e$	-2.69
$2Be + 6\ OH^- = Be_2O_3^= + 3\ H_2O + 4e$	-2.62
$Mn + 2\ OH^- = Mn(OH)_2 + 2e$	-1.55
$Zn + 2\ OH^- = Zn(OH)_2 + 2e$	-1.245
$Zn + 4\ OH^- = ZnO_2^= + 2\ H_2O + 2e$	-1.216
$Cr + 4\ OH^- = CrO_2^- + H_2O + 3e$	-1.2
$Sn + 3\ OH^- = HSnO_3^- + H_2O + 2e$	-0.91

TABLE VI (Continued)

Reduction Potentials

Couple	E°
$Fe + 2\ OH^- = Fe(OH)_2 + 2e$	-0.877
$H_2 + 2\ OH^- = 2\ H_2O + 2e$	-0.828
$Cd + 2\ OH^- = Cd(OH)_2 + 2e$	-0.809
$Co + 2\ OH^- = Co(OH)_2 + 2e$	-0.73
$Ni + 2\ OH^- = Ni(OH)_2 + 2e$	-0.72
$2\ Cu + 2\ OH^- = Cu_2O + H_2O + 2e$	-0.358
$Cu_2O + 2\ OH^- + H_2O = 2\ Cu(OH)_2 + 2e$	-0.080
$Pd + 2\ OH^- = Pd(OH)_2 + 2e$	+0.07

On the basis of these data, only Ca, Mg, Be and Mn oxides or hydroxides would not be expected to be reduced to metal at the zinc electrode. Romanov has given up on $Ca(OH)_2$ and $Mg(OH)_2$ and the data of this report show that addition of CaO has no beneficial effect.

BeO is quite soluble in strong NaOH, to the extend of 3 + gm/100 gm saturated solution. While it would be a simple matter to saturate the solution (assuming that it would have a similar solubility in KOH) and then add excess BeO to the plate, the solid phase in existence with BeO in concentrated solutions is not BeO, but $BeO \cdot NaOH \cdot H_2O$ (Seidell, "Solubilities of Inorganic and Metal Organic Compounds," 4th Ed., Vol. I, p. 412. D. VanNostrand Company, Inc., New York, 1958). If a similar compound were to form in KOH solutions, the crystal structure would be changed, of course.

Solubility data for $Mn(OH)_2$ in NaOH solutions show 0.03 grams per 4.14 molal solution with solubility increasing with concentration (Seidell, Vol. II, p. 558). The presence of manganese in the system is to be eschewed, however, because soluble permanganates are certain to be formed on charge at the silver oxide plate which would oxidize

the separator.

It is concluded from the available information that this approach appears to be hopeless, and abandonment is recommended.

H. Development of Failure Analysis Techniques

No work has been done this year other than use of techniques already established, except to take many more microphotographs of failed plates, and to begin work on the alternative method of surface area determination described below in section L. Much of the contemplated work is waiting on cycle life improvement possibilities.

I. Sizes of Zincate Ion and Soluble Silver Species in KOH

In an attempt to achieve a better understanding of concentrated KOH solutions, available data from the literature have been treated as discussed herein. It is of interest to achieve a better understanding of battery strength KOH solutions as a firm basis for further studies on zincate ion and the soluble silver species. For example, it would be desirable to have a separator material which would allow free migration and diffusion of KOH and yet screen out the passage of zincate ion and soluble silver species. In order for this to be achievable, a sufficient difference in ionic (or molecular) diameters would have to exist between K^+ and OH^- on the one hand and zincate and soluble silver on the other. If an appreciable difference were to be found, then it would make sense to try to develop separator materials with a pore size large enough to admit free diffusion of KOH, but small enough to block zincate ion and silver. Conversely, if ionic (or molecular) sizes of KOH (K^+, OH^-) were to be found to be nearly equivalent to zincate and silver sizes, then attempts to develop separator materials to achieve the desired end on a pore size basis would be useless, and different approaches would have to be found.

The work herein reported may be regarded as a first approach to the problem and is incomplete in the sense that data for the several

separate ions have not been achieved except in terms of upper and lower limits; however, data in the existing literature can be treated to obtain molecular volumes for hydrated KOH in battery strength solutions.

Partial Molal Volumes

As a first step in the procedure, the density data* for KOH solutions up to 50% by weight (68°F.) were used to calculate the volumes of solutions containing 1000 grams of water. The data are shown in Table VII.

TABLE VII

Volumes of KOH Solutions (68°F.)

Weight % KOH	Density	Volumes of Solutions Containing 1000 gm. H_2O (c.c.)	Weight KOH Grams	Molality n_2
0	0.997	1003	0	0
2	1.016	1004	20	0.36
6	1.053	1010	65	1.16
10	1.090	1022	112	2.00
16	1.147	1037	190	3.39
24	1.226	1074	317	5.65
30	1.288	1110	430	7.66
40	1.396	1193	668	11.9
50	1.512	1322	1000	17.8

From these data, the solution volume may be plotted against the molality, as in Figure 35. The tangent to the curve at any value of molality provides data for the calculation** of the partial molar volume. As an example, from the tangent at 40% by weight, the volume

*JACS, Apr. 1941, p. 1088.

**See, for example, "Textbook of Physical Chemistry," Glasstone, 2nd Ed. p. 239, D. VanNostrand Co., Inc. 1946.

of KOH in solution is calculated to be 20.5 c.c. This may be compared with 27.4 c.c. calculated for the molar volume from the handbook value of 2.044 gm. per c.c. for the density of solid KOH.

From the molar volume, the volume per molecule of KOH in solution may be calculated, using Avagadro's number

$$\frac{20.5}{6.023 \times 10^{23}} = 3.41 \times 10^{-23} \text{ c.c.}$$

or $3.41 \times 10^{-23} \times 10^{24} = 34.1$ cubic Angstroms.

If the molecule is treated as a sphere, the molecular diameter is calculated to be

$$d^3 = \frac{6 \times 34.1}{\pi} = 65$$

$$d = 4 \text{ A}^\circ$$

On this basis, the diameter of either the K^+ or the OH^- ion would be less than 4 A°.

From the shape of the curve, it is evident that the molar volume of the KOH gets progressively smaller as the concentration of solution decreases. Thus at $n_2 = 2$ (10% by weight KOH), the molar volume is calculated from the tangent to be 12 c.c. per mole. Evidently, KOH solutions are quite non-ideal, and the molecular volumes of dissolved KOH and water are far from being additive. Just how far they are from being additive is described in Figure 36 where the volume per mole for KOH solutions is plotted against the mole fraction of KOH. These data were calculated from Table VII.

The deviation from ideality means, of course, that the ions from dissolved KOH are more-or-less hydrated in solution. As a consequence, the molecular volume and diameter previously calculated for KOH in 10% solutions may be considered to be effective values for KOH stripped of waters of hydration, and therefore, not representative of the real situation in solution. While Figure 36 says that there is a good deal of solute-solvent interaction, the data of the figure do not provide quan-

titative means of determining how much water is tied up by dissolved KOH as water of hydration.

Degree of KOH Hydration

A very thorough review of the literature has not yet been made in terms of ionic hydration numbers in strong KOH solutions; however, some information is available for comparison with the treatment which will be made below. For example G. Yagil has found a hydration number of 3 for OH^- ion in concentrated KOH and NaOH solutions (JACS 85 (16), 2376-80, 1963) by means of reaction rate studies, in good agreement with Ackermann (CA 55, 13054 a) who studied hydration by means of infrared techniques. Brady and Krause found a hydration number of 4 for K^+ ion in concentrated KOH solutions (11.36% and 18.81% KOH, by weight) using X-ray diffraction (Norelco Report 5, 111, 1958). The latter article also contains reference to theoretical means of calculation of hydration numbers. Textbook values (Glasstone, "Textbook of Physical Chemistry, p. 921, 2nd Ed. D. VanNostrand and Co., New York, 1946) of hydration numbers for K^+ ion in KCl solutions of 5.4 and 10.5 are given.

At any rate, a treatment which enables calculation of hydration numbers of KOH as a function of concentration is proposed, hereby, which is believed to be novel and which indicates that hydration numbers depend substantially on concentration.

The concept and treatment of data are very simple.

Determination of molecular weights from freezing point depression, boiling point elevation, vapor pressure reduction, etc., are all commonly used techniques, and any standard elementary physical chemistry text provides the theoretical basis for making such determinations. Furthermore, the same texts discuss solutions of strong electrolytes, where 100% ionization is assumed to be the case. The major problem seems to be that such experimental data are good only for relatively dilute solutions (1 to 2 molal, or less).

When freezing point depression data, boiling point elevation data, and vapor pressure lowering data for KOH solutions are examined, it is apparent that the quantities involved are substantially larger than those which can be calculated on the basis of the simple theory, assuming 100% ionization, as concentration increases beyond 1 or 2 molal. It is suggested, therefore, that this result occurs simply because of the hydration of ions (and/or molecules), and that comparison of the actual data with that calculated as theoretical based on 100% ionization (from Raoult's Law) can provide a means of determining the extent of hydration. What this means is: because of hydration, the water of hydration becomes a component of the solute* and, consequently, the real concentration of solute becomes appreciably larger than that calculated from the straight molal quantities of each component originally added in making up the solution.

The vapor pressure lowering relationship is chosen to illustrate the method of data treatment. In Figure 37 are shown the measured values of vapor pressure of water for solutions of KOH up to 50% by weight at 68°F. (International Critical Tables, Vol. III, p. 373). On the same graph are shown values of the vapor pressure calculated from Raoult's Law based on 100% ionization (this latter curve is different from the one shown in Figure 24, Second Quarterly Report, because Raoult's Law was improperly handled in calculating the theoretical vapor pressure lowering in the earlier report, as pointed out by Professor Dirkse in a private communication dated May 15, 1967).

The tie-lines drawn in the figure indicate that a 3 molal solution behaves like a theoretical 4.5 molal solution, a 5 molal solution behaves like a theoretical 9.3 molal solution, an 8 molal solution behaves like a 21.8 molal theoretical solution, and so forth.

Now, a 9.3 molal solution contains 55.6 moles of water in the ratio 9.3/55.6, so the 5 molal solution behaves as though it contains water in the same ratio.

---

*See, for example: "Ionic Sizes," Stern and Amis, Chem. Rev. 59, Feb. 1959, p. 23.

$$\frac{5.0}{X} = \frac{9.3}{55.6}$$

$$X = 29.9$$

But, inasmuch as the 5 molal solution actually contains 55.6 moles of water, then 55.6-29.9 = 25.7 moles of water have become part of the solute as water of hydration. Therefore, 25.7 moles of water are associated with 5 moles of KOH for a hydration number of 5.14. In similar fashion, a hydration number can be calculated for each concentration of KOH, and the curve described in Figure 38 is obtained. The curve indicates that the number of moles of water associated with one mole of KOH falls off as concentration is increased.

Now we are in a position to calculate the size of the hydrated molecule. Using a 40% by weight solution (11.9 m), from Figure 38 it is seen that 3.6 moles of water are tied up with 1 mole of KOH. Because there are 11.9 moles of KOH in a 40% solution, 42.9 moles of water are hydrated, leaving 12.7 moles of solvent water. If it is assumed that solvent water has the same specific volume as pure water, then the volume of solvent water is

$$12.7 \times 18.1 = 230 \text{ c.c.}$$

But, from Figure 35, an 11.9 molal solution containing 1000 grams of water has a volume of 1190 c.c. Therefore, the volume of hydrated KOH is

$$1190 - 230 = 960 \text{ c.c.}$$

or $$960/11.9 = 80.6 \text{ c.c/mole}$$

The value of 80.6 c.c. per mole may be compared with the additive value of 90.9 calculated from the molar volume of solid KOH and that for 3.6 moles of water.

Again, using Avagadro's number, the volume per hydrated molecule for KOH in a 40% solution is

$$\frac{80.6}{6.023 \times 10^{23}} = 13.4 \times 10^{-23} \text{ c.c.}$$

or $13.4 \times 10^{-23} \times 10^{24} = 134$ cubic Angstroms.

If the hydrated molecule is treated as a sphere, the molecular diameter is calculated to be

$$d^3 = \frac{6 \times 134}{\pi} = 255.5 \text{ cubic Angstroms}$$

$$d = 6.35 \text{ A}^\circ$$

For a 4 molal solution (hydration number 5.6), the volume per molecule is calculated to be 187 cubic Angstroms and the spherical diameter to be 7.1 A°. On this basis, the diameter of either the hydrated K^+ ion or the hydrated OH^- ion would be less than 7.1 - 6.35 A°, over the concentration range involved.

The phase diagram for KOH - H_2O solutions indicates formation of the solid compound, $KOH \cdot 4H_2O$, at 44% KOH by weight (-28°F.). This is 13.9 molal, for which there are exactly 4 moles of water per mole of KOH available for hydration. At the freezing point, the degree of hydration may be regarded as corresponding perfectly to the available water. It is interesting that the projected curve of Figure 38 lies under 4 waters of hydration for the 44 weight % solution. It would be expected on this basis that the degree of hydration should decrease as temperature increases, and it would be interesting to go through similar calculations for vapor pressure curves at other temperatures, as well as similar treatments of the freezing point depression curves and boiling point elevation curves.

It is interesting, also, that at 4 molal (18.8% by weight) the total hydration obtained by the scheme used in this section is 5.6. This may be compared with a possible expected total of 4.0 + 3.0 = 7.0 from the references quoted at the beginning of this section.

Figure 39 shows the total moles of both bound and free water, calculated from the data of Figure 38, as a function of concentration. The data of this curve corrects the upper curve of Figure 26 in the Second Quarterly Report.

On the basis of the fact that the phase diagram shows the concentra-

tion of KOH to be 52.8% by weight (20 m) at a freezing point of 68°F., another point can be located on the curve of Figure 39 for 20 molal and it would correspond, of course, to 55.6 moles of bound water. (This assumes that the vapor pressure of water at the freezing point would be substantially nil). Extrapolation of the actual vapor pressure curve of Figure 37 to zero indicates zero vapor pressure around 20-22 molality for a hydration number of 2.6 - 2.8.

Ion-Ion Association

In the Second and Third Quarterly Reports, some speculation was given to the possibility of ion-ion association in st ong KOH solutions, on the basis of Figure 26 in the Second Quarterly Report, and on the basis of the fact that the product of the conductivity and the viscosity divided by the molarity was found to be not a constant at 20°C. Professor Dirkse in a similar calculation (private communication dated May 25, 1967) showed constancy of the function $\eta\lambda/C$ for KOH solutions at 25°C. Consequently, the data were recalculated for 25°C. using the viscosity data given in Table 5, page 155, of "Characteristics of Separators for Alkaline Silver Oxide Batteries - Screening Methods". These data were found to agree exactly with viscosity data given by Hitchcock and McIlhenny (Ind. & Eng. Chem., Vol. 27, p. 466). Data for conductivity at 25°C. were obtained from the resistance values of KOH at 25°C. given in Table 2, pages 149-150 of the Screening Methods reference given above. Table VIII shows the data and the calculated values of $\eta\lambda/C$.

TABLE VIII

Data for the Function $\eta\lambda/C$ for KOH Solutions at 25°C.

Concentration (Molarity)	η	λ	$\eta\lambda$	$\eta\lambda/C$
0.6	0.91	0.130	0.118	0.198
0.8	0.93	0.170	0.159	0.197

TABLE VIII (Continued)

Data for the Function $\eta\lambda/C$ for KOH Solutions at 25°C.

Concentration (Molarity)	η	λ	$\eta\lambda$	$\eta\lambda/C$
1.0	1.00	0.200	0.200	0.200
1.5	1.03	0.295	0.304	0.204
2.0	1.10	0.360	0.396	0.198
4.0	1.40	0.575	0.805	0.201
6.0	1.83	0.640	1.17	0.195
8.0	2.42	0.620	1.50	0.187
9.0	2.82	0.583	1.64	0.182
10.0	3.30	0.541	1.78	0.178
11.0	4.00	0.505	2.03	0.184
12.0	4.83	0.460	2.22	0.184
13.0	6.20	0.405	2.50	0.193
13.4	7.00	0.387	2.71	0.202
			Avg.	0.193 ± 3.6%

While there is some variation in the values of $\eta\lambda/C$, and, possibly a minimum in the value near 10.0 molar, actually the values lie within an average deviation of ± 3.6% which is probably not outside the limits of experimental error.

The point is this: if $\eta\lambda/C$ is truly a constant, then there should be no ion-ion association effects in KOH solutions, even up to 45% by weight, and, consequently, no regard need be given to such possible effects on the values of hydration numbers and ion sizes, as was attempted in the Third Quarterly Report (see text, pps. 4 and 5, and illustration, Figure 2). Again, it may be suggested that a body of such data should be obtained with temperature as a parameter. These data are very interesting in terms of KOH solutions, in view of the existing theory concerning ion-ion association in strong electrolytes. Similar work for solutions (other than KOH) of high-concentration, strong electrolytes is also suggested, in order to check out electrolyte theory in this respect.

It seems possible that a good deal of this might be accomplished with data already existing in the literature.

Zincate Ion

A simple technique was used to measure the volume increase of a 45% solution of KOH as increasing amounts of ZnO were added at 72°F. A 500 c.c. volumetric flask was filled to the calibration mark with 45% KOH. Weighed amounts of ZnO were added and when solution was complete, the increase in the height of the meniscus in the neck of the flask was measured with a centimeter scale. The internal diameter of the neck of the flask was measured, and so, knowing the i.d. and the increase in height of the liquid level, the volume change could be calculated. The results are shown in Figure 40. The shape of the curve is slightly S-like; however, a straight line was drawn through the points and its slope = 20.9 c.c./mole. This may be compared with 14.86 c.c./mole calculated from the handbook value for the density of solid ZnO. Therefore, the oxide occupies more volume when dissolved in 45% KOH at room temperature than it does in the dense solid state.

Treating the ZnO as a dissolved molecule and assuming a spherical configuration, the diameter may be calculated.

$$\frac{20.9 \times 10^{24}}{6.023 \times 10^{23}} = 34.6 \text{ cubic A}^\circ = \text{volume/ZnO molecule}$$

$$r^3 = \frac{3}{4} \times \frac{34.6}{\pi} = 8.25$$

$$r = 2.2 \text{ A}^\circ$$

$$d = 4.04 \text{ A}^\circ$$

This value may be regarded as a value for unionized and unhydrated ZnO. However, as Dirkse's data show the molecule is likely to exist as the $Zn(OH)_4^{=} \cdot 2H_2O$ ion in solutions of strongly alkaline KOH. This is equivalent to $ZnO_2^{=} \cdot 4H_2O$, or a $ZnO_2^{=}$ ion with 4 waters of hydration.

We can estimate a minimum volume for $ZnO_2^{=} \cdot 4H_2O$ in the following way. From the data of Figures 35 and 36 the volume of one mole of bound water in 45% KOH may be calculated to be 13.4 c.c. per mole. Next, using the value of 14.36 c.c./mole for ZnO in the solid crystal and adding 4 x 13.4 = 53.6 c.c., we obtain 68.5 c.c. per mole for $ZnO_2^{=} \cdot 4H_2O$ without accounting for the extra oxygen atom. Then,

$$\frac{68.5 \times 10^{24}}{6.023 \times 10^{23}} = 113.4 \text{ cubic Angstroms}$$

$$d^3 = \frac{6 \times 113.4}{\pi} = 217$$

$$d = 6 \text{ A}^\circ$$

so, a minimum dimension for a spherical $ZnO_2^{=} \cdot 4H_2O$ ion is 6 A° diameter, which is not very different from the values 6.4 - 7.1 A° calculated previously for hydrated KOH molecules. While 6 A° is unquestionably slightly too small, it could be concluded that the construction of a separator membrane which would screen out zinc diffusion, yet allow uninhibited diffusion of KOH, is simply out of the question based on pore size alone.

However, it should be remembered that the diffusing zincate ion has to drag along two hydrated K^+ ions with it, so some differential could be involved. This can be estimated using the value of 80.6 c.c. per mole for hydrated KOH previously calculated. Thus, if one-half the value of 80.6 is assigned to a hydrated K^+ ion, then the total volume per mole for 2 K^+ ions (hydrated) and $ZnO_2^{=} \cdot 4H_2O$ would be 149.1 c.c. per mole. Then,

$$\frac{149.1 \times 10^{24}}{6.023 \times 10^{23}} = 249 \text{ cubic Angstroms}$$

$$d^3 = \frac{6 \times 249}{\pi} = 475$$

$$d = 7.8 \text{ A}^\circ$$

This value still doesn't appear to be sufficiently larger than those calculated for hydrated KOH to attempt to meet the problem by reduction of pore size in separators.

The question might also be asked: is there any experimental evidence bearing on the situation in terms of relative diffusion rates through membranes? In Table 5 of APL-TDR-64-85 (final report on Air Force Contract Nr. AF33(657)-10643, dated 1 August 1964) flux rates for KOH and zincate ion diffusion through regular pore size fibrous sausage casing (RPS) were measured to be 1.1×10^{-3} for KOH under a concentration difference of 12 M and 4.0×10^{-6} for $ZnO_2^=$ for a concentration difference of 1.3 M (in 45% KOH). Using an estimated average value of D for KOH of 1.4×10^{-5} cm^2/sec. and a value of 1.8×10^{-6} for D of zincate ion in 44% KOH, the value of flux for KOH might have been expected to be $\frac{14}{1.8} \times \frac{12}{1.3} = 72$ times that for zincate ion. Thus, $4.0 \times 10^{-6} \times 72 = 288 \times 10^{-6} \cong 0.3 \times 10^{-3}$, and for this membrane KOH diffusion was 1.1/0.3 = 3.7 times larger than expected in terms of our previous conclusion regarding the possibility of obtaining screening on a pore size basis. This could mean that some screening of zincate ion was being achieved. Comparing the small pore size (SPS) membrane in the same table of reference, the factor was 0.75/0.22 = 3.4, which represents less screening than was achieved by the regular pore size material. Going on down the table, values of the screening factor lying between 1.3 and 4.6 (the latter for control fibrous sausage casing) are obtained. For the best of the RAI materials, i.e. 2.2XH (Table 6, same reference) a value of 3.2 for the screening index was found. These data, if reliable, would indicate some hope for being able to obtain screening of zincate ion through pore size reduction in spite of the previously estimated values for ionic (molecular) sizes.

It can only be concluded that additional information is necessary, either by way of preparation of smaller pore size membranes or by way of more refined measurements of ionic sizes, or both.

Soluble Silver

While no experimental work has been done on the determination of the size of soluble silver species, some information is available. First of all, negative ions do not vary greatly in terms of ionic dimensions* and, furthermore, if the soluble silver species is AgO^-, it should have a smaller hydration sheath than the doubly charged zincate ion. From the experimental point of view, however, in the just-mentioned Tables of reference, values of soluble silver flux equivalent to those for zincate ion were measured. On this basis, it is concluded that remarks apropos of zincate ion diffusion also apply to diffusion of the soluble silver species.

J. Membrane Pore Size Measurements in KOH

This work is just getting underway. It is expected to be done by competitive diffusion rates of different size neutral molecules in solutions of battery strength KOH. The first step is to find some neutral molecules of different sizes that are sufficiently soluble in strong KOH to give a satisfactory concentration gradient, that are stable in strong KOH, and that are not adsorbed in the separator membranes.

K. Stoichiometric Ratios of Formed Zinc

This work is scheduled to start in the first quarter of the second year.

---

*See Stern and Amis, "Ionic Sizes," Table 14, p. 30, Chem. Rev. 59, Feb. 1959.
See also Monk, "Electrolytic Dissociation," Table 14.4, p. 271, Academic Press, New York, 1961.

L. Alternate Method of Surface Area Measurement

This proposed method of investigation of surface area of zinc electrodes is based on the fact that zinc can form a passive layer on discharge because a ZnO or $Zn(OH)_2$ solid product can be formed film-wise on the surface, at high rates of discharge and low concentrations of KOH and at low temperatures, much faster than it will go into solution. C. M. Shepherd (Naval Research Laboratories, Unreported Work) has observed discharge voltages as high as 40 volts on passivating zinc surfaces. This was accompanied by the formation of a bright blue color. The bright blue color is frequently observed on zinc electrodes which have failed on cycle life testing, particularly at low temperatures (30-40°F.), although it is sometimes observed on failed zinc electrodes from cells cycled at room temperature.

The bright blue color bespeaks the possibility of an oxide film thickness which could be of the order of 500-700 A° thick (Kubaschewski and Hopkins, "Oxidation of Metals and Alloys," see p. 100 et seque, Butterworth Scientific Publications, London, 1953; see also the discussion by U. R. Evans, "Metallic Corrosion, Passivity and Protection", Arnold, London, 1946).

Because of the thinness of these passivating films and their constant value as indicated by color, the amount of current that is passed in order to achieve passivation should be descriptive of the surface area even on rough surfaces and porous electrodes provided particle size of the metallic zinc is several orders of magnitude greater than the thickness of the passivating film. Thus, one could, for example, measure the time to passivation over a range of high current densities on a flat sheet zinc and determine film thickness from the number of coulombs passed. Then, at the same electrolyte concentration and temperature, the current at which passivation occurs for a porous electrode for the same time interval would be found. Assuming a surface roughness factor of one for the flat zinc sheet, the surface area of the porous electrode would correspond to the ratio of current values necessary to achieve passivation at the same value of time.

It is interesting that this method has been used recently by E. A. Butler and A. U. Blackham (Final report on JPL Contract No. 951554, Contract NAS7-100), "Studies of Reaction Geometry in Oxidation and Reduction of the Alkaline Silver Electrode," Section II, April 10, 1967; see also J. A. Allen, Trans. Far. Soc. 48, 273, 1952) to determine the surface area of sintered silver electrodes.

On this program, work on the zinc electrode has just been started by T. P. Dirkse at Calvin College. The following surface treatment of sheet zinc electrodes was used for 99.999% zinc. They were degreased in ethylene dichloride, given a slight etch in dilute HCl, rinsed thoroughly and dried. Next they were painted with a polystyrene cement to expose an area $\frac{1}{8}$" x $\frac{1}{8}$" to the electrolyte. Just before use the zinc surface was rubbed with a fine (3/0) silicon carbide paper and rinsed with distilled water. They were then placed in a 10% KOH bath at room temperature, soaked for five minutes, and discharged over a range of currents against working charged nickel oxide electrodes. The range of currents was selected to obtain voltage drop to zero volts in 10 seconds or less. Amalgamated zinc electrodes were also run. Amalgamation was accomplished by dipping each zinc electrode in a solution containing 50 gm/l. of $HgCl_2$ and thoroughly rinsing with water.

A summary of the results is given in Figure 41. The data indicate that there is not any appreciable difference between the plain and the amalgamated zinc. From the data of Figure 41 a plot of time-to-passivation vs. current can be made as in Figure 42. From both figures, it is evident that as current decreases, the number of coulombs of zinc used increases, consequently some film solution is indicated, if the discharge process is formation of a ZnO or $Zn(OH)_2$ film followed by solution.

Taking the 4 second data from Figure 41 it is seen that 1.08 coulombs have been passed. Using Faraday's law,

$$W_{Zn} = \frac{1.08 \times 32.7}{96,500} = 3.68 \times 10^{-4} \text{ gms of Zn}$$

were reacted. Assuming a surface roughness factor of one, this would mean

that the following thickness of zinc has reacted:

$$t = \frac{3.68 \times 10^{-4}}{7.14 \times 1.61} = 0.313 \times 10^{-4} = 3130\ A^{\circ}$$

Due to the roughening treatment given the sample with the silicon carbide paper, the roughness factor is unknown. If the roughness factor were as large (say) as 10, then the thickness of zinc reacted could be as small as 313 A°.

After establishing the calibration curve for sheet zinc some Delco-Remy negatives were run which had a geometric area of $\frac{1}{2}$" x $\frac{1}{2}$". The results were as shown in Table IX.

TABLE IX

Passivation Times for Porous Electrodes

Electrode #	Current (amperes)	Time (seconds)	Coulombs (ampere-seconds)
1	2.4	4.0	9.6
2	1.8	5.2	9.4
3	1.8	7.2	13.0
4	2.1	8.1	17.0

Comparing these with the zinc sheet data from Figure 42, the relative current values indicate surface areas of: 8.9, 7.2, 8.1 and 9.9 times the surface area of the sheet zinc electrodes, for electrodes numbers 1 through 4, respectively.

If the roughness factor of the sheet zinc electrode were (say) 10, then the surface areas would be calculated to be 89, 72, 81 and 99. A 0.25 sq.in. section of a Delco-Remy negative contains 0.4 gm. of zinc in the fully-formed condition, so a surface area of around 200 sq.cm. per gram of zinc would be estimated from these data.

It should be recognized, however, at this point in the experimental program that all these data are illustrative only. The uncertainty in the roughness factor of the sheet zinc is high. The sharp slope of the increase in the coulombs passed vs. current is a good indicator that the technique for establishing passivity on the sheet zinc electrodes needs to be examined in more dilute electrolytes and at lower temperatures in order to induce a lower solubility rate of the zinc oxide formed on discharge. Hydrogen gassing on the zinc surface before the discharge (i.e. cathodic preelectrolysis) should be examined as a means of surface reduction of any oxides which might be existing on the surface. It is planned to continue this work in order to be able to achieve a realistic estimate of surface area of porous zinc plates. The primary objective is to use the technique as a tool in failure examination work; however, it could be useful in relating capacity to particle size and surface area in the interest of designing for high initial capacities.

M. Separator Development

The First Quarterly Report from RAI Research Corporation is attached.

N. Electrolytes

A study of electrolyte mixtures, using percentages of 45% and 50% KOH and 45% NaOH in addition to varying layers of separator material, was accomplished.

Table X shows the cell construction cycle data and failure analysis of some 60 cells tested. The best combination was one layer of acrylonitrile monomer and four layers of cellulosic membrane in 50% KOH yielding a cycle life of 220 cycles. Additional work is planned in which strongly basic tertiary amino hydroxides will be used as electrolytes.

The mixtures of KOH and NaOH were tried out because previous experience at lower depths-of-discharge (25% and 40%) had shown that NaOH increased cycle life over equivalent weight concentrations of KOH. The

TABLE X

Study: Electrolyte and Separator Test

Note: Cells 1, 2, 3, 4, 5, and 6 contain 1 layer acrylonitrile and 4 layers of reinforced cellulosic membrane.
Cells 7, 8, 9, 10, 11 and 12 " 2 " " " " " "
Cells 13, 14, 15, 16, 17 and 18 " 3 " " " " " "
Cells 19, 20, 21, 22, 23 and 24 " 4 " " " " " "

Cell No.	Cycles	Initial Capacity	Pos. Plate Construction	Neg. Plate Construction	Electrolyte	Extent of Zinc Formed & Accumulative Overcharge		Negative Plate Treeing	Creeping	Washout
1-3	192	28 a.h.	Eight plates	Seven plates	45% KOH	90% Zinc	+ 11 a.h.	Light	around 2 layers	25-35%
4-6	220	29 "	.020"-.023"	20 g ZnO	50% KOH	"	"	"	"	"
7-9	192	30 "	15 g Ag + 1% Pd	+ 2% HgO + .5% BC610	45% KOH	"	"	"	"	"
10-12	192	28 "			50% KOH	"	"	"	"	"
13	192	30 "	"	"	45% KOH	"	"	"	"	"
14	60	30 "	"	"	"	90% ZnO	"	None	"	"
15	192	30 "	"	"	"	90% Zn	"	Light	"	"
16-17	192	29 "	"	"	50% KOH	"	"	"	"	"
18	180	29 "	"	"	"	"	"	"	"	"
19	60	30 "	"	"	45% KOH	90% ZnO	"	None	"	"
20	192	30 "	"	"	"	90% Zn	"	Light	"	"
21	192	30 "	"	"	"	"	"	"	"	"
22	180	28 "	"	"	50% KOH	"	"	"	"	"
23-24	192	28 "	"	"	"	"	"	"	"	"
25-30	210	34 "	"	"	100%(45% KOH)					
31-36	162	30 "	"	"	80%(45% KOH), 20%(45% NaOH)					
37-42	70	28 "	"	"	60%(45% KOH), 40%(45% NaOH)					
43-48	33	21 "	"	"	40%(45%KOH), 60%(45% NaOH)					
49-54	33	22 "	"	"	20%(45% KOH), 80%(45% NaOH)					
55-60	33	18 "	"	"	100% (45% NaOH)					

NaOH-containing electrolytes just could not support the rates of charge necessary on the 2-hour cycle regimen at 60% depth-of-discharge. Charge voltages went way up; the cells heated up, and gassing resulted indicating inefficiency of charge.

O. Factors Controlling Zinc Particle Size Growth

The original work plan called for examination of the influence of the following factors on zinc particle size growth in cycling cells:

Current density and time
Mechanical barriers
Surfactants
Initial ZnO particle size and shape
Overgrowth sites
Combinations of the preceding factors.

Photomicrographs have been made of all variations of zinc plates tested on this program, or are in process of being made. It is recalled that the reason for this portion of the program was the remarkable effect of the Emulphogene BC-610 in keeping the zinc particle size small and disperse in comparison with the 2% PVA as evidenced by Figures 47 through 51 in AFAPL-TR-66-79. In the current program it should be remembered that 0.5% BC-610 has been used in all negative plate formulations, except those where the surfactant itself is under study. As a consequence it is to be expected that fineness of particle size and dispersity will be at least equivalent to that of the control cells containing 0.5% BC-610, unless some factor resulting from a variation under study were, actually, to increase the particle size. Another consideration is the fact that, in the first year of this program, no variation has been found which extends life of the cell beyond that obtained with the use of 0.5% BC-610 and Kadox-15. Kadox-15 has a particle size of 0.11 μ, and so far under the current program, only two materials have been tested which have a finer particle size, i.e. the high surface area wet process materials 243-63-1 (0.031 μ) and 243-67-2 (0.025 μ). The point being driven at here

is this: that use of the BC-610 and the Kadox-15 may have extended cycle life to the point where particle size and dispersity no longer control life, i.e. another factor now needs to be controlled. The factor of concern is believed to be the loss of negative active material from around the edges and at the top of the plate. It is specifically noted that this does not represent any appreciable loss of weight of active material, but it does represent a redistribution of the active material on the plate. The result of this redistribution is, effectively, to almost double the current density to the active material, based on the geometric area (i.e. not necessarily true current density based on active material true surface area). Nevertheless, doubling the current density on the basis of the geometric area might almost double the IR loss through the separator causing a drop in voltage which would contribute to shortened life. However, the active material photomicrographs may be examined for particle size and dispersity effects.

The effects of current density, time and temperature will be determined in conjunction with the studies on stoichiometric ratios of formed zinc, scheduled for investigation during the second year.

Most of the photomicrographs shown in this report are concerned with the use of mechanical barriers to agglomeration (Figures 1 through 18). All these may be compared to Figure 1 which shows the control plate containing 0.5% BC-610 from a cell which failed at 140 cycles. Figures 2, 3 and 4 for the asbestos fiber additions show that particle size and agglomeration are, indeed, reduced for an equivalent number of cycles (134). Asbestos is a magnesium silicate and it tends to dissolve and gelatinize in strong KOH, which may have been the reason it interfered so badly with the formation process, even in concentrations as low as 5% by weight in the plates. At any rate it did not increase cycle life.

The shredded sausage casing (Figures 5, 6, 7 and 18) also kept the zinc from agglomerating, but the photomicrographs show large void areas, probably due to the gradual dissolution of the material. Except in very large quantities (30% by weight, Figure 18, Table I),

it did not prevent shedding around the top and sides. The large void spaces might be expected to result in loss of contact of the metallic zinc resulting in loss of capacity also. At any rate, its use didn't increase cycle life.

The fact that the 30% by weight sample prevented shedding almost completely brings up another point for discussion. Unless relatively little (say 5%-10% or less) of the organic fibers turn out to be useful in extending cycle life, their practical effect is to increase the plate volume considerably because of their low density, which would mean a reduction in the volume performance. Moreover, because of sheer bulk their use could result in loss of metallic zinc contact and consequent reduction in performance. Thus, at 30% by weight, the shredded sausage casing yielded only 21 a.h. on the initial capacity test and gave only 300 cycles (at 40% depth-of-discharge) in spite of the fact that shedding was prevented.

The effects of metallic zinc additions to the original formulation are shown in Figures 8, 9 and 10. The state of agglomeration of the 5% sample (Figure 8) looks very much like that for the control cell (Figure 1) allowing for the difference in magnification, and the 5% addition may have provided a slight increase in cycle life. This material (#1208 zinc metal), while elongated in shape, is more nodular than fibrous. The use of fibrous zinc should probably be reinvestigated if a source of real fibers can be obtained.

The lignosulfonic acid additions are interesting. Their photomicrographs are shown in Figures 11, 12 and 13. Figure 14 shows a control plate also at 200X magnification for comparison. This material did not prevent agglomeration; in fact it is much more advanced for equivalent numbers of cycles (compare Figures 12 and 14). In spite of this the 1.2% lignosulfonic acid additions yielded slightly better cycle life than the controls (cells 132 through 137 vs. cells 123, 124 and 125, Table I). This additive should be reinvestigated both by itself and in combination with varied amounts of the BC-610.

Of all the materials tried out as mechanical barriers to agglomeration, the one that worked best was the cotton fibers. Photomicrographs

are shown in Figures 15, 16 and 17. These are at the 100X magnification and may be compared with Figure 1. One percent of this material (Figure 15) is sufficient to keep the metallic zinc in a very finely divided state and while these cells yielded only 144 cycles (Table I, cells 163 through 167), they averaged better than their controls (cells 168 through 173) which gave an average of 122 cycles. It is planned to reinvestigate this material.

The Avicel photomicrographs are not yet available.

As far as the surfactant series is concerned, i.e. BC-420, BC-610, BC-720 and BC-840, photomicrographs for which are shown in Figures 19 through 25 (Figure 25 is for a 0.5% BC-610 control), the sections taken show such large void spaces that little comparison can be made of their possible effects on particle size control. At any rate cell life is poorer for the BC-720 and BC-840 than for the controls. The BC-420 gives cell life equivalent to that for the BC-610. (See Table II, cells 91 through 120). The BC-420 and the BC-610 seem to be equivalent. (BC-840 has also been shown to be inferior to BC-610 at 40% depth-of-discharge, previously (AFAPL-TR-66-79, Table 11, p. 49). On the basis of these data, the use of either BC-420 or BC-610 could be recommended. No further work is planned and 0.5% BC-610 will continue to be used in the standard plate formulation.

Figures 26 through 31 show photomicrographs of failed zinc plates at several concentrations of BC-610 tested at 40°F. and 100°F. These are at 200X magnification and may be compared with Figure 14.

Figures 32, 33 and 34 show photomicrographs for concentrations of 0.1, 0.6 and 1% of the anionic surfactant FC-95. These are at 200X also and are to be compared with Figure 14. Particle size seems to be about the same as in Figure 14, although particles are more disperse for the FC-95. More work over broader concentration ranges and at different temperatures is planned for this material and for companion anionic and cationic materials from the same manufacturer.

The photomicrographic information on the influence of the ZnO morphology, particle size, etc. are not presented in this report because all the samples have not yet been tested and all the photomicrographs are not yet available.

Photomicrographs are not yet available for the experimental work on the CaO additions, nor has any work been done on combinations of the three factors: mechanical barriers, sites for overgrowths, and surfactants. Combinations on mechanical barriers and 0.5% BC-610 have been presented above.

III. General Discussion

As a prelude to examination of the effects on cycle life of the several variations incorporated in the negative plate during this program, consideration should be given to the pure effect of the depth-of-discharge factor. That is to say, the question should be asked: what actual capacities are available from these nominal 25 a.h. cells at various rates of discharge for the cell design concerned? Reduction in capacity as a function of discharge rate is expected for any electrochemical cell and it may vary as a function of cell design. In order to determine this for the 15-plate, 4-layer Visking, 0.5% BC-610, cells were discharged at 25 and 50 amperes and found to have capacities of 19.0 and 15.0 a.h., respectively. The average of all the control cells run on this program to date is 26.7 a.h. at the 15-ampere rate. On the basis of these data, Table XI was constructed.

TABLE XI

Capacity Available at Cycle-Life Test Rates

Depth-of-Discharge (% of Nominal Capacity*)	Required Depth-of-Discharge a.h.	Required Rate on 2-Hour Cycle (35-min. discharge) amperes	Capacity Available at Cycle-Life Test Rates a.h.
100	25	43	15.5
80	20	34.3	17
70	17.5	29.8	18
60	15	25.8	19
40	10	17.2	23
25	6.25	10.7	31

*Nominal Capacity = 25 ampere-hours at 15-ampere rate.

On the basis of the data of Table XI it is apparent that this cell design would not be able to cycle at all on the 2-hour regimen at depth-of-discharges

of 100% or 80%, because it does not have sufficient capacity at the required test rate of discharge.

From Table XI we may construct another table relating the allowable capacity loss before failure from the data in columns 2 and 4 of the table for depth-of-discharges of 70% or less. This is shown in Table XII.

TABLE XII

Allowable Capacity Loss Before Failure Related to % DOD

% DOD	Allowable Capacity Loss Until Failure a.h.	Expected Cycle Life
70	0.5	28
60	4	226
40	13	735
25	24.7	1400*

*Actual cycle life from data of Table 12, AFAPL-TR-66-79.

Now, assuming that there is a direct ratio between the allowable capacity loss until failure and the actual cycle life, data for expected cycle life as a function of DOD may be calculated, as in the third column of the table. The actual cycle life at 25% DOD was used to estimate expected cycle life at the higher depths-of-discharge. An actual cycle life of 600 cycles at 40% DOD for negative plates with 0.5% BC-610 Emulphogene additions may be compared with the value of 735 from the table. (See Table 11, AFAPL-TR-66-79.) The average cycle life of 33 control cells on this program, so far, is 164 ± 36 cycles with some groups going over 200 cycles. This may be compared with the value of 226 cycles in Table XII.

In estimating the expected cycle life as a function of depth-of-discharge and the allowable capacity loss, it is obvious that the condition of the negative plate will be much better at the end of life at 60% depth-of-discharge

than it is at 40% depth-of-discharge and so on. This is evident from the fact that if the depth-of-discharge is reduced after failure at 60%, the cell will continue to cycle.

The point of this discussion is this: during the first year of this program we have been looking very intensively at the effects of the several variations on agglomeration and dispersity of the active material. This was a natural sequitur to the discovery that cycle life could nearly double with the use of Emulphogene BC-610 and that this resulted from reduction of the rate of agglomeration (AFAPL-TR-66-79, Table 11 and Figures 47 through 51), and the maintenance of dispersity of the metallic zinc. It seems possible, judging from the photomicrographs, that even at 60% depth-of-discharge there is sufficient true surface area (i.e. lack of agglomeration or particle size growth) to support the discharge and that loss of active material around the top and sides of the plate may have been a predominant factor in determining life. (Actually, true surface area of the available zinc needs to be measured to support this possible conclusion.)

Several other possible effects can be thought of that could come into play in shortening life: one, the loss of small amounts of active material would be more serious in reducing life at the higher depths-of-discharge; two, the loss in geometric area of the active material would be more serious, due to increased IR losses; and three, if availability of electrolyte is a controlling factor in determining capacity (as could be the case based on the information in NARMCO's report attached), then the reduced geometric area might mean that the electrolyte at the top and the sides is not available for reaction, and, moreover, the change in the electrolyte concentration due to inhibition of diffusion by the separator would be more serious, due to the increase in geometric current density and the reduced geometric area.

If these effects are dominating factors in determining cycle life, there are two obvious ways to go in order to alleviate the situation. One way is to find the cause for the rearrangement of the active material from the tops and sides to the center and bottom of the plate and see what

can be done about it. In a very interesting study made recently (J. McBreen and G. A. Dalin, "The Mechanism of Zinc Shape Change in Secondary Batteries," Extended Abstracts of the Battery Division of the Electrochemical Society - Fall Meeting, Philadelphia, 1966, p. 123), gravitational effects, "washing" caused by rise and fall of the electrolyte in the negative plate compartment, and cell case taper were ruled out as possible causes. The second way to go is to provide a separator which will reduce the extent of electrolyte concentration change, and, perhaps provide a higher energy yield in the equivalent cell volume.

It might have been expected that some of the mechanical barriers tested under this program would have reduced the rate of change of the geometric area, if washing and gravitational effects were at play, so these results substantiate those of McBreen and Dalin. Of the several investigated, only the cotton fibers seemed to have any effect, so investigation of this material will be continued. Cotton fiber should withstand chemical attack in the KOH much better than its regenerated cellulose counterpart, i.e. fibrous sausage casing, or cellophane, because of its much higher molecular weight. The molecular weight of cotton fibers is probably of the order of 600,000, containing 3000 - 3500 anhydroglucose units ("Cellulose and Cellulose Derivatives," Part I, 2nd Ed., edited by E. Ott, H. M. Spurlin and M. W. Grafflin, p. 53, Interscience Publishers, Inc., New York). The process of making cellophane involves reduction in molecular weight to achieve processability, i.e. the shredded sausage casing fibers should be more readily amenable to attack in the environment which should result in more rapid loss of any possible effect they might exert as mechanical barriers.

Based on the predominance of short-circuiting failures when only three layers of fibrous sausage casing were used, and the low cycle life resulting (around 110 - 120 cycles, see Table II), four layers of fibrous sausage casing will be continued in use for standard construction in order to insure zinc plate failure, until a better separator material is found.

The use of zinc fibers will be reinvestigated.

The lignosulfonic acid, in view of the fact that it did not prevent zinc

particle size growth but yet yielded good cycle life, will be continued to be investigated because it appears to function differently than the other surface active agents such as the Emulphogenes and the FC-95. The FC-95 and similar surface active agents will be investigated because it appears to function at least as well as the Emulphogenes, so the possibility exists that a better surfactant of this class could be found. The FC-95 will be investigated at 30 - 40°F. and 100°F. to determine whether it might function better than Emulphogene BC-610 at these temperatures.

Tests of several of the alcohols, for example the best (ethanol) and the worst (propanol) will be repeated because these groups of cells did not get sufficient overcharge to keep the zinc plate in a charged condition. These tests will be run along with those on the series of carbowaxes of varying molecular weight, which are scheduled for early test in the second year program.

Discussion of the possible effects of the ZnO variations will be withheld until all variations have been tested.

The use of XX-601 in combination with Kadox-15 will be reinvestigated because the cells tested on this program failed due to undercharge (Table IV). XX-602 will also be checked out because it is the most acicular of the oxides available for test, i.e. it has the longest needles (see Fig. 45, AFAPL-TR-66-79).

Use of the $ZnSO_4$ admixture will be reexamined because 5% additions of this material appear to give good results at room temperature, in combination with cotton fibers.

IV. Recommendations

The most urgent and emphatic recommendation that can be made as a result of this work is that every effort be made to determine the cause of loss of material around the sides and edges of the plates, because this result seems to be the major contributing factor to loss of capacity as cycling progresses. If this is true, it is quite possible that adequate testing of the variations checked out so far may not have been achieved. Conversely, however, it can also be said that, with the exception of the cotton fibers, none of the variations tested was effective in slowing down loss of material around the top and sides.

In addition to the second year work plan already laid out, the reinvestigations called for above are recommended.

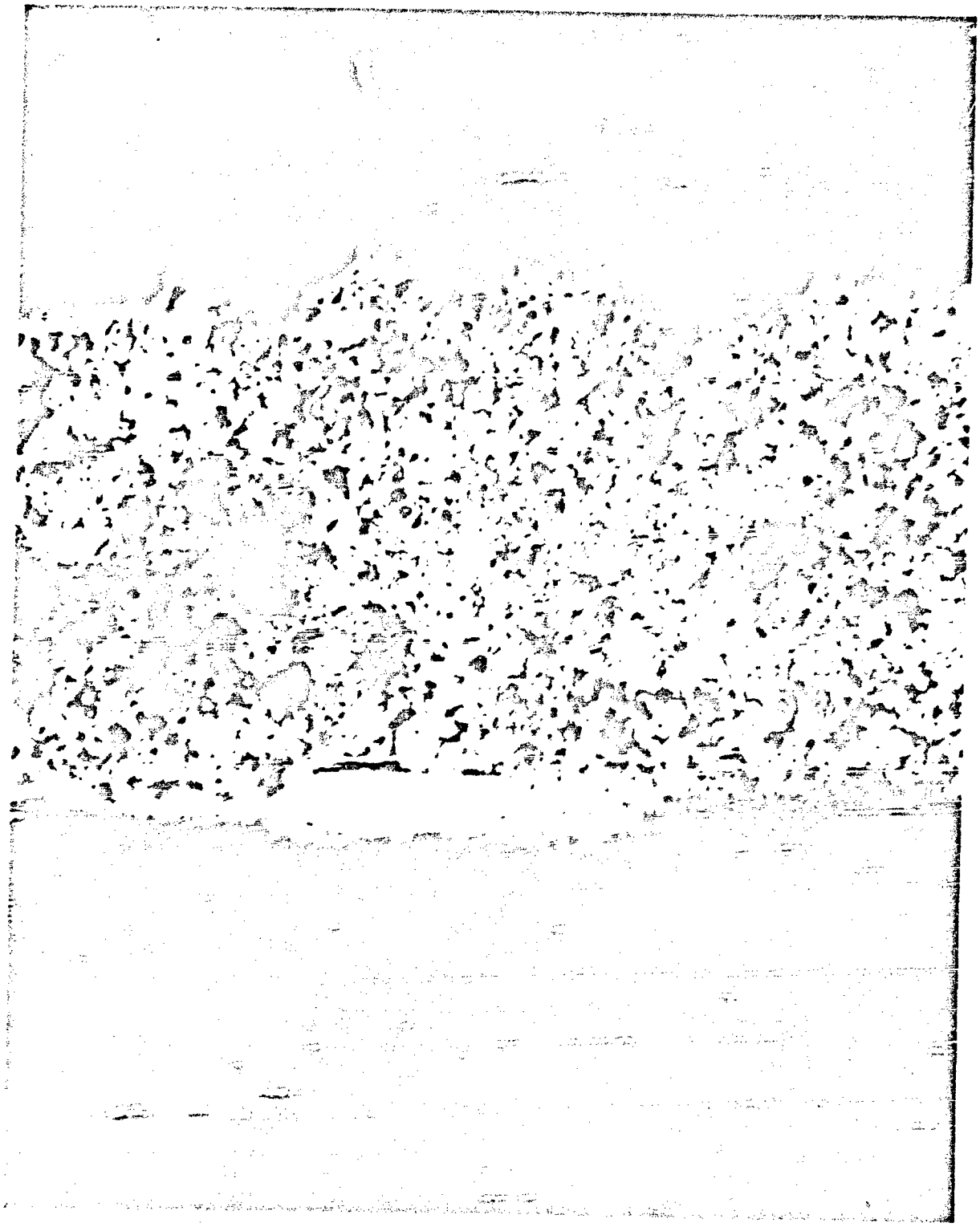

Figure 1. Negative Plate in Control Cell at 140 Cycles. 100X.

Figure 2. Negative Plate Containing 5% Asbestos Fibers at 134 Cycles. 14CX.

Figure 3. Negative Plate Containing 10% Asbestos Fibers at 134 Cycles. 14CX.

Figure 4. Negative Plate Containing 15% Asbestos Fibers at 134 Cycles. 1.0X.

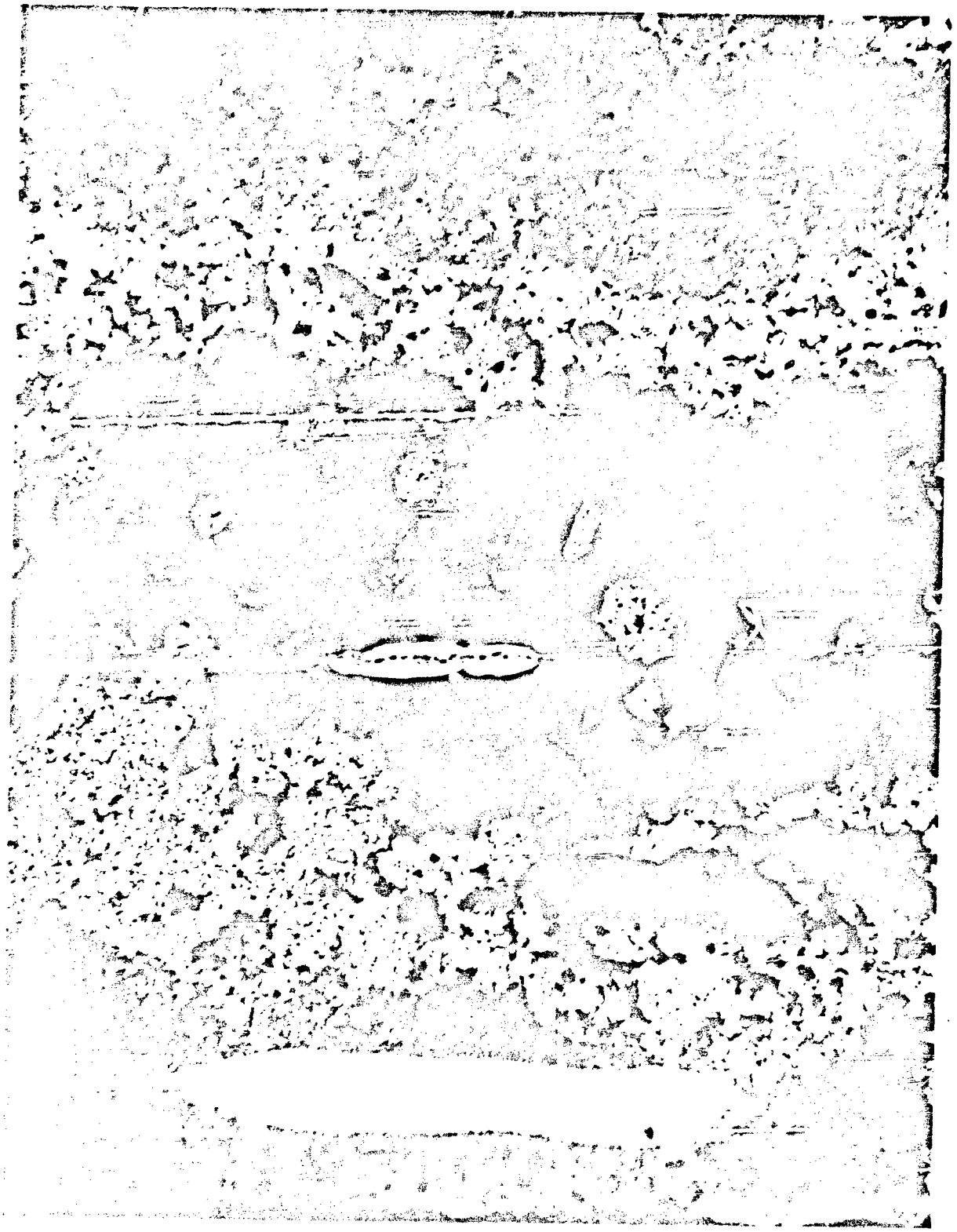

Figure 5. Negative Plate Containing 5% FOO Fibers at 146 Cycles. 140X.

Figure 6. Negative Plate Containing 10% FC Fibers at 146 Cycles. 140X.

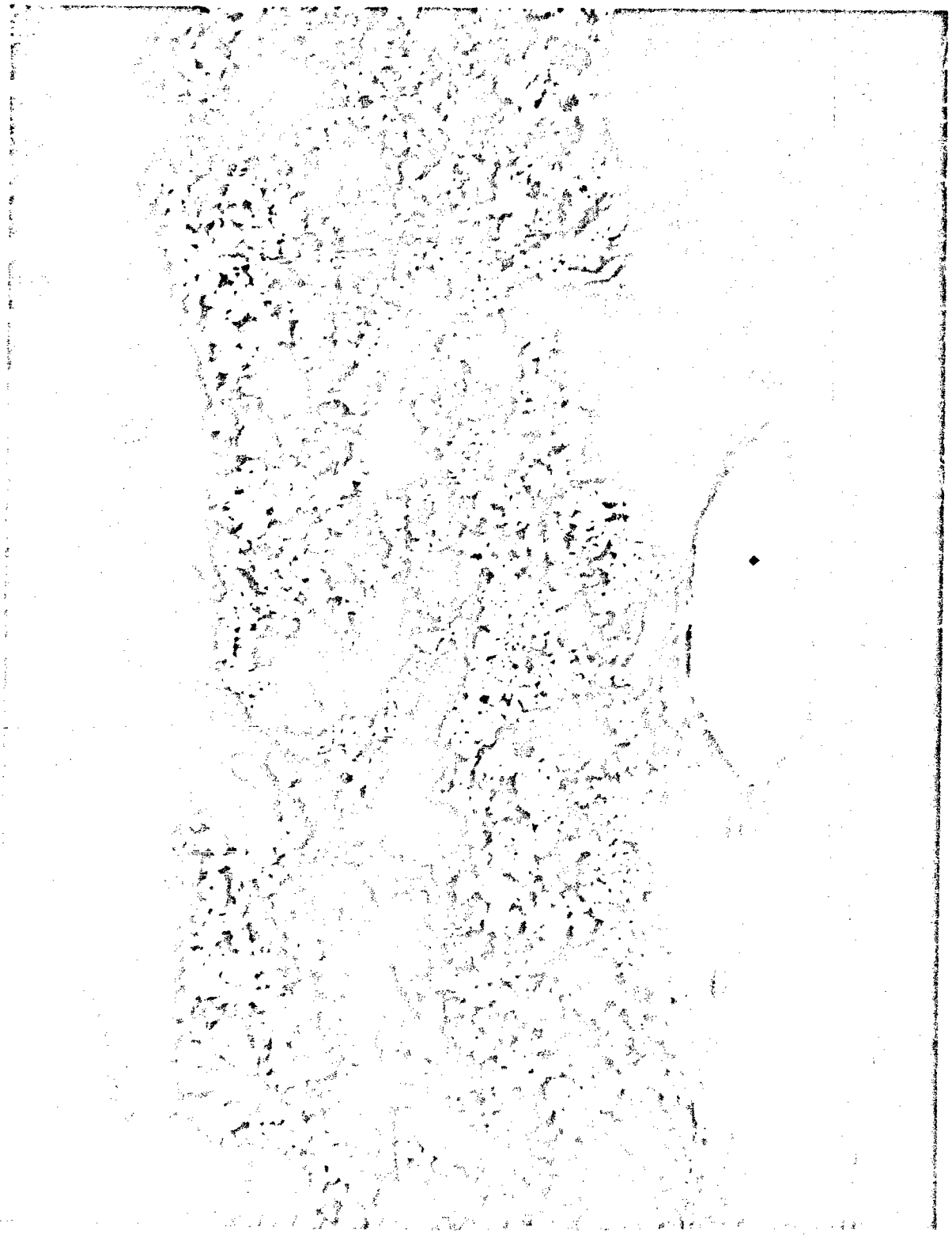

Figure 7. Negative Plate Containing 15% F.C Fibers at 1:6 Cycles. 1.7 X.

Figure 8. Negative Plate Containing 5% Zinc Fibers at 171 Cycles. 140X.

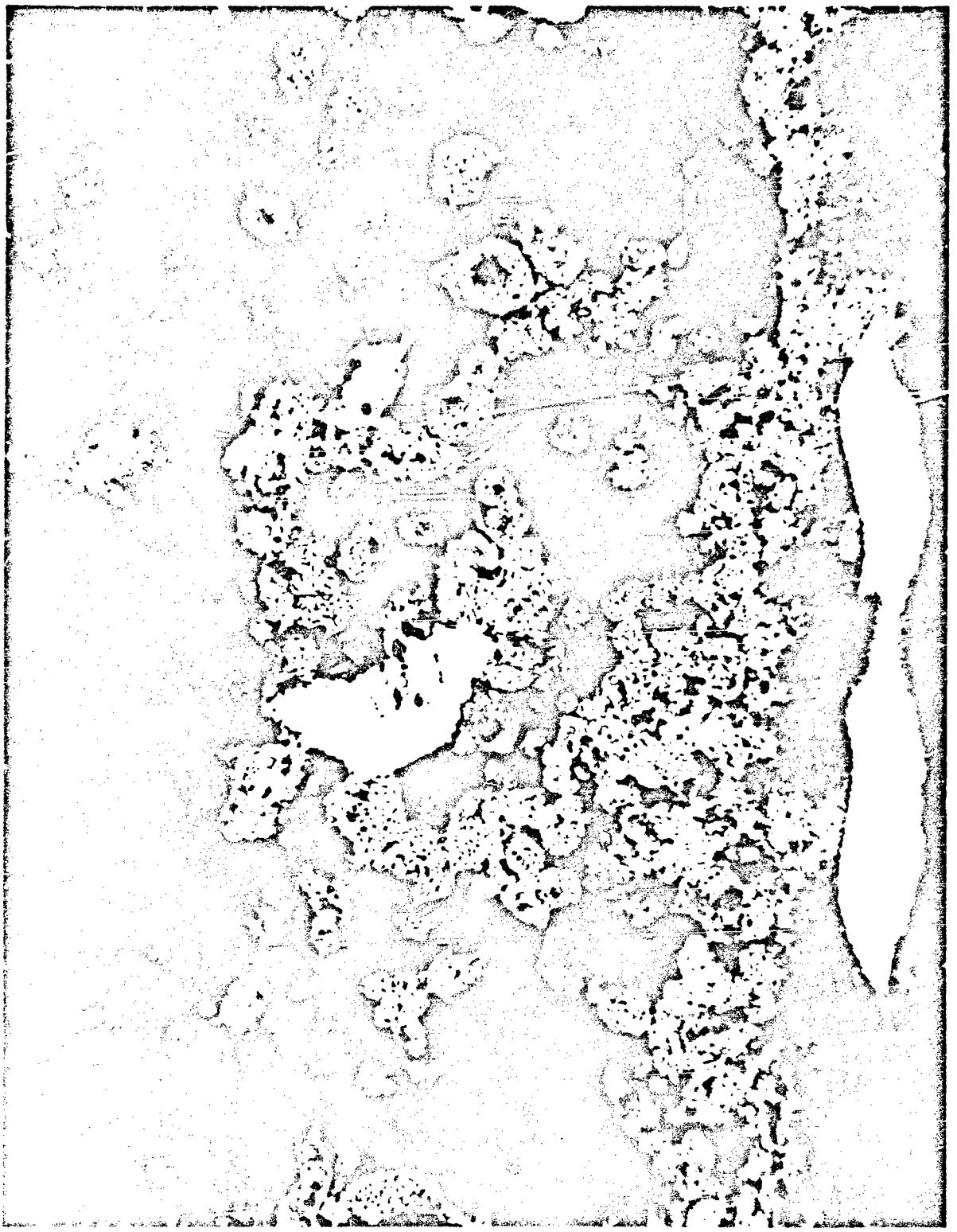

Figure 9. Negative Plate Containing 10% Zinc Fibers at 108 Cycles. 140X.

Figure 10. Negative Plate Containing 15% Zinc Fibers at 168 Cycles. 14CX.

Figure 11. Negative Plate Containing .2% LSA at 84 Cycles. 200X.

Figure 12. Negative Plate Containing 1.2% LSA at 168 Cycles. 200X.

Figure 13. Negative Plate Containing 2% LSA at 144 Cycles. 200X.

Figure 14. Negative Plate as Control at 157 Cycles. 200X.

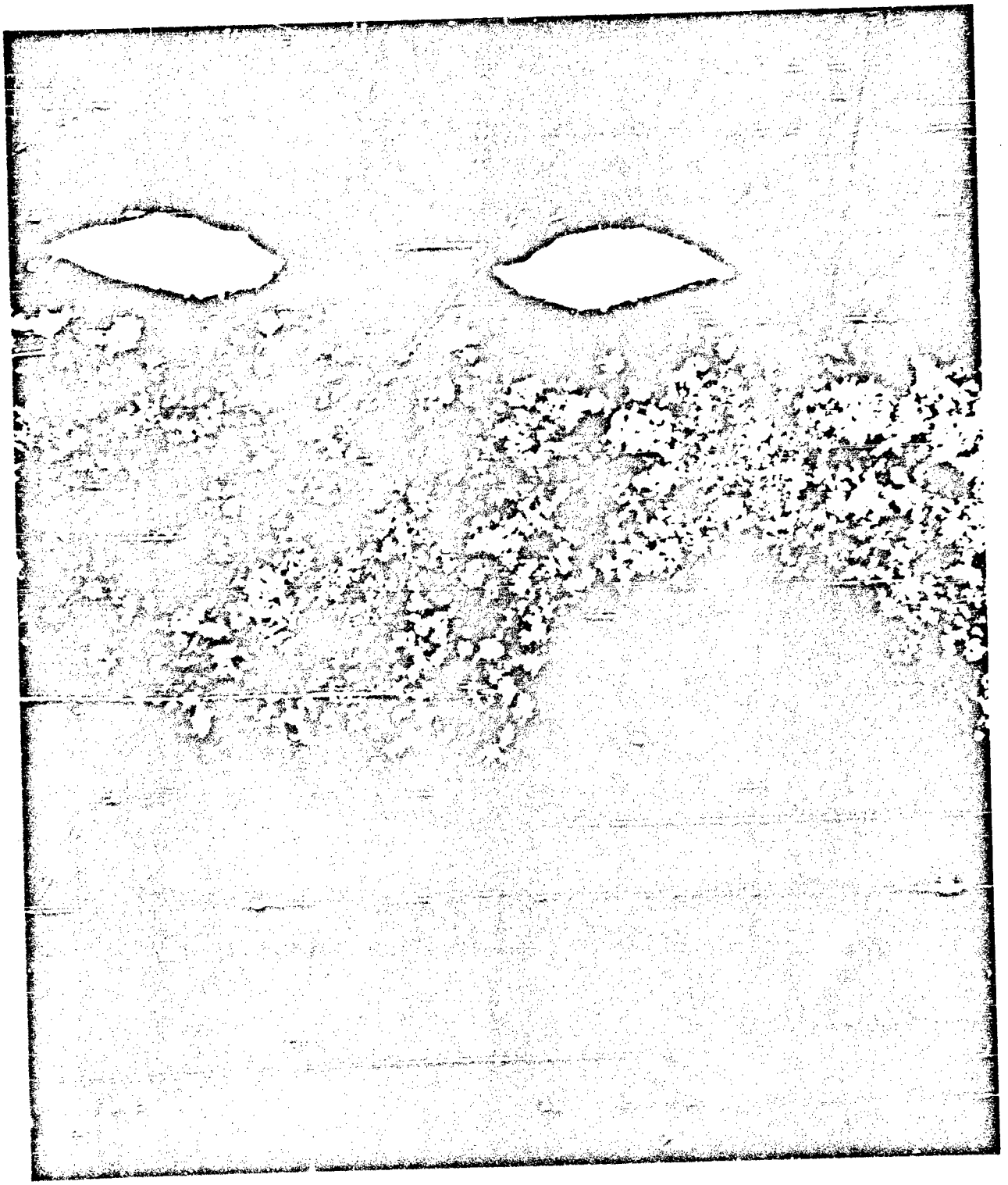

Figure 15. Negative Plate Containing 1% Cotton Fibers at 144 Cycles. 100X.

Figure 16. Negative Plate Containing 3% Cotton Fibers at 144 Cycles. 100X.

Figure 17. Negative Plate Containing 5% Cotton Fibers at 144 Cycles. 100X.

Figure 18. Negative Plate Containing 30% Cellulosic Fibers at 300 Cycles. 100X.

Figure 19. Negative Plate Containing .15% BC-420 at 168 Cycles. 200X.

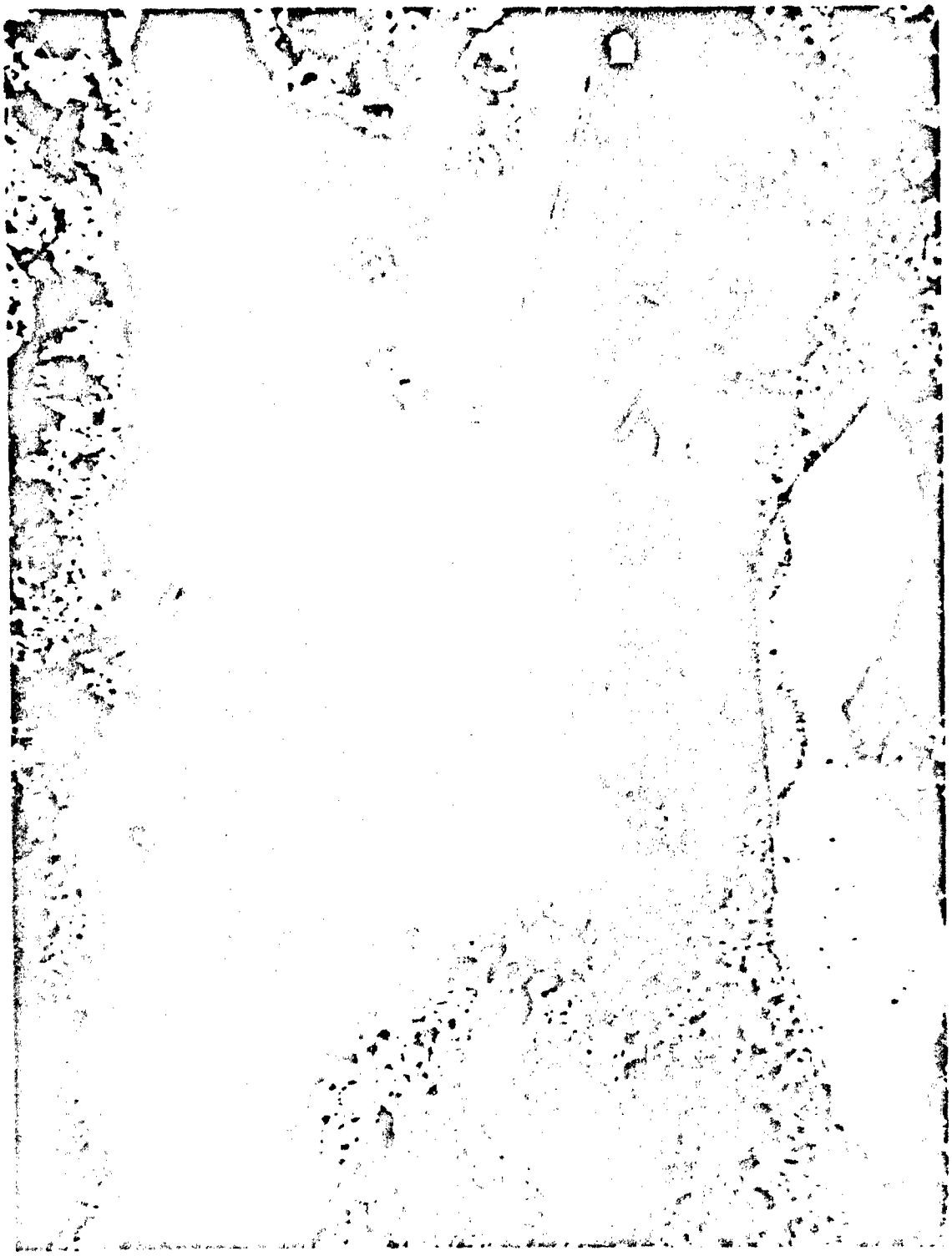

Figure 20. Negative Plate Containing 1% BC-420 at 160 Cycles. 200X.

Figure 21. Negative Plate Containing .15% BC-720 at 120 Cycles. 200X.

Figure 22. Negative Plate Containing 1% BC-720 at 108 Cycles. 200X.

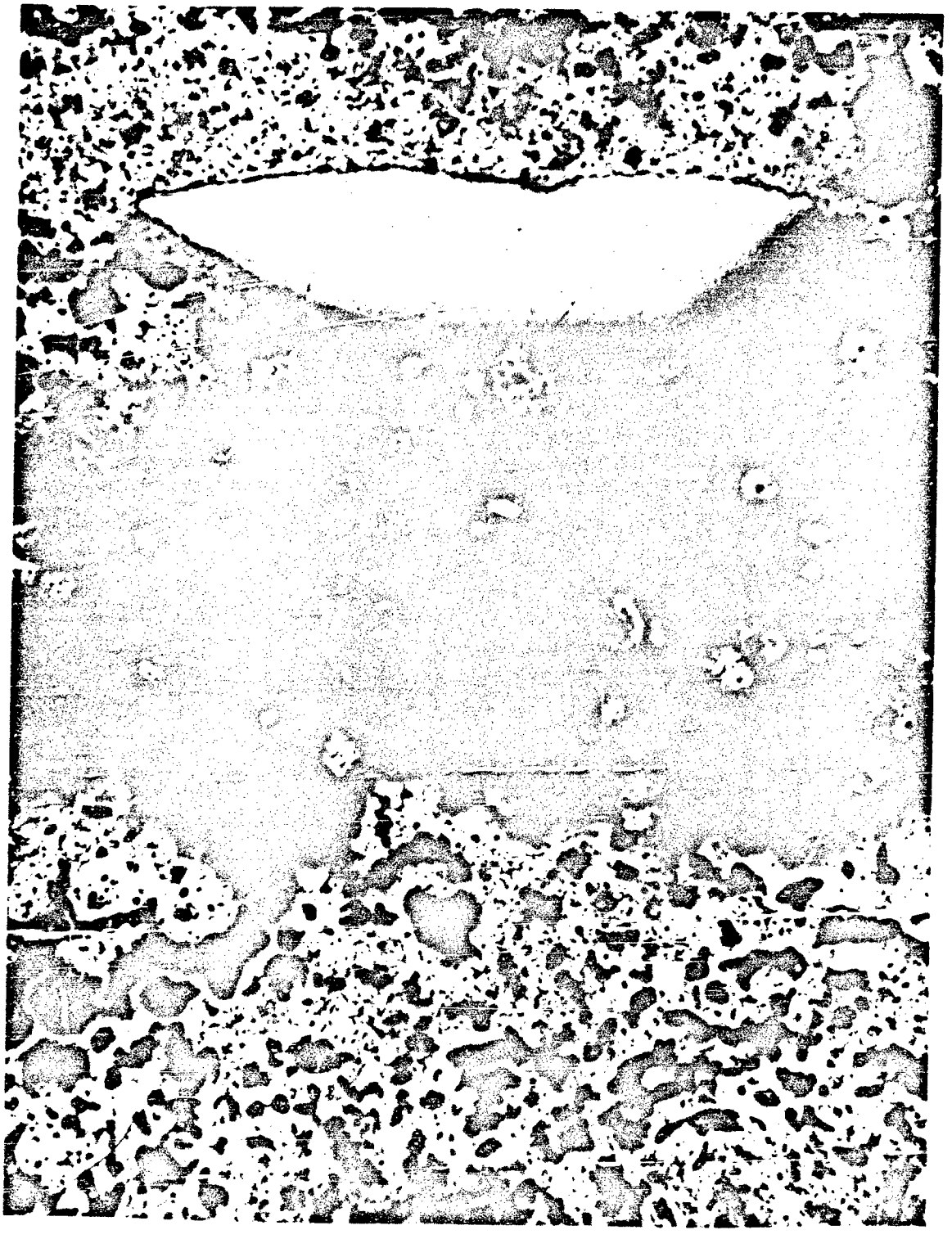

Figure 23. Negative Plate Containing .15% BC-840 at 168 Cycles. 200X.

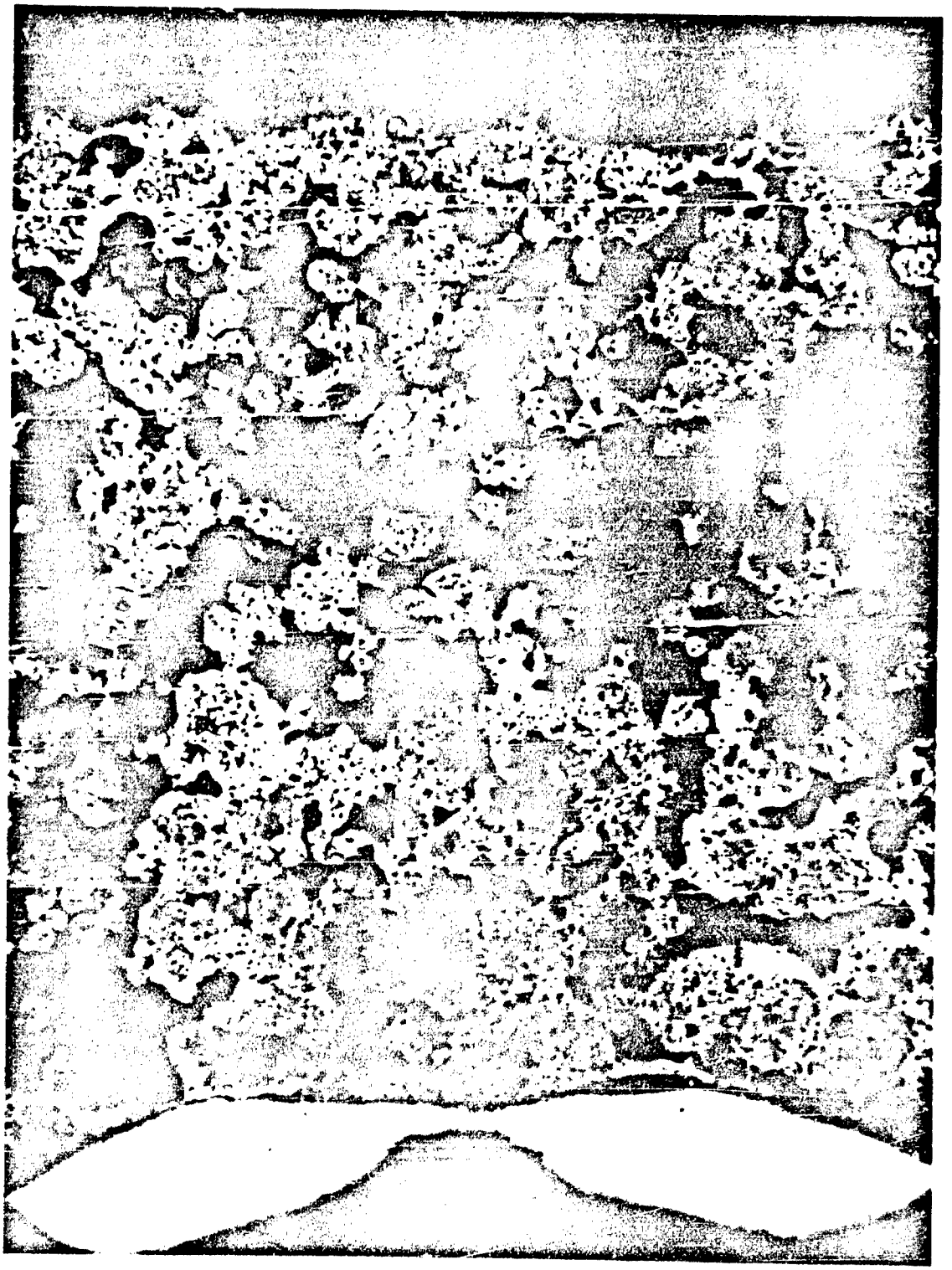

Figure 24. Negative Plate Containing 1% BC-840 at 144 Cycles. 200X.

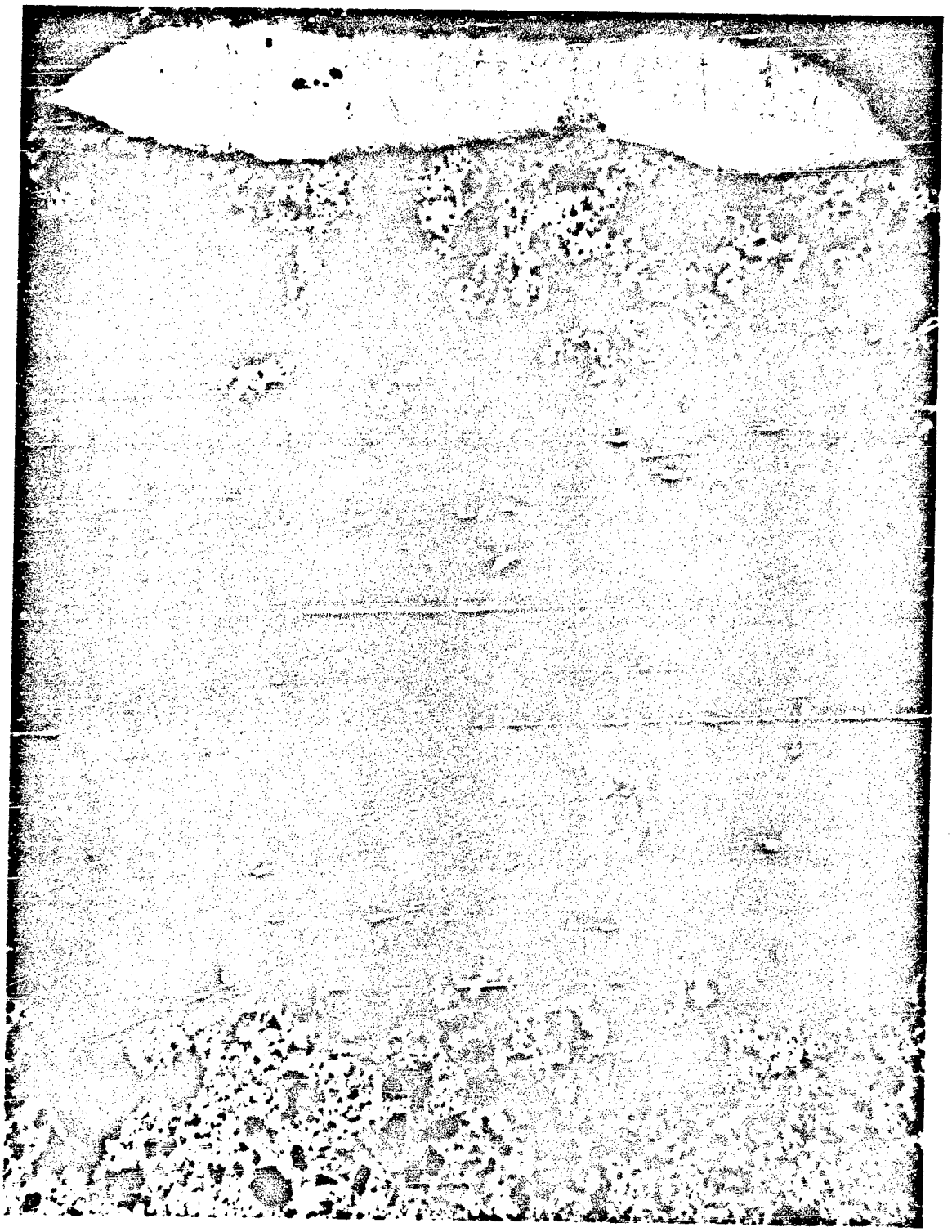

Figure 25. Negative Plate Containing .5% BC-610 at 168 Cycles. 200X (Control)

Figure 26. Negative Plate Containing .15% BC-610 at 76 Cycles at 40°F. 200X.

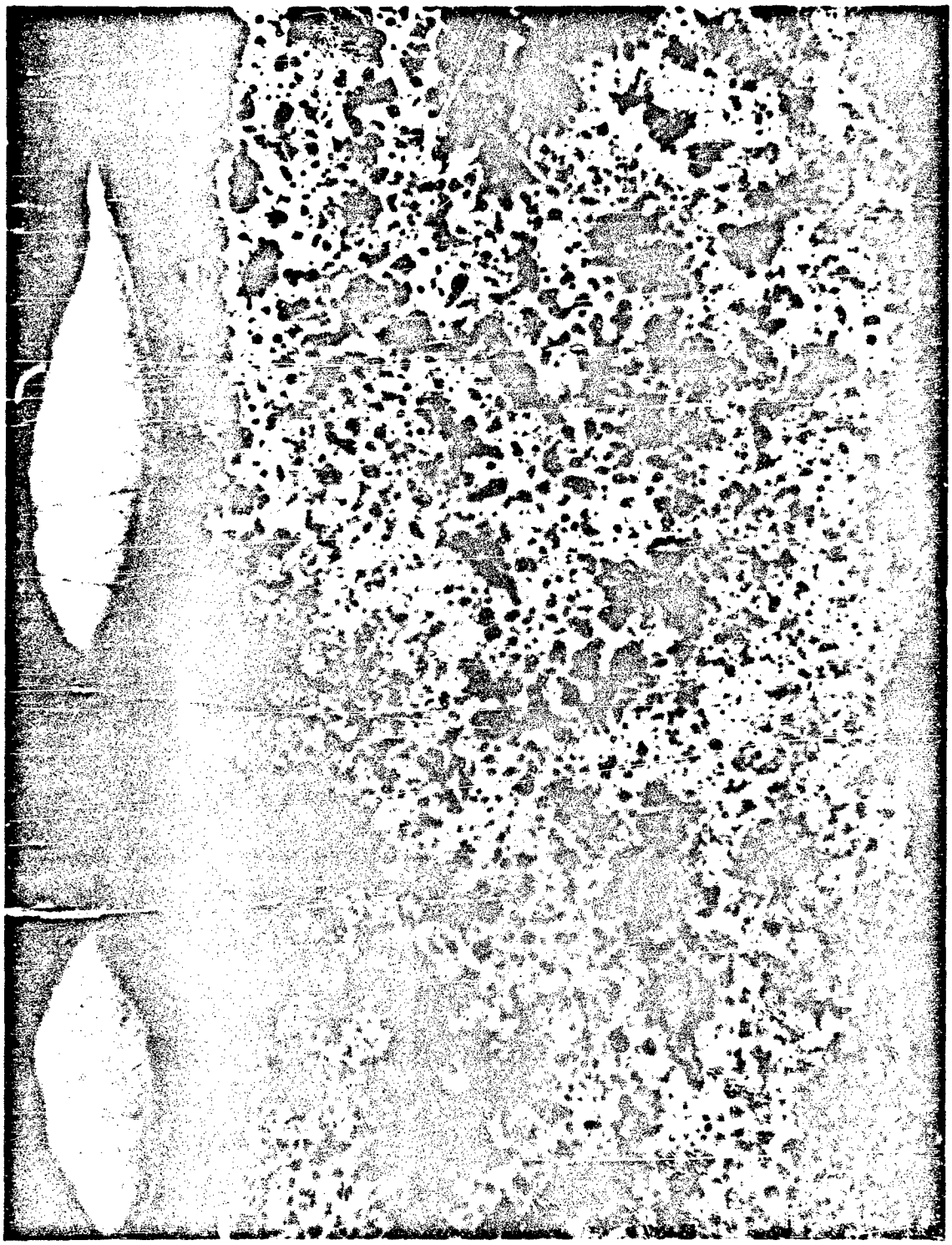

Figure 27. Negative Plate Containing .6% BC-610 at 52 Cycles at 40°F. 200X.

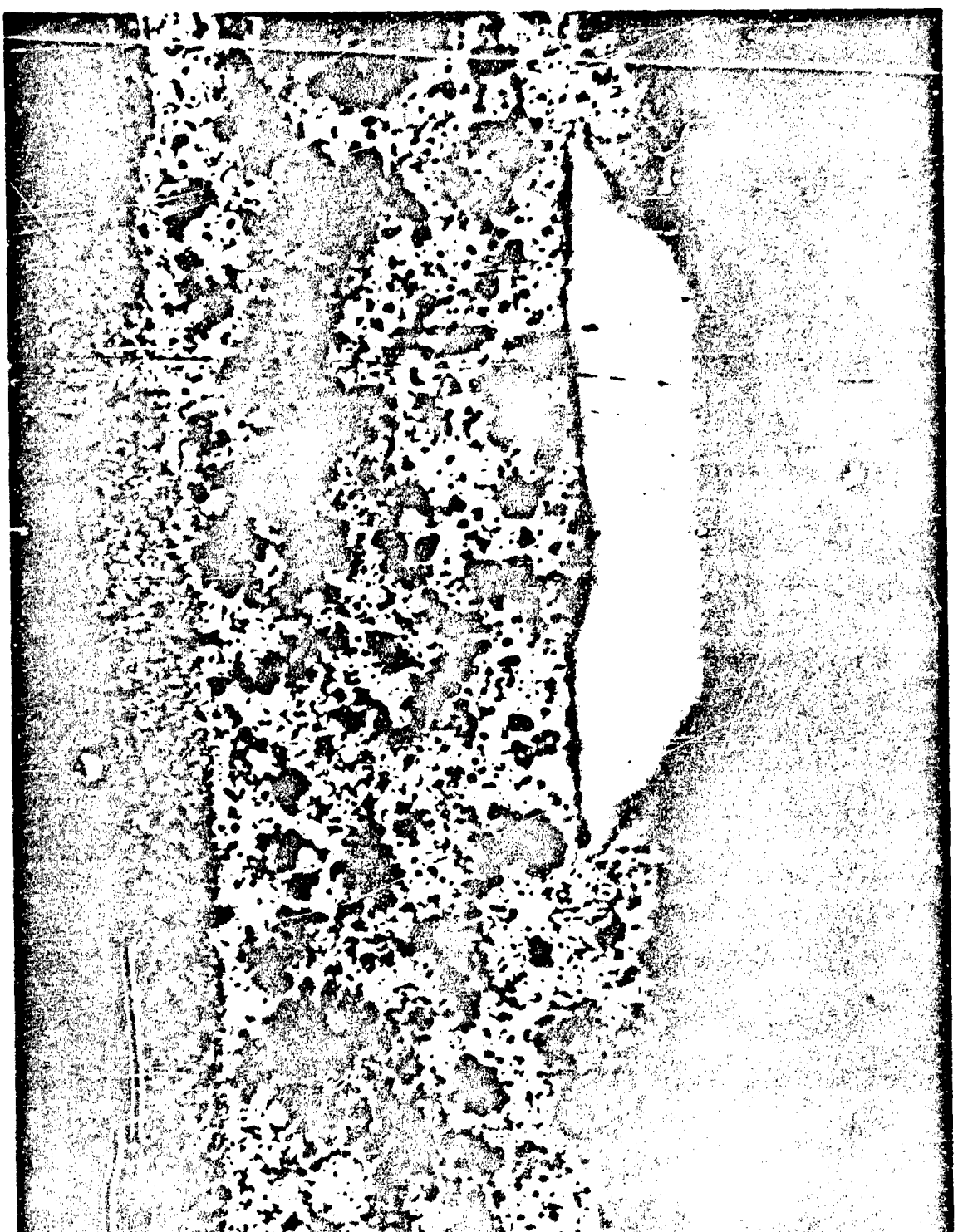

Figure 28. Negative Plate Containing 1% BC-610 at 58 Cycles at 40°F. 200X.

Figure 29. Negative Plate Containing .15% BC-610 at 110 Cycles at 100°F. 200X.

Figure 30. Negative Plate Containing .6% BC-610 at 121 Cycles at 100°F. 200X.

Figure 31. Negative Plate Containing 1% BC-61C at 124 Cycles at 100°F. 200X.

Figure 32. Negative Plate Containing .1% FC-95 at 150 Cycles. 200X.

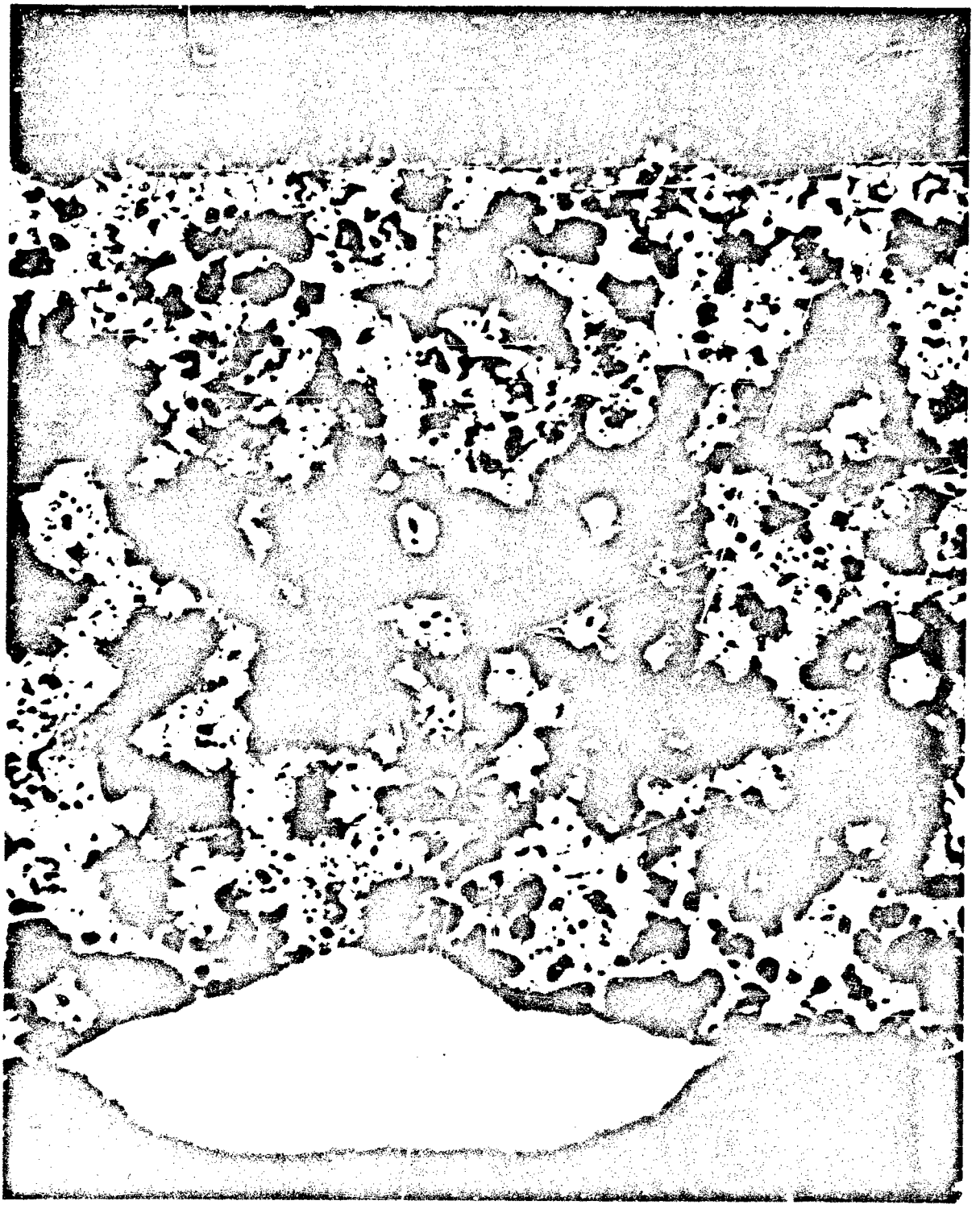

Figure 33. Negative Plate Containing .6% FC-95 at 152 Cycles. 200X.

Figure 34. Negative Plate Containing 1% FC-95 at 168 Cycles. 200X.

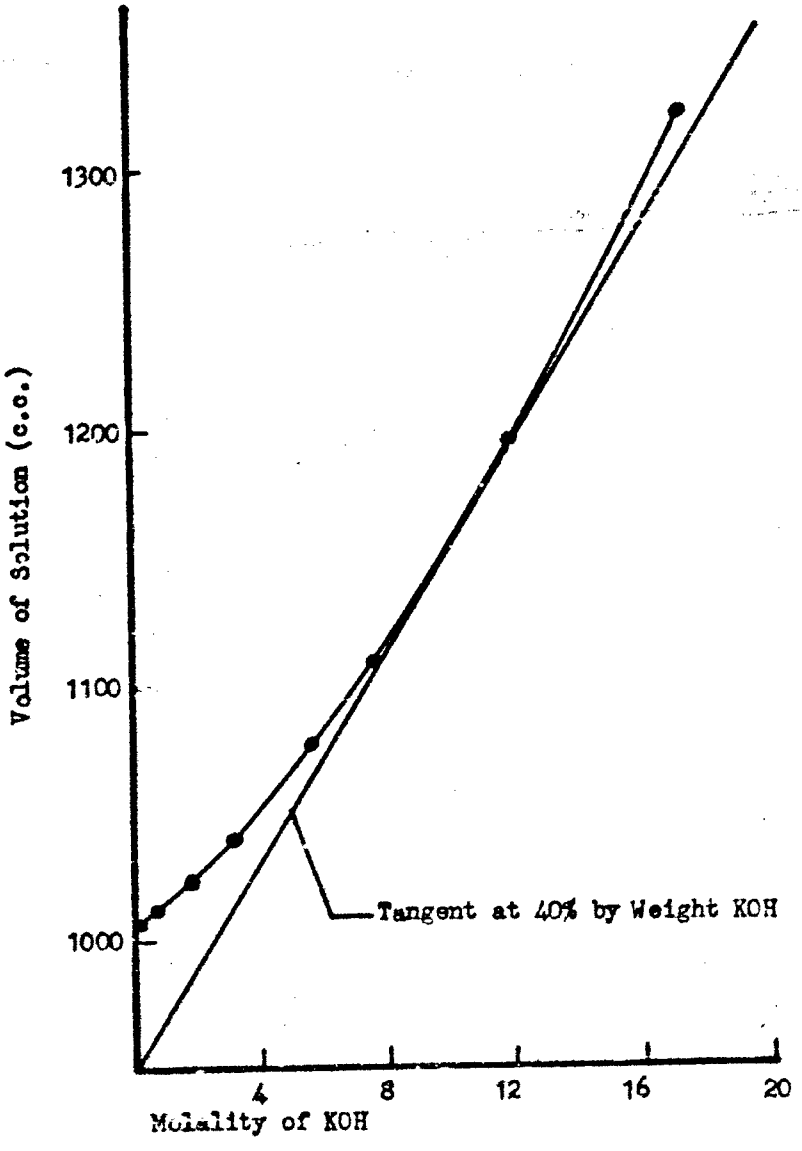

Figure 35. Volume vs. Molality KOH Solutions at 68°F.

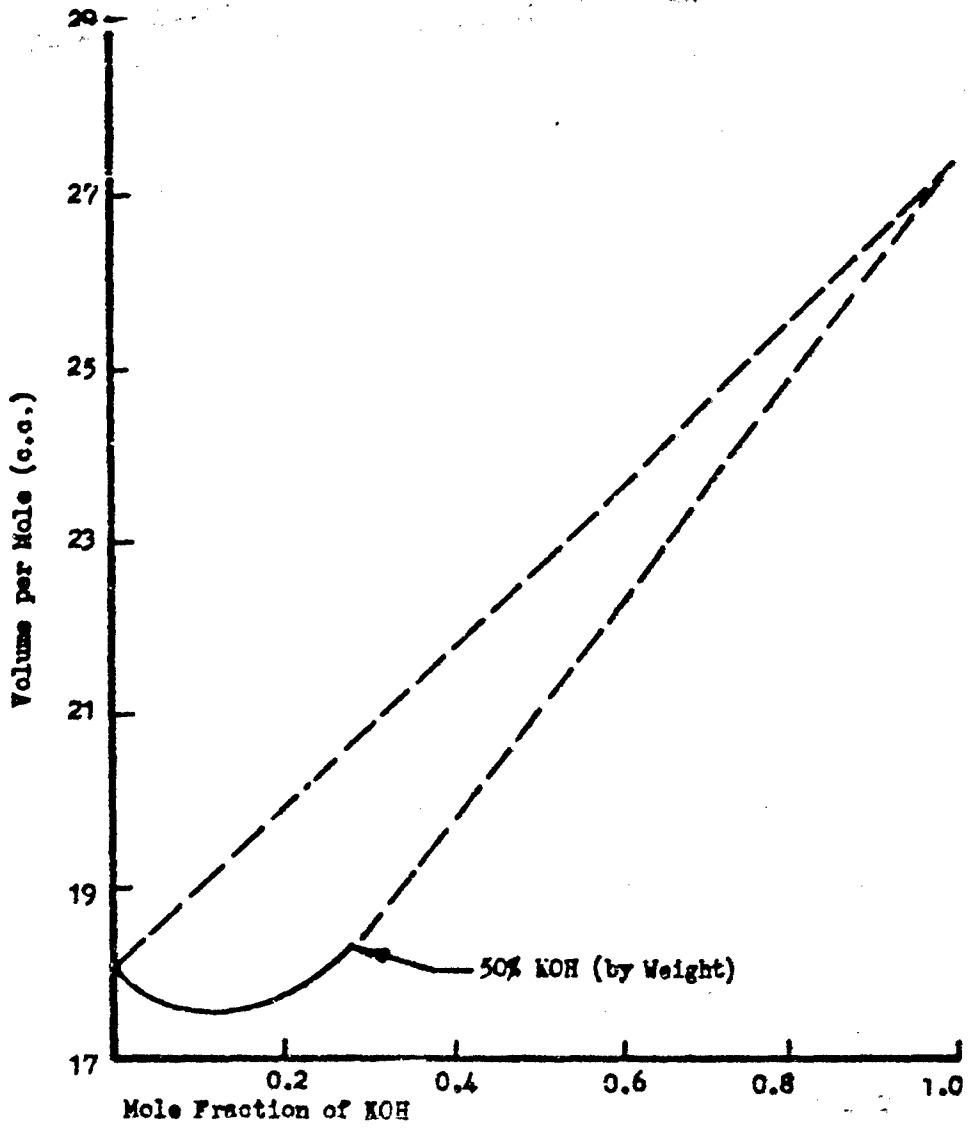

Figure 36. Illustrating Non-Ideality of KOH Solutions

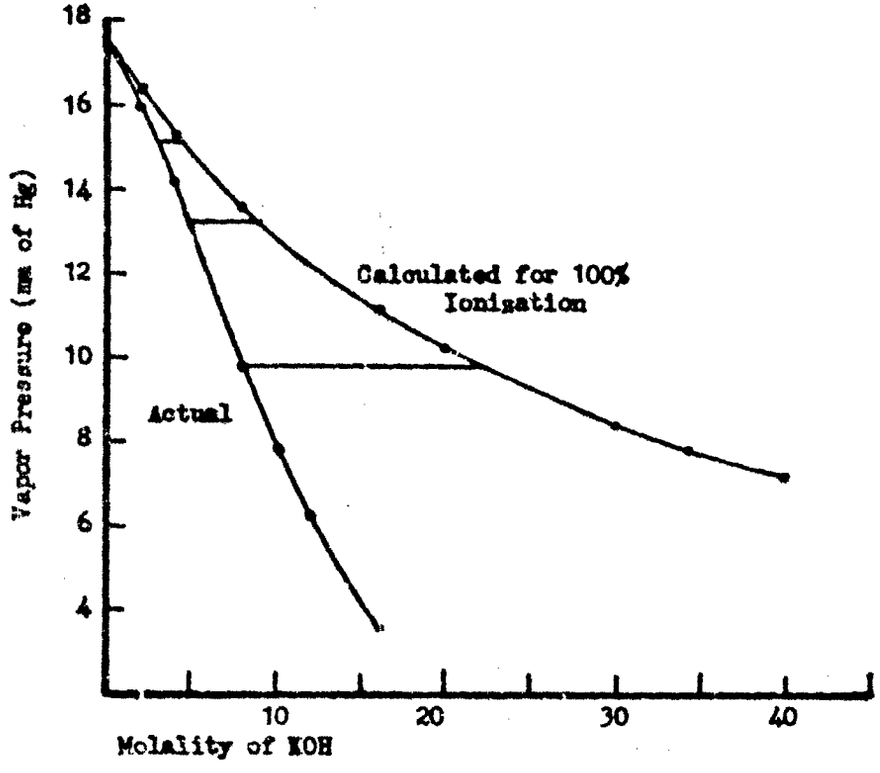

Figure 37. Vapor Pressure of Solutions of KOH. 68°F.

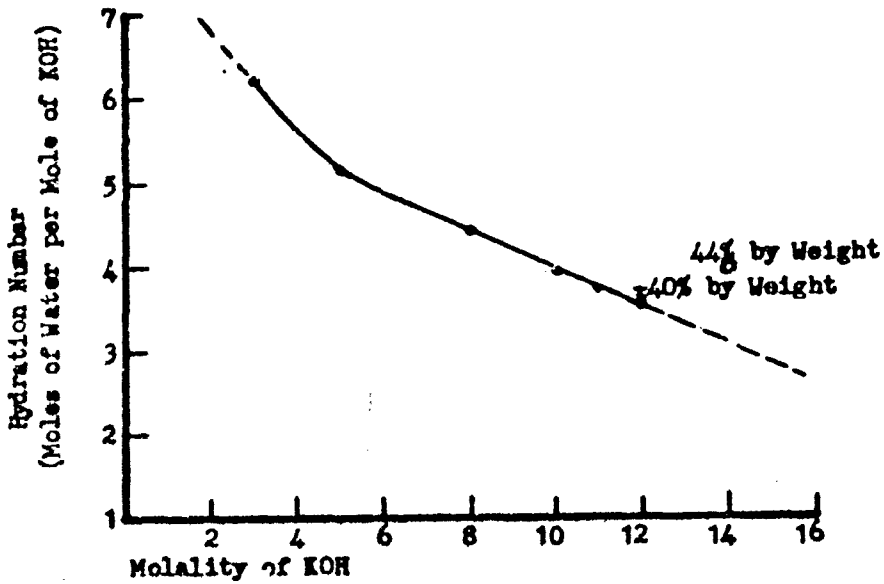

Figure 38. Hydration of [illegible] 68°F.

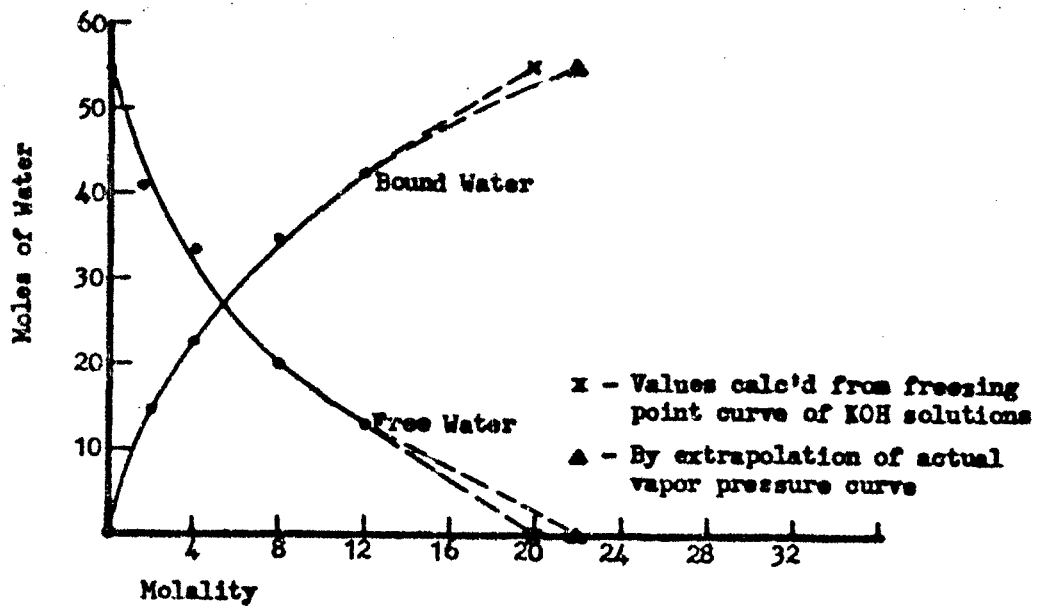

Figure 39. Bound and Free Water in KOH Solutions. 68°F.

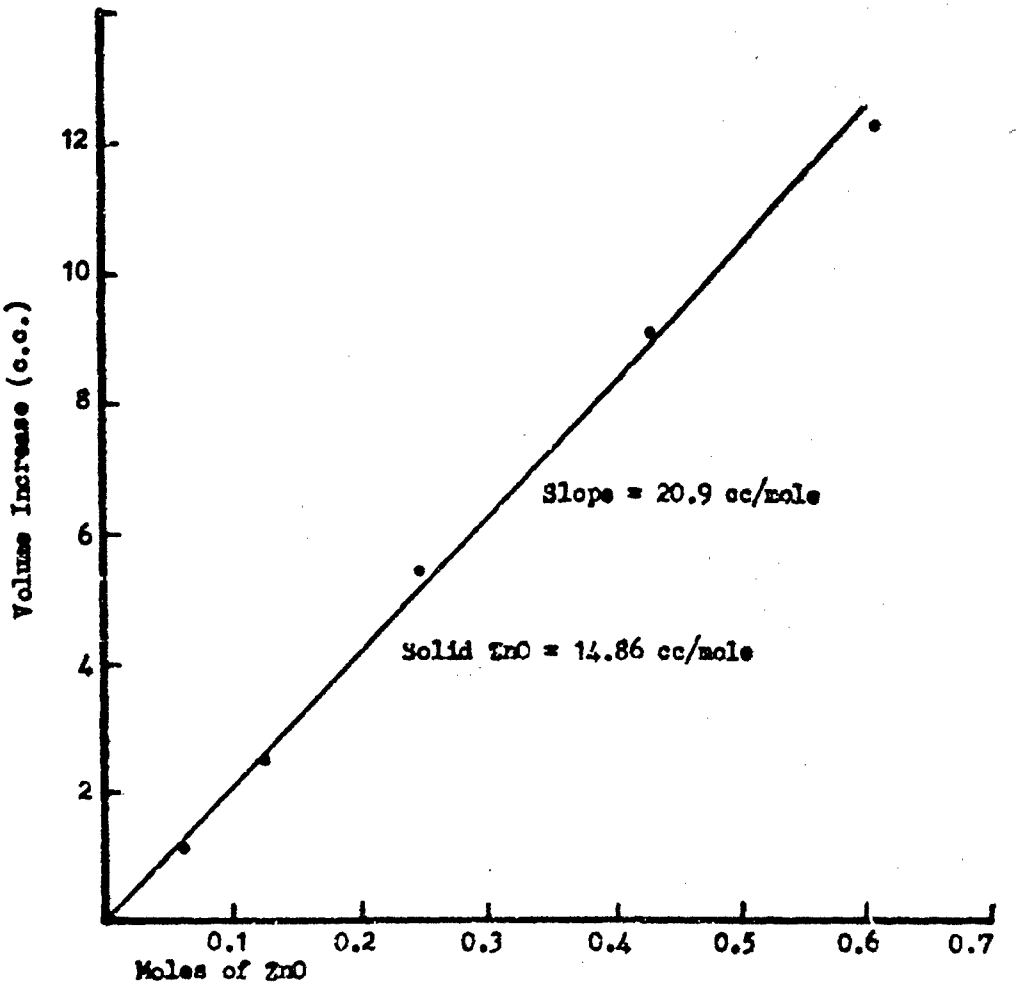

Figure 40. Volume Change of Solutions of ZnO in 45% KOH. 72°F.

Best Available Copy

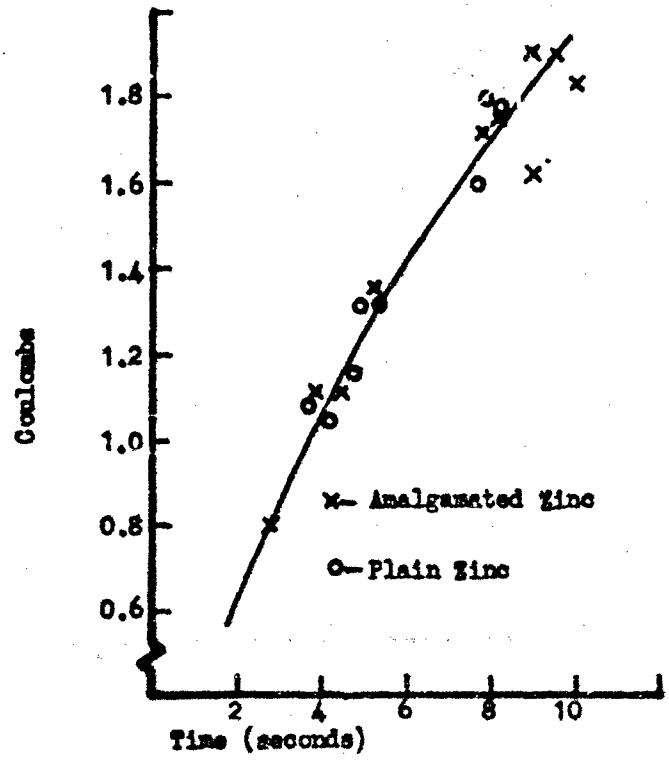

Figure 41. Time-to-Passivation vs. Coulombs Discharge on Sheet Zinc Electrodes Room Temperature. 10% KOH.

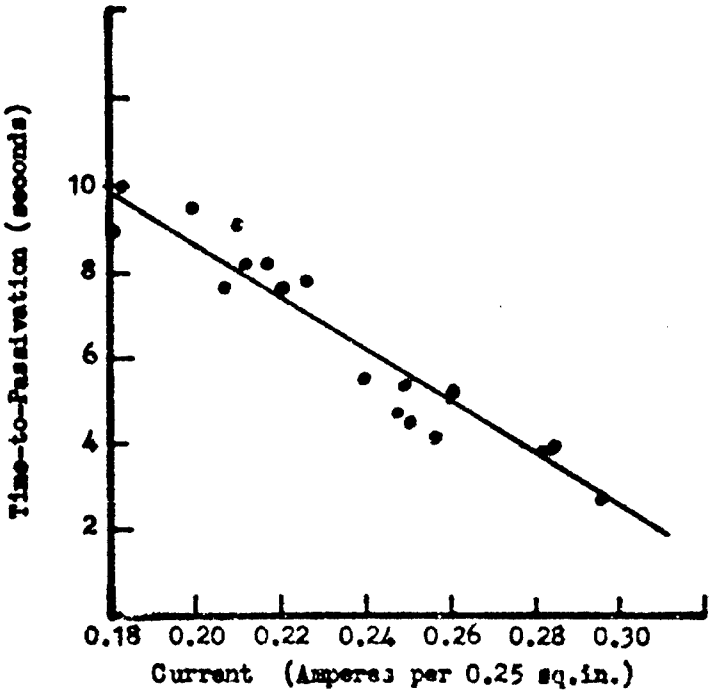

Figure 42. Time-to-Passivation vs. Current

APPENDIX I

A LITERATURE SURVEY ON THE SOLUBILITY OF ZnO IN OTHER DIVALENT METAL OXIDES AND OF $Zn(OH)_2$ IN OTHER DIVALENT METAL HYDROXIDES

In the search for a possible host lattice for ZnO and $Zn(OH)_2$, the only compounds considered are those containing a divalent cation. This limitation immediately eliminates compounds of the alkali metals, lanthanides, actinides, and other metals which do not normally show the +2 oxidation state.

The compound ZnO has a hexagonal (Wurtzite) lattice with the following cell parameters, a = 3.24 Å, c = 5.19 Å [1]. Among the commonly occurring metal oxides only beryilium oxide, BeO, has a hexagonal structure. Its lattice parameters are: a = 2.69 Å, c = 4.3 Å [2]. Even though the difference between these sets of parameters is somewhat greater than 15%, BeO and ZnO do appear to form a solid solution on which conductivity and X-ray diffraction measurements were made [3]. No other information on phase relationships between BeO and ZnO is available in the literature.

Diadochy, rather than isomorphism, is the primary criterion in solid solution formation, so that a hexagonal compound may form a solid solution with a non-hexagonal one if the ionic sizes are correct[4]. Substitution of one cation for another in a particular lattice is often possible if the difference in the ionic sizes is less than about 15%. Using this criterion and Pauling's

---

1. C. W. Bunn, Pr. phys. Soc., 47, 835 (1935).

2. W. M. Lehman and M. Haase, Z. Kryst., 65, 537 (1927).

3. I. D. Tretyak and M. A. Emchik, Pitannya Fiz. Tverd. Tila L'vivs'k Derzh. Univ., 1964, 80 (Ukrain).
C. A., 62: 12560f

4. B. Mason, Principles of Geochemistry, 2nd ed., J. Wiley and Sons, Inc., New York, 1958, p. 85.

empirical values for crystal radii[5], the following ions may be diadochic in oxide structures:

Zn	0.74 Å	Mn	0.80 Å
Co	0.74	Cr	0.84
Ni	0.72	Pd	0.86
Fe	0.76	Cu	0.69

This is born out also by the fact that in minerals the Zn ion is often replaced by Mn, Fe, Co, or Cu.

The crystal structures and cell parameters of the oxides of these metals are as follows:

CrO , probably cubic, parameters not determined[6]

MnO , cubic, a = 4.47 Å [7]

FeO , cubic, a = 4.27 Å [8]

CoO , cubic, a = 4.25 Å [9]

NiO , cubic, a = 4.17 Å [10]

CuO , monoclinic, a = 4.65, b = 3.41, c = 5.11 Å, β = 99°29' [11]

PdO , tetragonal, a = 3.02, c = 5.31 Å [12]

---

5. L. Pauling, The Nature of the Chemical Bond, 3rd ed., Cornell University Press, Ithaca, N. Y., 1960, p. 518.
6. H. Lux, L. Eberle, and D. Sarre, Ber., 97 (2), 503 (1964).
7. H. Ott, Z. Krist., 63, 222 (1926).
8. V. M. Goldschmidt, Ber., 60, 1285 (1927).
9. H. P. Walmsley, Phil. Mag., 7, 1101 (1929)
10. J. Brentano, Proc. Phys. Soc. London, 37, 184 (1925)
11. G. Tunell, E. Posnjak, and C. J. Ksanda, Z. Krist., 90, 120 (1935).
12. W. J. Moore, and L. Pauling, J.A.C.S., 63, 1393 (1941).

The compound CrO has not been well characterized. It is not affected by pure water but is readily oxidized by atmospheric oxygen [13]. The most stable and the most easily prepared appear to be the oxides of Co, Ni, Cu, and Pd.

No references were found in the literature (up to Dec., 1966) on solid solution formation between ZnO and CrO. ZnO does form solid solutions with the other six oxides listed above. In addition, ZnO forms solid solutions with BeO (see p. 1 of this report), and with MgO, CdO, and SnO.

Some aspects of the phase relations among these compounds are given in the following references:

14. R. Rigamonti, Gazz. Chim. Ital., 76, 474 (1946) C. A., 41, 71911

Formation of solid solutions of ZnO in MgO, NiO, CoO, MnO and CdO. Preparation, X-ray data, cell parameters, and limits of solubility are discussed.

15. R. Isomatsu, and S. Kitagawa, Doshisha Daigaku Rikogaku Kenkyu Hokoku, 5, (2), 67 (1964)

C. A., 62, 10167a

Phase diagram of the system ZnO-FeO is determined by X-ray diffraction.

16. J. Robin, Compt. Rend., 235, 1301 (1952)

C. A., 47, 47191

Preparation of mixed Co and Zn oxides, determination of phase diagrams.

17. E. Hayek, Monatsh., 66, 197 (1935)

C. A., 30, 39[1]

Mixed crystals of SnO with various oxides including ZnO are prepared by precipitation from solution.

---

13. H. Lux, and E. Pröschel, Z. anorg. Chem., 257, 73 (1948)

18. G. Natta, and L. Passerini, Gazz. Chim. Ital., 59, 139 (1929)
C. A., 25, 633
Formation of solid solutions among the oxides of Ca, Cd, Mn, Co, Ni, and Zn.

19. J. A. Hedvall, Z. anorg. allgem. Chem., 103, 249 (1918)
C.A., 13, 3098[5]
Formation of solid solutions of NiO with ZnO and other metal oxides.

20. H. Kedesdy, and A. Drukalsky, J.A.C.S., 76, 5941 (1954)
C.A., 49, 15599c
Formation of NiO-ZnO solid solutions, structure and X-ray data are given.

21. T. Ando, and R. Umemoto, Ceram. Abstr., 1952, 151 (in J. Am. Ceram. Soc., 35, no. 8)
C.A., 47, 6669g
Describes formation of ZnO-CoO solid solution from ZnO and $CoCO_3$ in a CO_2 atmosphere.

22. V. D. Balarev, Annuaire fac. sci.-phys. et math. Chemie, 47, 3 (1952)
C.A., 48, 7976e
Fusion of ZnO with CuO may indicate the existence of a eutectic in this system.

23. G. Yamaguchi, and H. Miyabe, Kogyo Kagaku Zasshi, 63, 562 (1960)
C.A., 57, 9278h
Composition and lattice constants are given for various solid solution phases in the ternary system ZnO-CoO-MgO.

The following references are less directly related to this problem but may be of interest:

24. V. P. Chalyi, and O. I. Shor, Ukrain. Khim. Zhur., 27, 7 (1961)
C.A., 55, 17325g
A thermographic study of hydroxide mixtures. Dehydration gives solid solutions of NiO and ZnO, depending on concentrations.

25. C. Frondel, Am. Mineral., 25, 534 (1940)

C.A., 35, 7111

Discusses exsolution growths of ZnO in MnO.

26. H. P. Rooksby, Trans. Brit. Ceram. Soc., 56, 581 (1957)

C.A., 52, 17871c

Distortion of the NiO structure by ZnO substitution.

27. O. Schmitz-Dumont, K. Brokopf, and K. Burkhardt, Z. anorg. allgem. Chemie, 295, 7 (1958)

C.A., 53, 1915g

Absorption spectra of solid solutions of CoO and ZnO.

Information available in the literature suggests only two possible host lattices for $Zn(OH)_2$, namely $Ni(OH)_2$ and $Co(OH)_2$. $Zn(OH)_2$ occurs at at least five different phases, two of which have been characterized rather well. The α-form is hexagonal, with lattice parameters a = 3.11 and c = 7.8 Å (28). The ε-form is rhombic with a = 5.16, b = 8.53, and c = 4.92 Å (29). $Co(OH)_2$ occurs in two forms. It is blue when freshly made, but changes to the more stable pink form on standing. It is slightly soluble in alkaline solutions, and is easily oxidized by atmospheric oxygen. $Co(OH)_2$ has a trigonal structure with a = 3.19 and c = 4.66 Å (30).

---

28. W. Feitknecht, Ang. Chem., 52, 202 (1939)

29. R. B. Corey, and R.W.G. Wyckoff, Z. Krist., 86, 8 (1933)

30. G. Natta and A. Reina, Atti Linc. Mem., 4, 51 (1926)

$Ni(OH)_2$ is more stable toward oxidizing agents. It also has a trigonal structure with a = 3.07 and c = 4.60 Å (31).

The following references deal with the phase relations between the hydroxides of An, Co, and Ni.

32. W. Feitknecht and W. Lotmar, Helv. Chim. Acta, 18, 1369 (1935)

C.A., 30, 2077[4]

Solid solution formation in mixed precipitates of Zn, Ni, and Co hydroxides. Structure and composition of crystals is given.

33. G. Natta and L. Passerini, Gazz. Chim. Ital., 58, 597 (1928)

C.A., 23, 1556

Discussion of solid solutions of $Zn(OH)_2$ with $Co(OH)_2$ and $Ni(OH)_2$.

34. Th. v. Hirsch, Z. Physik. Chem., 43, 227 (1964)

C.A., 63, 2451g

An investigation of coprecipitation and mixed crystal formation between Co and Zn hydroxide, and others.

35. W. Lotmar and W. Feitknecht, Z. Krist., 93, 368 (1936)

C.A. 30, 6260[2]

Changes in ionic distances in Zn, Ni, and Co hydroxide solid solutions.

Two miscellaneous references were found which deal with the phase relationships between ZnO and $Zn(OH)_2$.

36. G. F. Hüttig, and H. Möldner, Z. anorg. Chem., 211, 368 (1933)

C.A., 27, 3415.

A discussion of the relative stability of $Zn(OH)_2$ with respect to ZnO in H_2O.

---

31. G. Natta, Atti accad. Lincei, 2, 495 (1926)

37. R. Scholder, and G. Rendrich, Z. anorg. allgem. Chem., 247, 76 (1939)

C.A., 33, 5271[9]

Phase relations in the system of $ZnO-Na_2O-H_2O$.

APPENDIX II

PREPARATION AND CHARACTERIZATION OF SPECIAL ZINC OXIDES FOR EVALUATION IN SILVER OXIDE-ZINC SECONDARY BATTERIES

Purchase Order D-R115475
Under Contract No. AF33(615)-3487

PREPARATION AND CHARACTERIZATION OF SPECIAL ZINC OXIDES FOR EVALUATION IN SILVER OXIDE-ZINC SECONDARY BATTERIES

Second Quarterly Technical Progress Report

Covering the Period

15 January 1967 to 15 April 1967

Dated

19 April 1967

Prepared by

D. O. Carpenter

G. E. Snow

FOREWORD

This report was prepared by The New Jersey Zinc Company, Palmerton, Pennsylvania on Delco-Remy Division of General Motors Corporation Purchase Order D-R115475 under Air Force Contract No. AF33(615)-3487. The work was directed by Drs. C. E. Barnett and L. J. Reimert.

NOTICE

Foreign announcement and distribution of this report is not authorized. Release to the Clearinghouse for Federal Scientific and Technical Information, CFSTI (formerly OTS) is not authorized. The distribution of this report is limited because it contains technology identifiable with items on the Strategic Embargo Lists excluded from export or re-export under U. S. Export Control Act of 1949 (63STAT.7), as amended (50 USC APP 2020.2031), as implemented by AFR 400-10.

This report is being published and distributed prior to Air Force review. The publication of this report, therefore, does not constitute approval by the Air Force of the findings or conclusions contained herein. It is published for the exchange and stimulation of ideas.

TABLE OF CONTENTS

LIST OF TABLES

LIST OF FIGURES

V. Appendix - Electron Micrographs

ABSTRACT

The properties of the initial zinc oxide used to fabricate the zinc electrode may substantially affect the performance of silver oxide-zinc secondary batteries. The special zinc oxides prepared will allow investigation of the effect of surface area (fine particle size) of wet process zinc oxide, particle morphology of precipitation process zinc oxides, high electrical conductivity of doped French Process zinc oxides and the effect of a variety of intentionally added metallic cation impurities.

I. Introduction

The objective of this project is to prepare and characterize a variety of zinc oxides for evaluation (by Delco-Remy) in silver oxide-zinc secondary batteries. The samples prepared during the first quarter permitted investigation of the effects of particle size of nodular French Process zinc oxides (0.13 μ to 1.02 μ), particle morphology as represented by a highly acicular American Process zinc oxide, and the high surface area (20 to 33 m^2/g) of wet process zinc oxides prepared by thermal decomposition of a basic zinc carbonate. Second quarter work has been directed at preparation and characterization of samples covering the following possible variables in electrode performance:

1. Surface area. A basic zinc carbonate type zinc oxide with 50 m^2/g surface area was prepared, that is, higher than the earlier 33 m^2/g sample.

2. Particle morphology of precipitation process zinc oxides. Nodular and acicular zinc oxides were prepared by precipitation from zinc chloride solutions.

3. Impurities. French Process zinc oxides were doped with small amounts of Zn, Cu, Sn, Mn, Fe, Pb, Cd, or As.

4. Electrical conductivity. French Process zinc oxides with 10^6 to 10^8 higher than normal electrical conductivity were prepared by doping with trivalent metal cations (Al and In).

A brief discussion of some of the factors involved in addition of impurities to zinc oxide is given below.

Zinc oxide is a well-known n-type (excess electron) semiconductor. The excess electrons arise because the usual preparation

techniques yield a zinc oxide non-stoichiometric in the direction of excess zinc. The excess zinc, occupying interstitial lattice positions, ionizes to yield free or quasi-free electrons with significant lifetimes and mobilities. The concentration of free electrons can be changed by incorporating impurities in the zinc oxide lattice. Addition of trivalent metal cations, for example, Al or In, increases the free electron concentration. The structure of zinc oxide is close-packed hexagonal but, since the zinc and oxygen atoms occupy only 44% of the volume, relatively large (0.95 A) open spaces are available for accommodation of impurities. Impurity promoters of ZnO are divided into the following two groups:

1. Intracrystalline - impurities with ionic radius approximately 0.6 to 0.9 A which are internal to the crystalline lattice. Such materials give rise to solid solutions.

2. Intercrystalline - impurities are external to the crystalline lattice.

Such classifications can not be regarded as an absolute rule because intra- or intercrystalline occupancy of positions will be at least partially dependent on the preparation procedure.

A relatively common method for impurity additions involves preparation of an intimate blend of an oxide of the dopant with the zinc oxide followed by calcination. This is frequently a preferred procedure when addition of anion impurities is to be avoided. In some cases, thermally decomposable dopant oxalates or carbonates are also used.

II. Sample Characterization Tests

All samples are characterized by the following tests: (1) air permeability particle size, (2) nitrogen adsorption surface area, (3) electron micrographs, (4) qualitative spectrographic and, where necessary, chemical analysis. See the First Quarterly Report for a description of these tests.

In the case of the Al- and In-doped samples, changes in electrical conductivity were measured by a "Dry Powder Resistivity" (DPR) test developed at NJZ. In this test the ZnO powder is compressed in a glass tube and the resistance measured with an electrometer. Resistivity is computed from the sample dimensions and can be in the range of from 10^1 to 10^{10} ohm-cm. Factors such as compacting procedure, temperature, and humidity are important variables, especially for high resistivity samples. The measurement is a satisfactory quality control guide for high conductivity zinc oxides.

III. Description of Samples

A. Wet Process Zinc Oxide from Basic Zinc Carbonate

A third sample of wet process oxide (243-67-2) was prepared by the basic zinc carbonate method, as described in the First Quarterly Technical Progress Report (15 October 1966 to 15 January 1967). In order to obtain a finer particle size the calcination temperature was reduced to 310°C., while the time was increased to 4 hr. The characterization data are given in Table I, and the electron micrograph is shown in Figure 1.

In addition to sample characterization tests previously described, the particle size of this sample was measured by the method of X-ray diffraction line broadening. This method involves the measurement of the width of the lines in the X-ray diffraction pattern, and then estimating the particle size from the Scherrer formula. For this sample the estimated size was 0.018 μ. Air permeability particle size measurements are not too satisfactory for very fine particle samples. Hence the 0.018-μ line broadening size is probably more representative of the actual size than the 0.025-μ air permeability value.

B. Wet Process Zinc Oxide from Zinc Chloride

Samples of wet process ZnO were prepared by the reactions of $ZnCl_2$ with NaOH, KOH, and NH_4OH. The NaOH and KOH reaction products (Samples 243-71-1 and 243-75-1, respectively) are fine nodular oxides, with NaOH yielding the smaller particle size. The NH_4OH reaction product (Sample 243-79-1) is acicular.

The NaOH and KOH reactions were carried out by adding a solution of 5.4-M reagent grade $ZnCl_2$ to a 6.8-M solution of the base at 100°C. under moderate agitation. Two mols of base were used per mol of $ZnCl_2$ added. The addition time was 4 hr. for the NaOH reaction and 3 hr. for the KOH. The products were washed by reslurrying in distilled water to remove the residual chloride and dried in air at 110°C. The final dry cake was micropulverized.

No detailed conditions for the $ZnCl_2$ + NH_4OH reaction are presented, since this is considered proprietary information.

The characterization data are given in Table I, and the electron micrographs are shown in Figures 2, 3, and 4.

TABLE I

Wet Process Zinc Oxides

Sample No.	243-67-2	243-71-1	243-75-1	243-79-1
Method of Preparation	Basic Zinc Carbonate	$ZnCl_2$ + NaOH	$ZnCl_2$ + KOH	$ZnCl_2$ + NH_4OH
Air Permeability Particle Size	0.025 μ	0.092 μ	0.155 μ	0.155 μ
N_2 Adsorption Surface Area	51.0 M^2/G	18.3 M^2/G	10.5 M^2/G	7.1 M^2/G
CO_2 Content	0.34%	--	—	—
Cl_2 Content	—	0.13%	0.11%	0.43%
Qualitative Spectrographic Analysis				
Zn	vs	vs	vs	vs
Si	xf	w-m	w	w-m
Pb	vf	vf-f	vf-f	vf
Cd	xf	vf	vf-f	xf
Al	xf-vs	vf	vf	vf
Fe	xf	xf	xf	xf-vf
B	vf	vf-f	vf	vf
Cu	xf	vf	vf-f	vf
Mg	Trace	xf-vf	vf	f
Sb	Trace	xf	xf	vf
Ti	f	--	f	f
Mn	Trace	xf	xf	xf-vf
Ca	--	f	vf	—
Cr	--	xf	xf	xf
Ni	--	xf	xf	—
Particle Size by X-ray Line Broadening	0.018 μ			

C. Al- and In-Doped High Conductivity Zinc Oxides

The general methods for development of high conductivity in zinc oxide were described in the Introduction. The specific procedure for doping with Al^{+3} is described in U. S. Patent 3,089,856 by H. M. Cyr and M. S. Kanovic, assigned to NJZ, and issued May 14, 1963. Details of the procedure for doping with In^{+3} are considered proprietary information.

Characterization data for these samples are given in Table II and Figures 5 and 6. Note that normal French Process zinc oxides have "Dry Powder Resistivities" of the order of 10^{10} ohm-cm. The particle size of the Al-doped sample, No. 243-41-1 (1.02 μ), makes it particularly appropriate for comparison with a first quarter sample of reheated zinc oxide (No. 243-27-1) having a particle size of 1.02 μ.

TABLE II

Al- and In-Doped High Conductivity ZnO

Sample No.	243-41-1	243-45-1
Technical Plan Item No.	15	16
Amount and Type of Impurity	0.30% Al*	0.48% In
Dry Powder Resistivity	9.4×10^2 Ω-cm	3.5×10^3 Ω-cm
Air Permeability Particle Size	1.02 μ	2.3 μ
N_2 Adsorption Surface Area	1.3 m^2/g	0.36 m^2/g
Qualitative Spectrographic Analysis - Element		
Zn	vs	vs
Si	vf	vf
Pb	vf	f
Cd	xf-vf	xf-vf
Al	m-m	vf
Fe	vf	xf
B	vf	vf
Cu	vf	xf-vf
Mg	xf	xf
Sb	Trace	Trace
Ti	—	—
Ge	—	—
Sn	—	f
Mn	—	Trace
Ag	—	—
Ga	—	—
Bi	—	—
In	—	m-s

*Residual Cl^- content - 0.02%

D. Impurity-Doped Samples

1. Fe, Cd, Cu, Sn, Mn, Pb

The impurities were added to a French Process zinc oxide by a procedure involving intimate admixing of an oxide of each specific impurity, followed by calcination for 1 hr. at 600°C. in air. Metallic oxides were selected in order to avoid introduction of anion impurities. The 600°C. calcination temperature was used so as not to cause too large an increase in the particle size of the zinc oxide. Equal mole percentages of Fe, Cd, Cu, Sn, Mn, and Pb, rather than weight percentages, were added. Since each sample contains approximately equal numbers of impurity ions, intercomparisons, as well as comparisons with high purity zinc oxide, are possible.

2. As

Using the preceding procedure, a sample was doped with As at a level more than adequate to prevent growth of acicular particles in American Process ZnO manufacture. It was thought that this might reduce dendritic growth in zinc electrodes.

3. Zn

The excess interstitial zinc content of a French Process ZnO was increased from about 0.002 wt. % to 0.009 wt. % by calcination for 1 hr. at 800°C. in an atmosphere of 5% hydrogen - 95% nitrogen. The methods for quantitative determination of excess zinc in zinc oxide are not very satisfactory. The method used at NJZ is described in a paper by Secco and Moore (J. Chem. Phys. 26, 942 (1957)). Since excess zinc in zinc oxide tends to produce discoloration (grey), in the absence

of high levels of foreign impurities color is something of a qualitative measure of the excess zinc content.

Particle size and chemical analysis data for the impurity-doped samples are given in Table III. Complete characterization information will be provided in a later report.

TABLE III

Characterization Data for Impurity-Doped Zinc Oxides

Technical Plan Item No.	--	18	19	20	21	22	23
Sample No.	243-83-1*	243-87-1	243-91-1	243-95-1	243-99-1	243-103-1	243-107-1
Impurity	--	Sn	Cd	Cu	Fe	Mn	Pb
Wt. % Impurity	--	0.13	0.13	0.081	0.07	0.089	0.25
Mole % Impurity	--	0.09	0.1	0.1	0.1	0.13	0.1
Air Permeability Particle Size	0.43 μ	0.45 μ	0.44 μ	0.44 μ	0.45 μ	0.43 μ	0.42 μ

*Base ZnO calcined under same conditions as Items 18-24 but no impurities added.

IV. Future Program

Characterization data for all the zinc oxides covered in the technical plan will be completed. For comparison with the zinc oxide samples, two samples of zinc dust and a sample of flaked (small flattened particles) zinc dust will be prepared. Selection of appropriate future samples will depend on the results of electrode evaluations of the samples prepared to date.

V. Appendix

Electron micrographs at 25,200X magnification are shown for the previously described samples in Section III, A-C. Micrographs for the doped samples will be submitted with the Third Quarterly Report.

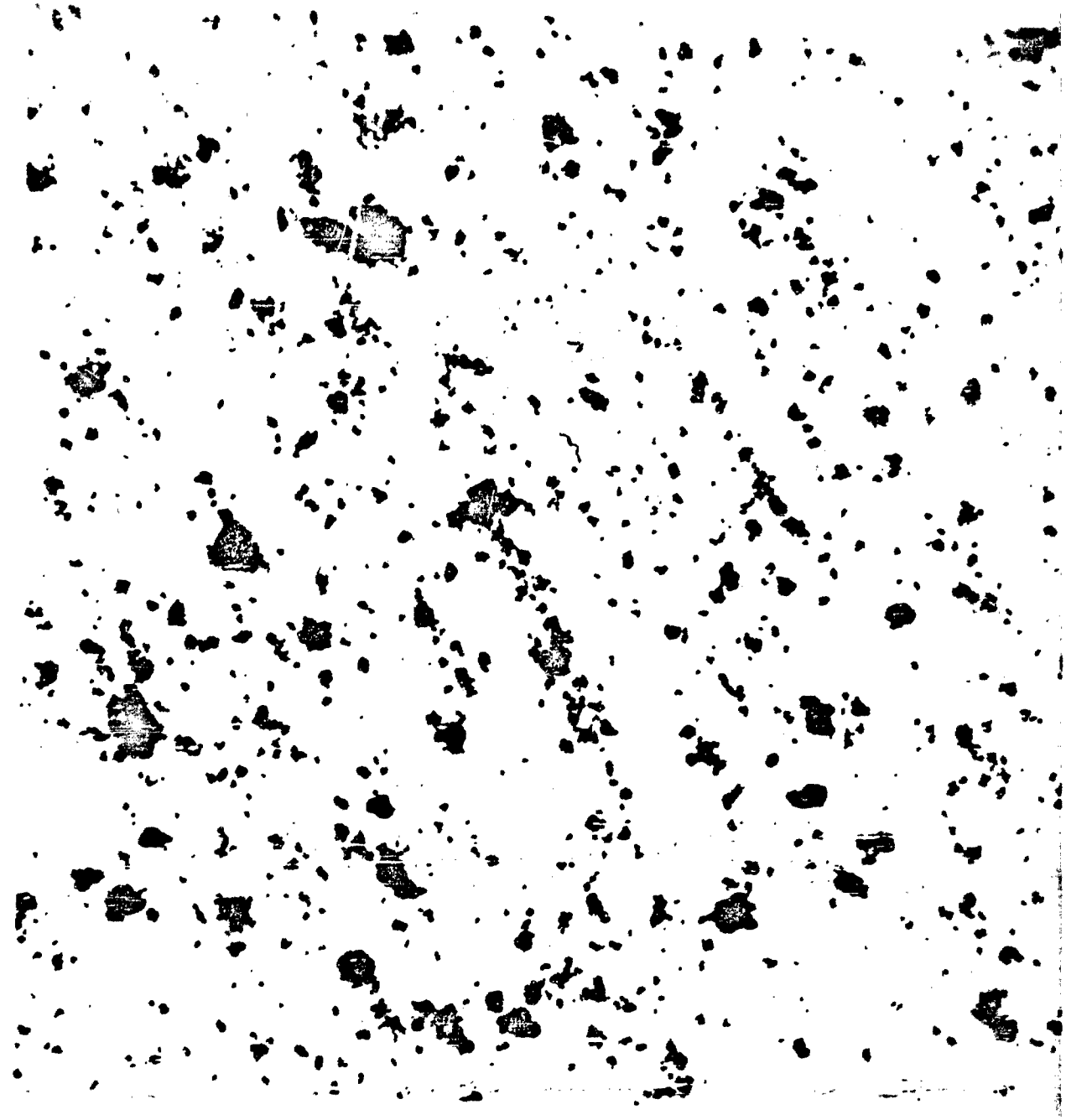

Figure 1. Sample No. 243-67-2 - High Surface Area Wet Process ZnO
Particle Size = 0.025 μ
Surface Area = 51 M^2/G
Magnification = 25,200X

Figure 2. Sample No. 242-71-1 - Precipitation Process ZnO ($ZnCl_2$ + NaOH)
Particle Size = 0.092 μ
Magnification = 25,200X

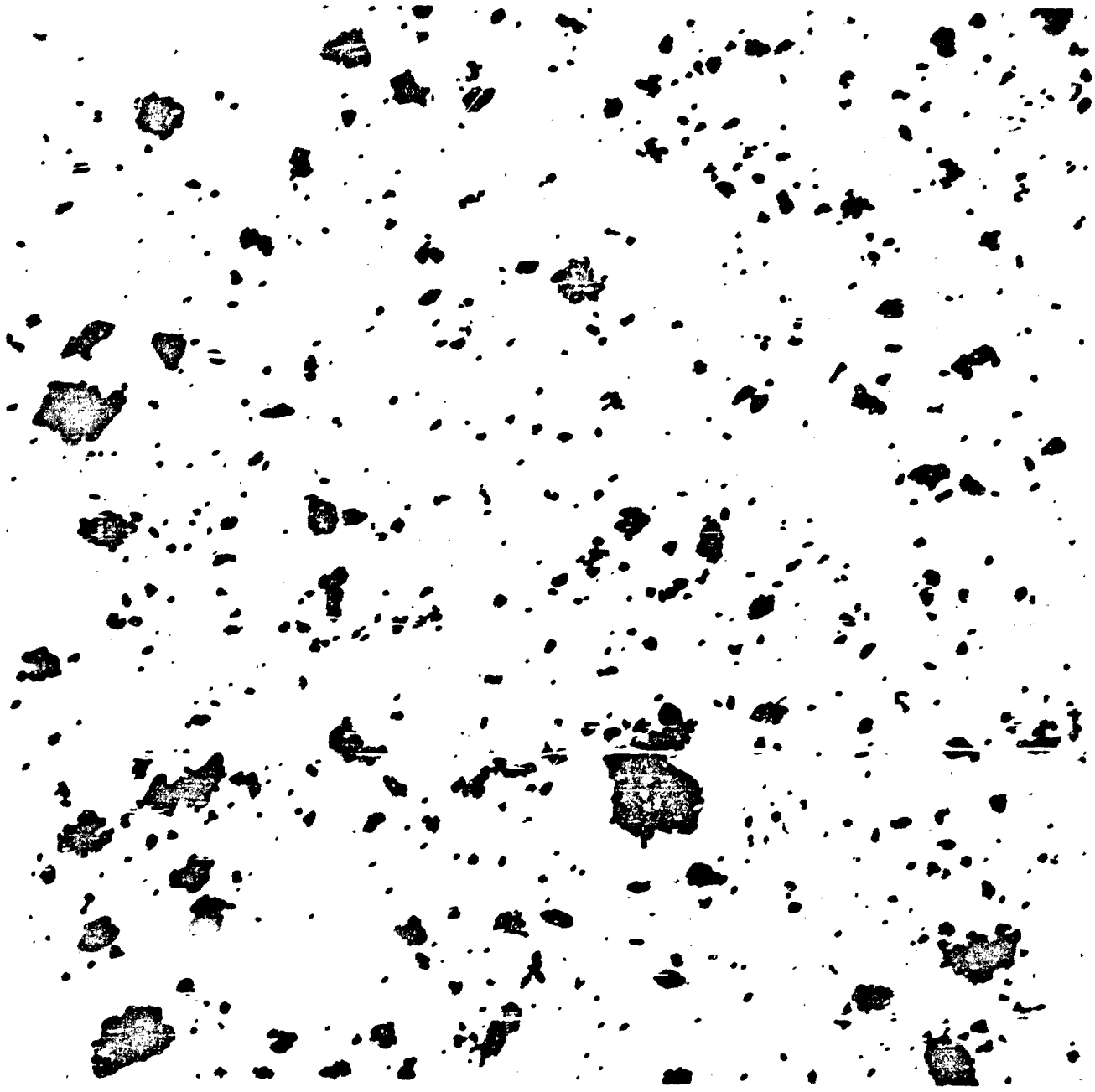

Figure 3. Sample No. 243-75-1 - Precipitation Process ZnO ($ZnCl_2$ + KOH)
Particle Size = 0.16 μ
Magnification = 25,200X

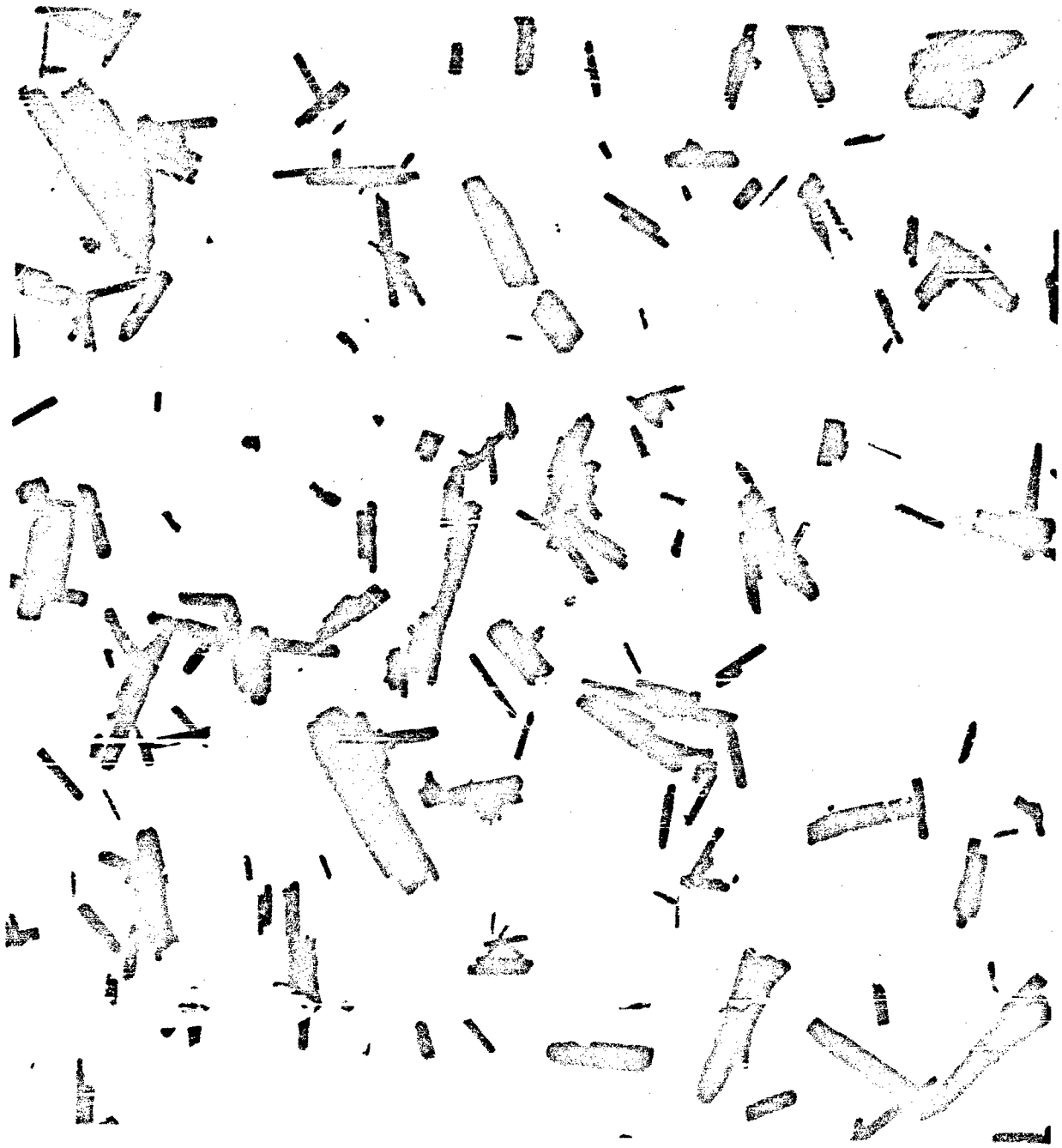

Figure 4. Sample No. 243-79-1 - Acicular Precipitation Process ZnO
($ZnCl_2$ + NH_4OH)
Particle Size = 0.16 μ
Magnification = 25,200X

Figure 5. Sample No. 243-41-1 - High Conductivity Al-Doped ZnO
Particle Size = 1.02 μ
Magnification = 25,200X

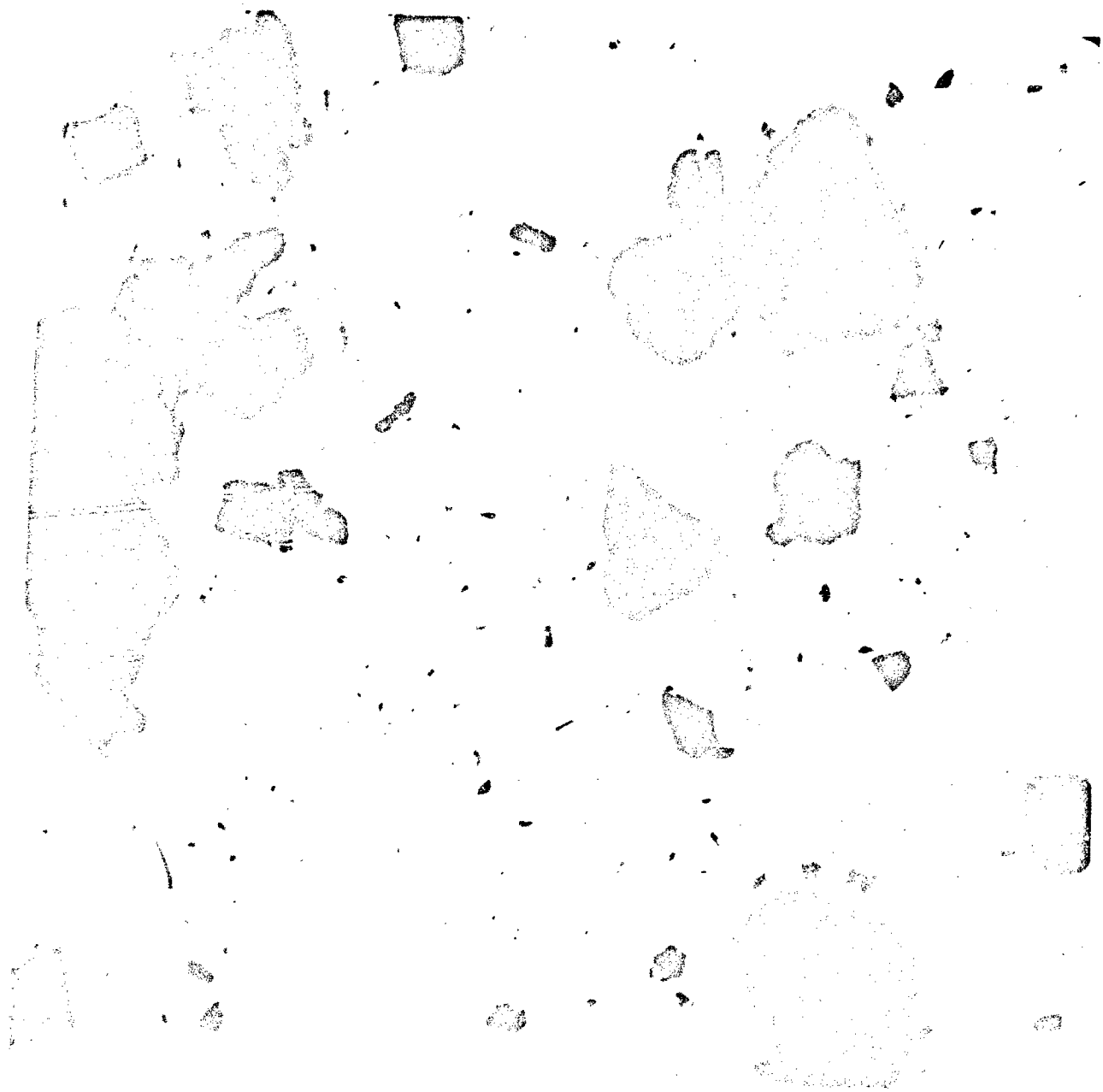

Figure 6. Sample No. 243-45-1 - High Conductivity In-Doped ZnO
Particle Size = 2.3 μ
Magnification = 25,200X

APPENDIX III

ADSORPTION OF ORGANIC MATERIALS ON ZINC ELECTRODES

ADSORPTION OF ORGANIC MATERIALS ON ZINC ELECTRODES

Second Quarterly Technical Progress Report

Covering the Period

15 January 1967 to 15 April 1967

Purchase Order D-R 120111

Under Contract AF 33(615)-3457

Prepared by

Dewitt A. Payne

Keith B. Prater

Allen J. Bard

The University of Texas

Austin, Texas

ADSORPTION OF ORGANIC MATERIALS ON ZINC ELECTRODES

Introduction

The chronocoulometric and the differential capacity apparatus were further tested by studying the adsorption of n-butyl alcohol on a mercury electrode from 0.1 N KCl. Work was then started on the Zn, $ZnO_2^=$ system in NaOH and KOH, with both mercury electrodes and zinc electrodes. The zinc electrodes used were both the stationary type and rotating disk type. The kinetics of the Zn, $ZnO_2^=$ system was studied to some extent.

Experimental

The techniques used in studying alcohol adsorption on mercury were the same as those mentioned in the last quarterly report. 5M NaOH and KOH were used as supporting electrolyte in the chronocoulometric study of the Zn system. There appeared to be no significant difference between the two electrolytes as long as the molarity of the two was the same. 5M was chosen because it allows for reasonable solubility of $ZnO_2^=$ without drastically affecting the viscosity of the solution. It was also felt that the glassware, especially the capillary of the Kemula drop apparatus would last longer at the lowest possible concentration.

Work at the rotating disc electrode was done in 1M KOH with the $ZnO_2^=$ concentration at 10^{-3} M. Work at higher concentrations was attempted but met with limited success due to the relatively large electrode area and the limited current available from the potentiostat. A smaller electrode is being prepared.

The system was studied by chronocoulometry[1] and potential scan amperometry using the apparatus previously described[2] for chronocoulometry, and a slightly modified form of the same apparatus for potential scan.

The Zn electrodes were machined from Zn bars and fitted with Teflon jackets to shield the portions which were not to be exposed to the solution. Just before an experiment, the electrode faces were polished flat to a shiny finish.

Results

The study of the adsorption of n-butyl alcohol gave results in complete agreement qualitatively with theory. No extensive quantitative experiment was attempted. Some results of these experiments are in the figures following.

The Zn, $ZnO_2^=$ system was first studied on a mercury electrode. Potential scan amperometry showed the system to probably be quasi-reversible, so it was decided to get some quantitative results. The literature[3] indicates that on Zn in strongly basic media the reaction was quasi-reversible and the rate was governed by a one electron step. Chronocoulometry indicated that the heterogeneous rate constant was on the order of 10^{-3} cm/sec and the charge transfer coefficient, α, was about .31.

It was then decided to study the reaction on a Zn metal electrode. Studies at a rotating disc electrode indicate that the reduction of $ZnO_2^=$ at a zinc electrode is diffusion controlled as indicated by a linear plot of $1/i$ *vs.* $1/w^{1/2}$ at a constant potential. In this case i represents the current and w the rotation rate in radians per second. From the slope and intercept of this plot, kinetic parameters may be obtained.[4]

Work was also done on the oxidation of zinc from the rotating disc electrode. This work was done in 1M and 5M KOH and, as before, owing to the large electrode area and the limits of the potentiostat, limiting currents were not obtained. Currents on the rising portion of the wave were found to obey the same equation as the $ZnO_2^=$ reduction giving a linear 1/i vs. $1/w^{1/2}$ plot.

For stationary electrodes it was found that with initial concentrations of zincate up to 0.01 M the zinc electrode was corroded by the solution with rapid evolution of hydrogen gas. Some Emulphogene BC-720 was added to the solution and the rate of corrosion became almost negligeable. As the Emulphogenes are not very soluble in electrolytes, it was decided to try adding propylene oxide to the solution instead. A solution containing approximately 1% propylene oxide exhibited similar behavior. Potential scan amperometry indicated that the system was quasi-reversible and that it was eventually diffusion controlled as the cathodic and anodic peak currents increased with scan rate, and that potential difference between the two peaks increased with scan rate. One would not normally expect the oxidation of a metal surface to be diffusion limited. But, in this case the reaction could be limited by diffusion of hydroxide to the electrode surface even at the extremely high concentration used.

The kinetics of the zincate reduction on zinc were studied by chronocoulometry and the results were very similar to the reduction on mercury. The heterogeneous rate constant is slightly larger and the charge transfer coefficient is approximately .42.

Conclusions

After studying the earlier work of Dr. T. P. Dirkse[5] we find that our experimental work agrees with his, but we feel that his interpretation of the results may be open to question. On the basis of the lack of corrosion of the zinc electrode in Emulphogene and propylene oxide solutions the hydrogen overvoltage must be significantly affected by these additives. Also, Dr. Dirkse's report makes no mention of the possible effect on his experimental results of the fact that the zinc system is complicated by kinetics.

We feel that work needs to be done of the effect of surfactants on the kinetics of both the zinc, zincate systems and the hydrogen system. It is also not clear from these experiments what is causing the limiting of the anodic currents. It might be diffusion of hydroxide to the surface of diffusion of zincate away from the surface. Work is continuing in an attempt to determine which is the case.

Literature Cited

1. C. H. Christie, G. Lauer, and R. A. Osteryoung, J. Electroanal. Chem., 7, 60 (1964).

2. D. A. Payne and A. J. Bard, First Quarterly Technical Progress Report (1967).

3. Parr and Hamson, Trans. Faraday Soc., 62, 3493 (1966).

4. D. Jahn and W. Vielstich, J. Electrochem. Soc., 109, 849 (1962).

5. T. P. Dirkse, Technical Report AFAPL-TR-66-5, 29 (1966).

TABLE 1

Kinetic parameters for the Zn, $ZnO_2^=$ system from chronocoulometric data[1]

1a
mercury electrode

potential stepped to (E-E°)	extrapolated intercept $t^{1/2}$ (sec)$^{1/2}$	
-.138	.164	5.42
-.158	.100	8.87
-.178	.080	11.06
-.198	.075	11.82
-.218	.050	17.73

slope of Log λ vs. (E-E°) = α/.0591 = 5.26 α = .31

Avg. slope of Q vs. $t^{1/2}$ plots = 88.7 microcoulombs/sec$^{1/2}$ = $2nFAD_o^{1/2}C_o/\pi^{1/2}$

$D_o^{1/2} = 1.85 \times 10^{-3}$

intercept of Log λ plot = log $k_o/D_o^{1/2}$ = .086 $K_o = 2.26 \times 10^{-3}$ cm/sec

1b
zinc electrode

-.094	.072	12.3
-.114	.053	16.7
-.134	.032	27.7
-.154	.027	32.9
-.174	.025	40.3

slope of Log λ vs. (E-E°) = 7.13 α = .42

intercept of plot = .413 $k_o = 4.79 \times 10^{-3}$ cm/sec

List of Figures

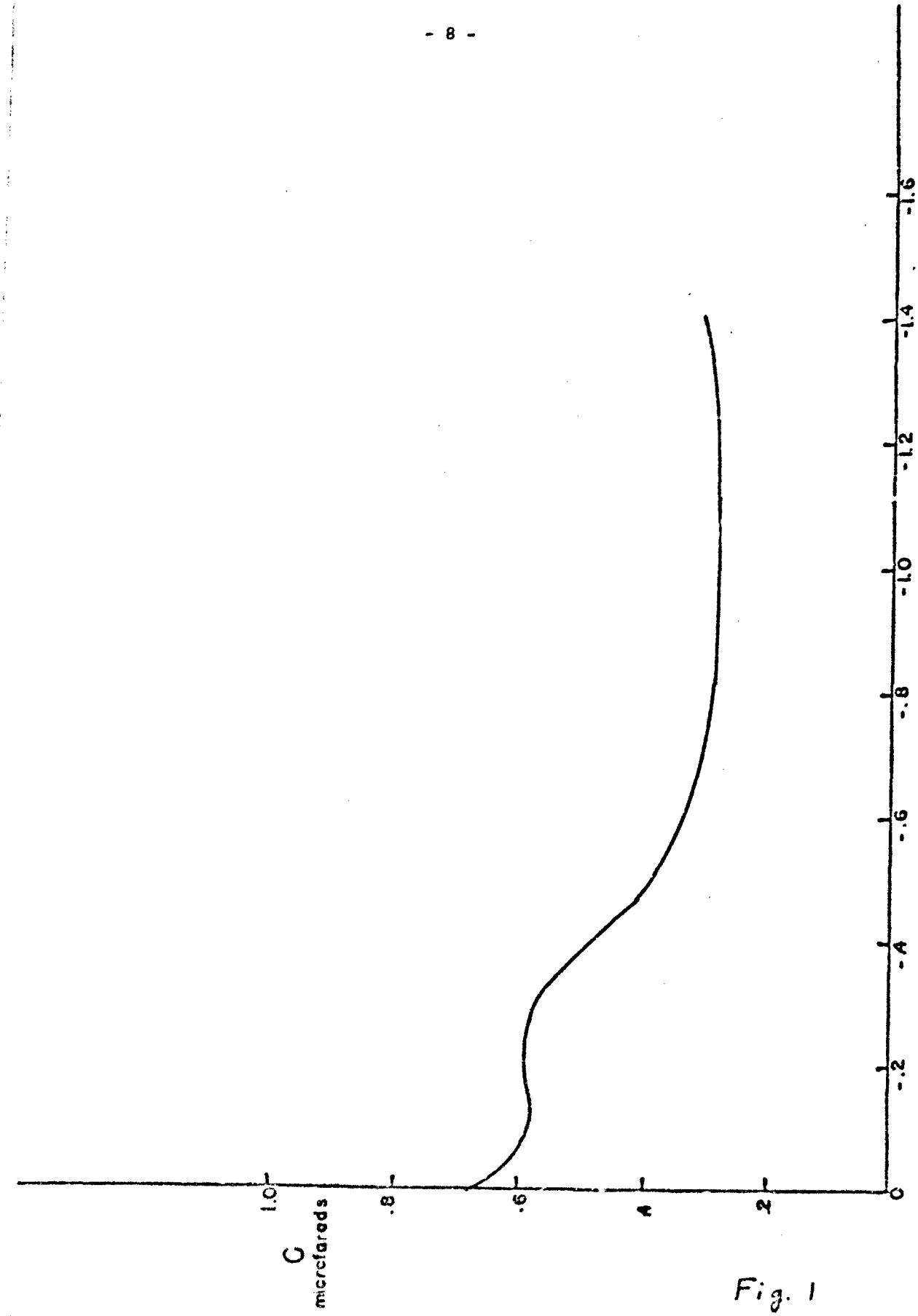

Fig. 1

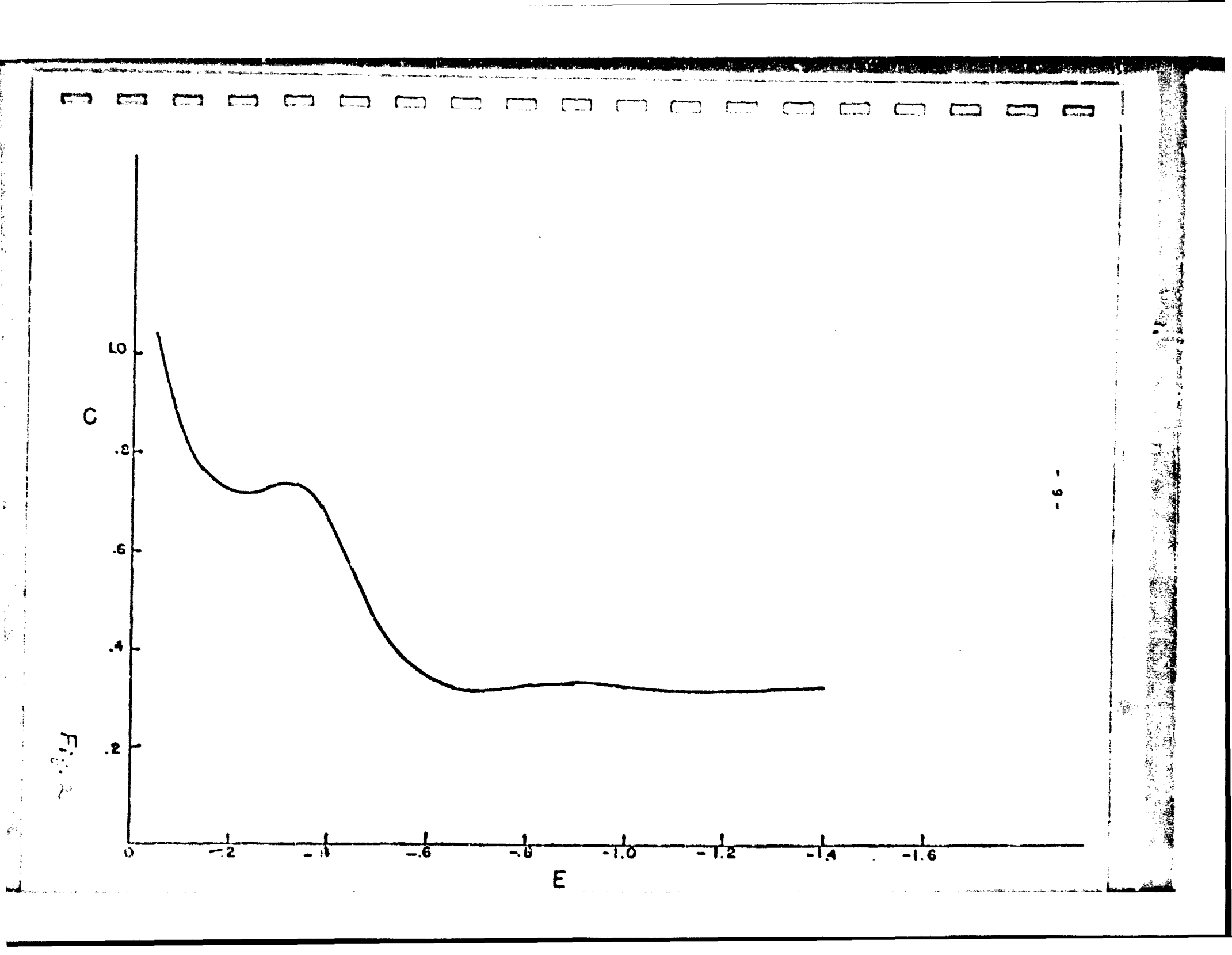

Fig. 2

Fig. 3

Fig. 4

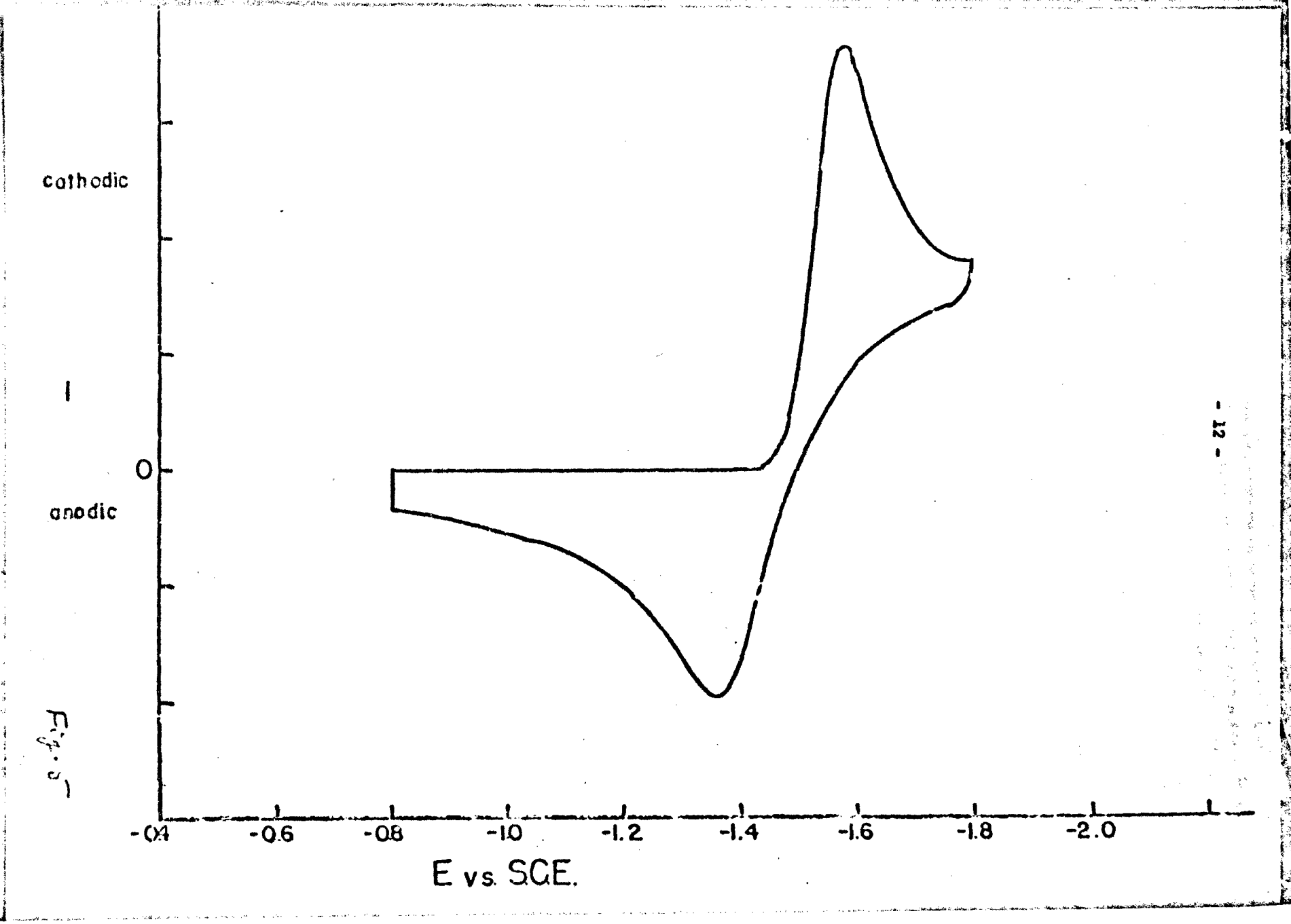

Fig. 3

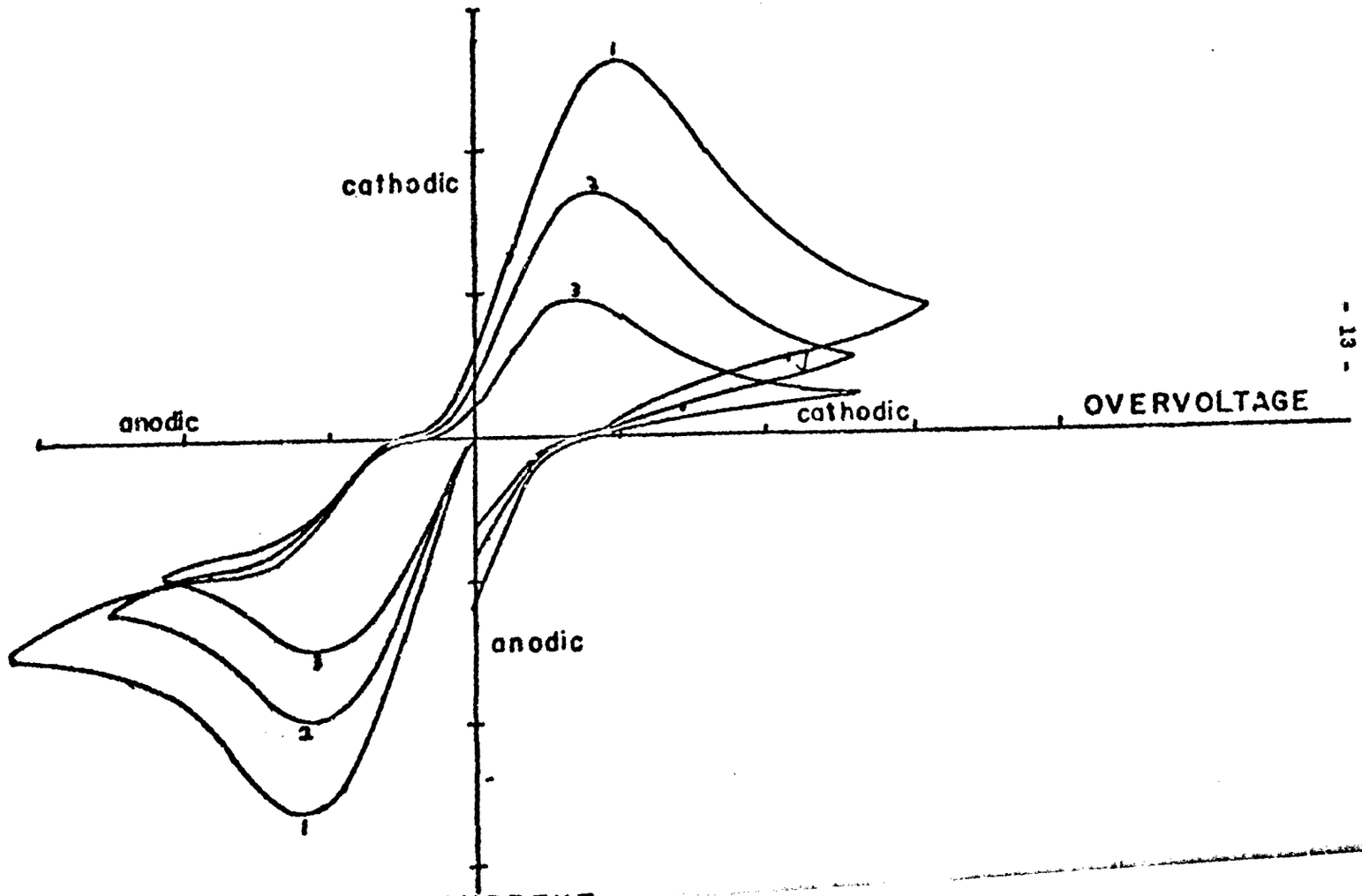
cathodic
anodic
cathodic
OVERVOLTAGE
anodic
CURRENT
1
2
3
1
2
3

Fig. 6

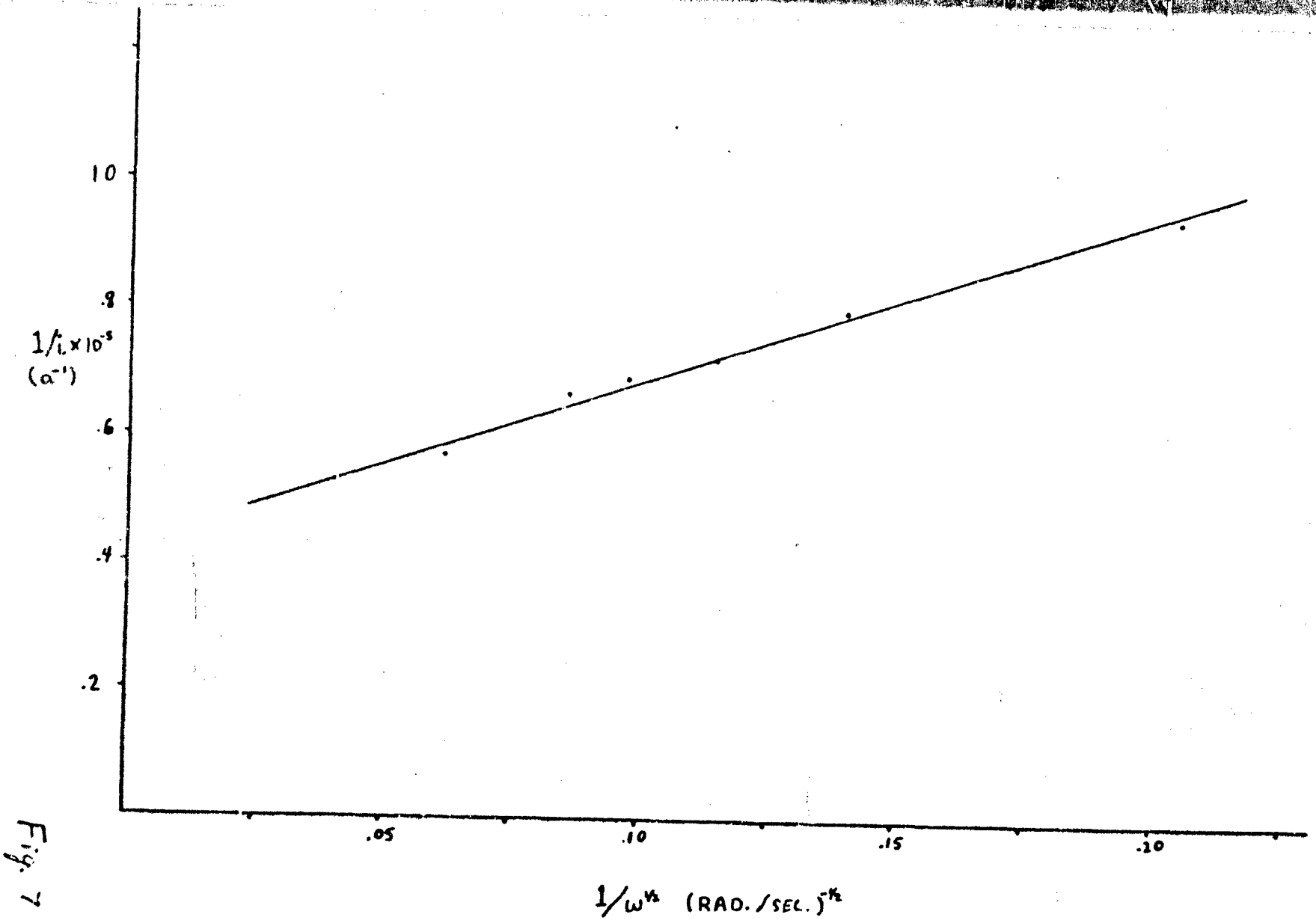

Fig. 7

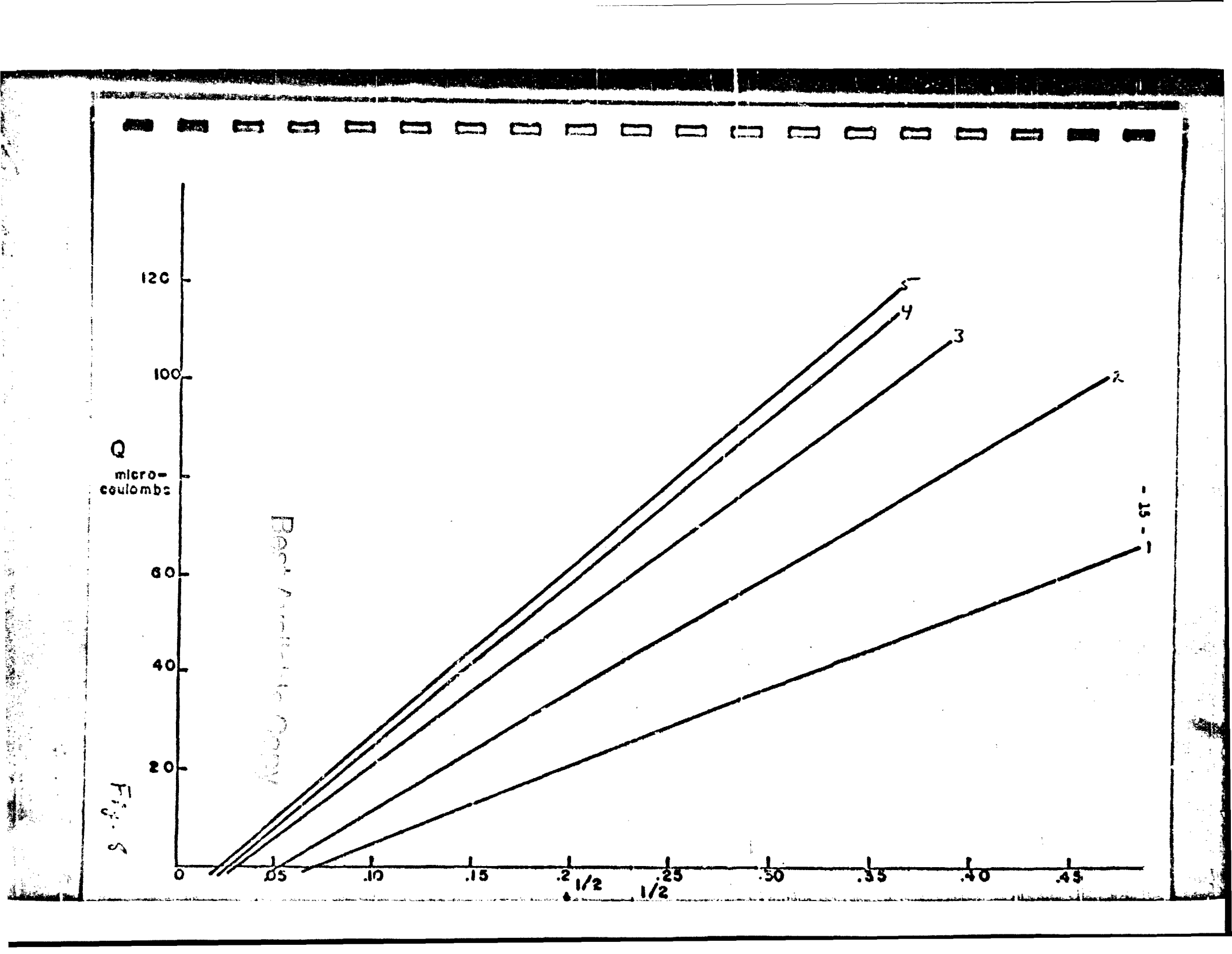
120
100
Q
micro-
coulombs
60
40
20
0
.05
.10
.15
.2
1/2
.25
1/2
.30
.35
.40
.45
5
4
3
2
1
- 25 -

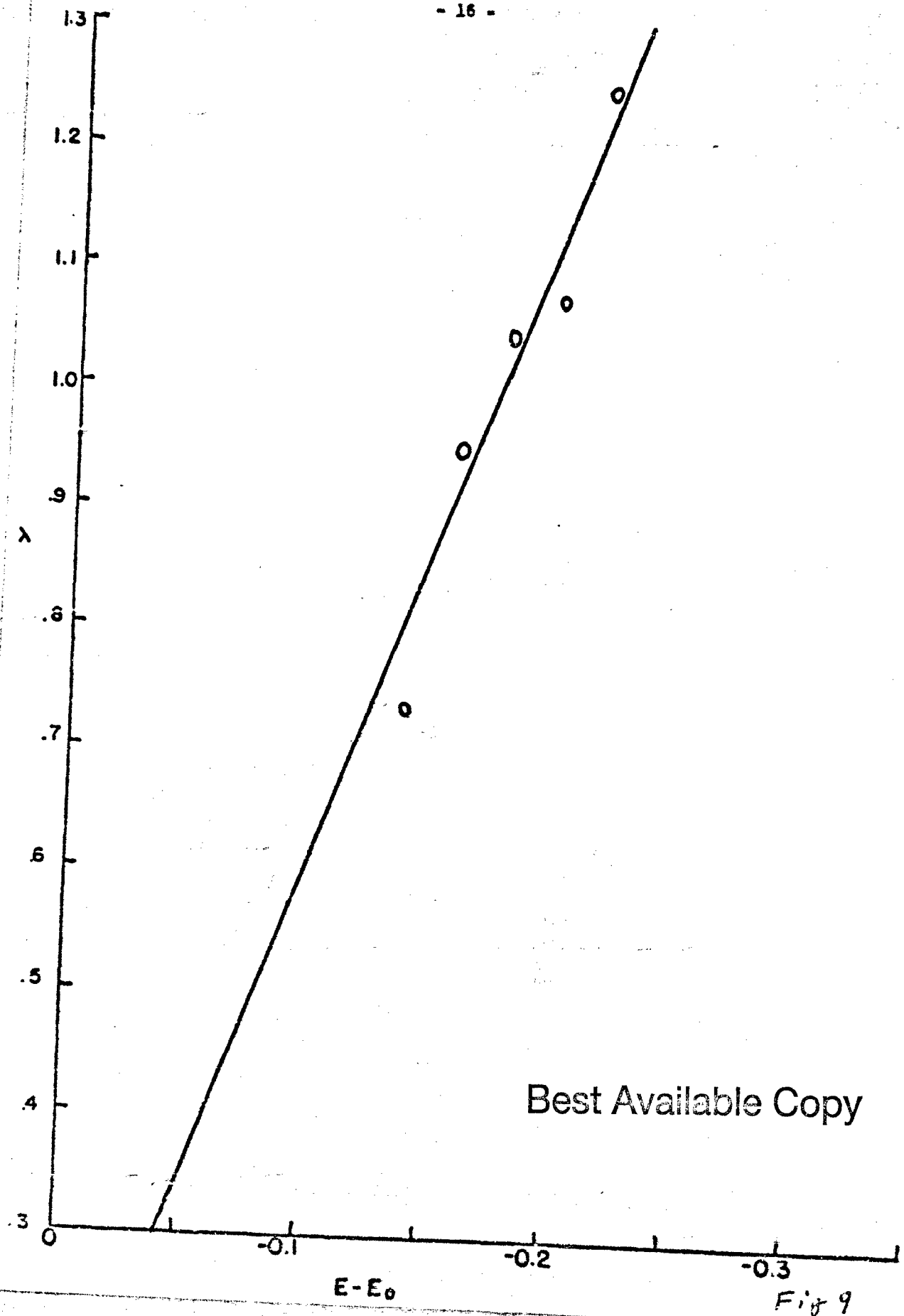

Fig 9

APPENDIX IV

INFLUENCE OF TRANSPORT CHARACTERISTICS OF SEPARATORS ON CELL ELECTROLYTE DISTRIBUTION

THIRD QUARTERLY REPORT

INFLUENCE OF TRANSPORT CHARACTERISTICS OF SEPARATORS ON CELL ELECTROLYTE DISTRIBUTION

March - May 1967

by

A. H. Remanick, Wm. I. Nelson, and M. Shaw

prepared for

Delco-Remy
Division of General Motors
Anderson, Indiana

June 16, 1967

Whittaker CORPORATION
NARMCO RESEARCH & DEVELOPMENT DIVISION
3540 Aero Court · San Diego, California 92123

ABSTRACT

Equations are presented permitting calculation of electrolyte distribution as a result of membrane absorption, from known weights of membrane and solution. KOH and water transference data, as a function of concentration, are presented for two typical battery membrane separators.

SUMMARY

Absorption data are presented to show the relationship between internal (within the membrane) and external molality of potassium hydroxide. Equations have been derived which permit the calculation of the equilibrium values of the weights of water and potassium hydroxide in the membrane and in the residual solution, as well as the internal and external molalities. These are calculated from the known weights of membrane, original solution, and original molality.

It has been calculated that for low membrane to solution weight ratios, the most pronounced effect is an increase in the hydroxide concentration within the membrane with respect to the concentration in the original solution. For higher membrane to solution weight ratios, a decrease in the hydroxide concentration in the residual solution is the most pronounced effect.

The effect of temperature on absorption does not appear to follow any definite pattern except for the fact that there exists temperature dependency in the absorption of both potassium hydroxide and water in Visking V-7 and PUDO-600 cellophane. Furthermore, concentration effects appear to be temperature dependent.

Transference numbers for both ionic species and solvent have been determined at 30° C. The values of t_+ indicate a slightly higher mobility of K^+ (relative to OH^-) in the membranes as opposed to free solution. The values of t_w show an expected concentration dependence.

I. INTRODUCTION

The poor performance of alkaline silver batteries at low temperature may possibly be attributed to concentration changes within the cell brought about by selective absorption of the membrane, as well as the transport characteristics of the latter, resulting in electrolyte freezing at higher temperatures than would be indicated on the basis of the initial concentration. It is the purpose of this program to measure such properties of typical membrane separators, correlate them with cell operation, and finally, to evolve practical mathematical expressions relating cell voltage as a function of time, temperature, current, electrolyte concentration, and membrane properties. Such relationships will be of value in the design of cells having improved low temperature performance.

II. RESULTS

A. Membrane Absorption of KOH

The measurement of KOH absorption by membranes has been completed. PUDO-600 cellophane, Visking V-7, and 2.2xH 20% acrylic acid graft polyethylene were investigated. Measurements for the latter material were extremely irreproducible, so that no cogent information could be derived. Although formal mathematical correlations for the absorption measurements have been presented earlier (Ref. 1), most of the experimental data was obtained during this period. Therefore, in order to maintain continuity, these are repeated here, together with the completed data.

The parameters of importance to membrane absorption are

1. Internal-external molality
2. Fraction absorption of KOH or water

1. Internal-external molality

Figure 1 shows a typical relationship between the concentration of KOH within the membrane (internal molality) and that in the residual solution (external molality), which can be expressed in the form:

$$\text{internal molality} = N\,(\text{external molality}) + P \qquad (1)$$

where N and P are functions of the membrane and the temperature, as shown in Table I.

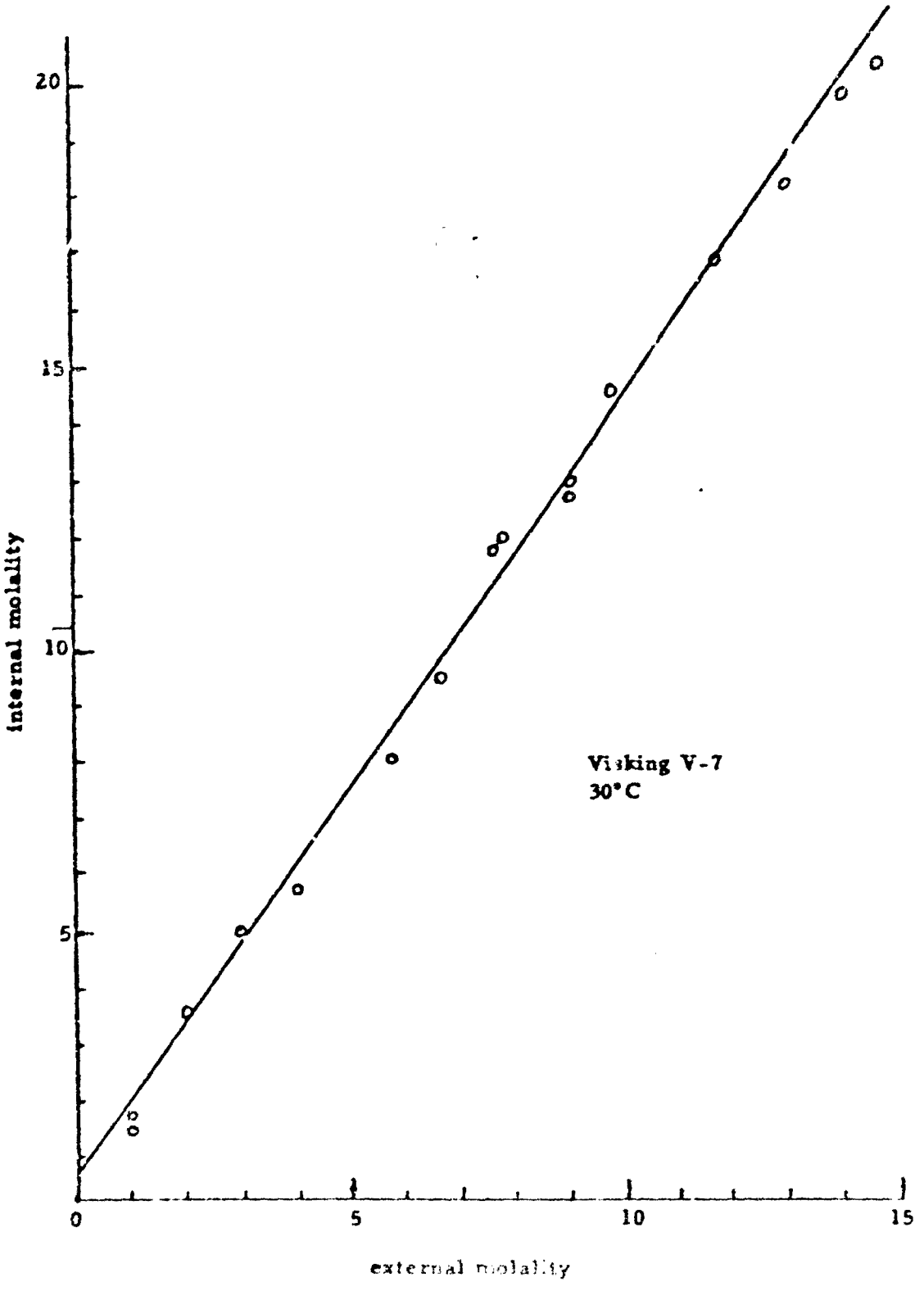

Figure 1 Relationship of membrane KOH concentration with residual solution concentration

TABLE I

Internal-External Molality Parameters

	0°C		30°C	
Membrane	N	P	N	P
Visking V-7	1.20	1.04	1.38	0.535
PUDO-600	1.13	1.49	1.12	2.22

Since the plotted data do not pass through the origin, values for P are not applicable at very low molality.

2. Fraction absorption of KOH or water

The fraction absorption of KOH by the membrane has been correlated with the external molality. This quantity is defined as

$$\text{Fraction absorption KOH} = \frac{w_i}{w_m} \qquad (2)$$

where w_i is the weight of KOH in the membrane at equilibrium, and w_m is the dry weight of the membrane.

The exact form of the mathematical relationship between the fraction absorption and the external molality is quite complex, if one considers the entire range of external molality. For mathematical simplicity, the total concentration range can be divided into a number of distinct regions. Within each region the data can be expressed according to the following relationship:

$$\text{Fraction absorption KOH} = J\,(\text{external molality}) + K \qquad (3)$$

with equilibrium conditions implied. J and K are constants for a given region.

A similar relationship exists for the fraction of water absorbed as a function of external molality, i. e. :

$$\text{Fraction absorption water} = L\,(\text{external molality}) + M \qquad (4)$$

It should be noted that no theoretical significance is attached to equations (3) and (4). Although empirical, they are, however, representative of the data on membrane absorption obtained under the experimental conditions.

Values of J, K, L, and M as a function of molality are given in Tables II and III.

3. Calculation of electrolyte distribution

The membrane absorption data permits the calculation of the KOH concentration within the membrane and the solution at equilibrium, as a function of weights of dry membrane and original solution, and the initial electrolyte concentration.

TABLE II ABSORPTION PARAMETERS - VISKING V-7

30° C — Fraction Absorption KOH

m	J	K
0.0 - 6.7	0.1330	-0.0114
6.7 - 8.3	-0.0552	1.28
8.3 - 15.0	0.0623	0.262

Fraction Absorption Water

m	L	M
0.0 - 1.0	0.908	0.823
1.0 - 2.1	-0.488	2.208
2.1 - 6.6	0.110	0.957
6.6 - 7.6	-0.456	4.700
7.6 - 10.0	-0.0668	1.746
10.0 - 15.0	-0.00092	1.064

0° C — Fraction Absorption KOH

m	J	K
0.0 - 6.4	0.183	-0.0744
6.4 - 8.1	-0.133	1.89
8.1 - 14.8	0.0787	0.179

Fraction Absorption Water

m	L	M
0.0 - 3.0	0.188	1.01
3.0 - 5.7	0.3506	0.547
5.7 - 7.8	-0.628	6.23
7.8 - 10.7	-0.0876	2.05
10.7 - 14.8	0.0654	0.406

TABLE III - ABSORPTION PARAMETERS - PUDO-600

30°C — Fraction Absorption KOH

m	J	K
0.0 - 3.5	0.105	0.0283
3.5 - 6.6	0.168	-0.170
6.6 - 8.7	-0.0546	1.29
8.7 - 15.0	0.0510	0.365

Fraction Absorption Water

m	L	M
0.0 - 1.0	0.267	0.872
1.0 - 2.1	-0.185	1.32
2.1 - 6.1	0.257	0.412
6.1 - 7.6	-0.450	4.70
7.6 - 10.0	-0.0888	1.96
10.0 - 13.0	-0.0122	1.18
13.0 - 15.0	0.0737	0.0653

0°C — Fraction Absorption KOH

m	J	K
1.0 - 6.2	0.2186	-0.141
6.2 - 8.4	-0.184	2.37
8.4 - 15.0	0.0874	0.0822

Fraction Absorption Water

m	L	M
1.0 - 2.1	-0.165	1.49
2.1 - 6.1	0.459	0.177
6.1 - 8.0	-0.849	8.08
8.0 - 10.2	-0.0645	1.85
10.2 - 11.9	0.0030	1.15
11.9 - 15.0	0.100	-0.0057

The following parameters are defined:

m_s	-	molality of original solution
w_s	-	weight of original solution
w_o	-	original weight of KOH (see Note 1)
W_o	-	original weight of water (see Note 1)
w_m	-	dry weight of membrane
w_e	-	weight of KOH in solution at equilibrium (see Note 2)
W_e	-	weight of water in solution at equilibrium
w_i	-	weight of KOH in membrane at equilibrium (see Note 2)
W_i	-	weight of water in membrane at equilibrium

Furthermore, it has been experimentally shown that at equilibrium

$$\text{fraction absorption KOH} = J\,(\text{ext. mol.}) + K \qquad (3)$$

$$\text{fraction absorption water} = L\,(\text{ext. mol.}) + M \qquad (4)$$

$$\text{internal molality} = N\,(\text{ext. mol.}) + P \qquad (1)$$

Note 1. w_o and W_o are determined from original solution parameters by the following relationships

$$w_o = \frac{m_s w_s}{17.8 + m_s} \qquad \text{and} \qquad W_o = \frac{17.8 w_s}{17.8 + m_s}$$

derived by linear combination of $w_o + W_o = w_s$, and $m_s = \frac{1000\, w_o}{56.1\, W_o}$

(mol. wt. of KOH is 56.1)

Note 2. The subscripts e and i correspond to "external" and "internal" relative to the membrane.

Although the values of J, K, L, and M are dependent on the particular value of the equilibrium external molality, only the final numerical solution will be dependent on the proper choice of J, K, L, and M. A mathematical solution for w_e, W_e, w_i, and W_i is dependent only on the form of equations (3) and (4) as will be seen.

Equations are presented on the next page which relate the weight of potassium hydroxide and water in both the membrane and residual solution under equilibrium conditions.

Equation (10) expresses W_e in terms of known quantities. From the value of W_e, w_e can be found by equation (9). Similarly, having w_e and W_e, w_i and W_i may then be determined from equations (7) and (8). However, since substitution of W_e in equation (9) would lead to a rather involved expression for w_e, it was decided that numerical solution for W_e should be made before substitution in equation (9). Since the expression for W_e is itself rather cumbersome, a computer was used for the mathematical solution. Certain restrictions on the final value of W_e aided in the choice of the proper values of J, K, L, and M. A value of W_e which is imaginary, negative, or greater than W_o is a physical impossibility. Therefore, an alternate choice of J, K, L, and M was necessary to establish a value of W_e within the limits $W_o > W_e > 0$.

Since it was anticipated that alternate choices of J, K, L, and M might be necessary, the computer program was written so as to allow facile substitution of such values. Having decided on the proper value of W_e, it was then possible to solve for w_e, W_i, w_i, equilibrium internal molality and equilibrium external molality. As a final check, the internal molality was determined from the external molality and equation (1). Since N and P in equation (1) are the most exact parameters, the value of W_e was adjusted until the value of the internal molality derived from w_i and W_i

The boundary conditions are

$$w_e + w_i = w_o \qquad (5)$$

$$W_e + W_i = W_o \qquad (6)$$

$$\frac{w_i}{w_m} = J\left(17.8\,\frac{w_e}{W_e}\right) + K \qquad (7)$$

$$\frac{W_i}{w_m} = L\left(17.8\,\frac{w_e}{W_e}\right) + M \qquad (8)$$

From these equations, the weight of KOH in solution at equilibrium is

$$w_e = \frac{w_o W_e - w_m W_e K}{W_e + 17.8\, w_m J} \qquad (9)$$

Further algebraic manipulation yields the weight of water in solution at equilibrium

$$W_e = \frac{1}{2}\left\{-17.8w_mJ - w_mM + W_o \pm \left[(17.8w_mJ + w_mM - W_o)^2 - 71.2w_m(w_oL - w_mKL + w_mJM - W_oJ)\right]^{\frac{1}{2}}\right\} \qquad (10)$$

agreed within 0. 1 m with that found using the computer value of equilibrium molality. This adjustment procedure was also written into the computer program. * The successful solution to equations (5), (6), (7), and (8) means that for a given membrane, it is possible to describe the distribution and concentration of electrolyte within any portion of the cell under equilibrium conditions.

Although direct comparisons of the values of J, K, L, and M for the membranes at two temperatures could be made, more meaningful information may be derived by comparison of the final electrolyte distribution under a given set of conditions. In Tables IV, V, VI, and VII, some of these calculations are presented. The initial conditions, weight of membrane, weight of solution, and solution concentration have been chosen for illustrative purposes and are not meant to indicate any limitation of the mathematical relationships.

Certain relationships are evident from inspection of the electrolyte distribution tables. It is apparent that for both membranes at each temperature, there is a marked reduction in the amount of residual electrolyte as the ratio of membrane to initial electrolyte becomes greater. Although the amount of residual electrolyte is dependent on the type of membrane and initial conditions, it appears that there is a maximum amount of membrane which should be used without deleterious effect on a battery system. Furthermore, it is seen that if the original weight ratio of membrane to solution is 1:10, the KOH concentration at equilibrium is significantly higher in the membrane than in the original solution, whereas

*The authors wish to thank Mr. Robert Elkin for writing the computer program. The computations were carried out on an Olivetti-Underwood Programma 101 digital computer.

TABLE IV ELECTROLYTE DISTRIBUTION - VISKING V-7, 30°C

w_m / g	w_s / g	m_s / m	w_e / g	W_e / g	Extern. Molal. / m	w_i / g	W_i / g	Intern. Molal. / m
10	100	9.0	25.7	54.6	8.3	7.8	11.9	11.8
20	100	9.0	16.4	38.5	7.6	17.2	28.0	10.9
30	100	9.0	6.31	16.8	6.7	27.7	49.6	9.8
35	100	9.0	3.59	9.78	6.5	30.0	56.6	9.4
40	100	9.0	0.60	1.87	6.3	32.9	64.6	9.1
10	100	14.0	33.3	45.7	13.0	10.7	10.4	18.5
20	100	14.0	23.7	34.9	12.1	20.3	21.1	17.2
30	100	14.0	15.2	24.0	11.3	28.9	32.0	16.0
40	100	14.0	7.33	12.4	10.5	36.7	43.6	15.0
47	100	14.0	2.49	4.43	10.0	41.5	51.5	14.3
50	100	14.0	0.48	0.88	9.80	43.5	55.1	14.1

w_m - dry weight of membrane

w_s - weight of original solution

m_s - original concentration

w_e - weight of KOH in solution at equilibrium

W_e - weight of water in solution at equilibrium

w_i - weight of KOH in membrane at equilibrium

W_i - weight of water in membrane at equilibrium

TABLE V ELECTROLYTE DISTRIBUTION - VISKING V-7, 0°C

w_m	w_s	m_s	w_e	W_e	Extern. Molal,	w_i	W_i	Intern. Molal,
g	g	m	g	g	m	g	g	m
10	100	9.0	25.1	53.0	8.5	8.4	13.5	11.2
20	100	9.0	17.5	39.4	7.9	16.1	27.1	10.6
30	100	9.0	5.0	12.5	7.1	28.6	53.9	9.4
33	100	9.0	0.44	1.2	6.7	33.1	65.2	9.0
10	100	14.0	31.9	43.1	13.2	12.2	12.9	16.8
20	100	14.0	20.9	30.0	12.4	23.1	26.0	15.8
30	100	14.0	11.2	17.1	11.6	32.9	38.9	15.0
35	100	14.0	6.7	10.5	12.0	37.4	45.5	14.6
40	100	14.0	2.4	4.0	10.9	41.6	52.0	14.2
42	100	14.0	0.7	1.2	10.8	43.3	54.8	14.1

w_m - dry weight of membrane

w_s - weight of original solution

m_s - original concentration

w_e - weight of KOH in solution at equilibrium

W_e - weight of water in solution at equilibrium

w_i - weight of KOH in membrane at equilibrium

W_i - weight of water in membrane at equilibrium

TABLE VI ELECTROLYTE DISTRIBUTION - PUDO-600, 30°C

w_m g	w_s g	m_s m	w_e g	W_e g	Extern. Molal. m	w_i g	W_i g	Intern. Molal. m
10	100	9.0	25.3	53.7	8.4	8.3	12.8	11.6
20	100	9.0	16.1	37.7	7.6	17.4	28.8	10.8
30	100	9.0	5.9	15.6	6.7	27.7	50.8	9.7
35	100	9.0	2.1	5.9	6.4	31.5	60.5	9.3
37.5	100	9.0	0.83	2.4	6.2	32.8	64.1	9.1
10	100	14.0	33.6	45.2	13.3	10.4	10.8	17.1
20	100	14.0	23.9	33.9	12.6	20.1	22.1	16.2
30	100	14.0	15.0	22.5	11.8	29.1	33.5	15.5
40	100	14.0	2.9	4.9	10.7	41.1	51.1	14.3
45	100	14.0	2.9	4.9	10.7	41.1	51.1	14.3
47.5	100	14.0	1.1	1.8	10.6	42.9	54.2	14.1

w_m - dry weight of membrane

w_s - weight of original solution

m_s - original concentration

w_e - weight of KOH in solution at equilibrium

W_e - weight of water in solution at equilibrium

w_i - weight of KOH in membrane at equilibrium

W_i - weight of water in membrane at equilibrium

TABLE VII ELECTROLYTE DISTRIBUTION - PUDO-600, 0°C

w_m	w_s	m_s	w_e	W_e	Extern. Molal,	w_i	W_i	Intern. Molal,
g	g	m	g	g	m	g	g	m
10	100	9.0	25.3	53.2	8.5	8.2	13.2	11.1
20	100	9.0	18.0	40.2	8.0	15.6	26.2	10.6
30	100	9.0	10.9	25.2	7.7	22.7	41.2	9.8
40	100	9.0	5.6	14.0	7.1	28.0	52.4	9.5
45	100	9.0	2.7	6.9	6.9	30.9	59.5	9.2
50	100	9.0	0.45	1.2	6.6	33.1	65.2	9.0
10	100	14.0	31.6	42.5	13.2	12.4	13.5	16.4
20	100	14.0	20.5	29.2	12.5	23.5	26.8	15.6
30	100	14.0	10.6	15.9	11.8	33.5	40.1	14.9
40	100	14.0	1.5	2.4	11.2	42.5	53.6	14.1

w_m - dry weight of membrane

w_s - weight of original solution

m_s - original concentration

w_e - weight of KOH in solution at equilibrium

W_e - weight of water in solution at equilibrium

w_i - weight of KOH in membrane at equilibrium

W_i - weight of water in membrane at equilibrium

the concentration in the residual solution is only slightly lower. On the other hand, for a ratio of about 1:2, the concentration of the residual solution is markedly lower than the original solution, whereas the membrane concentration is approximately the same as the original concentration.

For Visking V-7 at 30° C and 0° C, and for PUDO-600 at 30° C, it is seen that the amount of residual electrolyte is greater for the higher initial concentration, 14.0 m, than for the lower initial concentration, 9.0 m. That is, the overall membrane absorption is less at the higher concentrations than at the lower concentrations. This relationship is more complex in the case of PUDO-600 at 0° C although it appears that the amount of residual electrolyte is greater at the lower initial concentration, as opposed to the other cases.

A comparison of Tables IV and V reveals the fact that for both initial concentrations, Visking V-7 appears to absorb more electrolyte at the lower temperature. Although the effect is relatively small, it is of sufficient magnitude so as to be applicable in the design of batteries for low temperature operation. This effect appears to be more complex in the case of PUDO-600. At the lower concentration (9.0 m) more absorption occurs at the lower temperature, whereas at the higher concentration (14.0 m), greater absorption occurs at the higher temperature.

There are undoubtedly other electrolyte distribution relationships which may be derived by the methods previously described. However, since the absorption measurements are only a part of the investigation of transport characteristics of membranes, further discussion of electrolyte distribution will be deferred.

The method used to determine the absorption parameters involves a small weight of membrane in a relatively much greater weight of KOH solution. This method was chosen because of experimental simplicity. Since these experiments formed the basis for calculating the data presented in Tables IV-VII (where the weights of membrane and solution were within an order of magnitude comparable to more typical battery ratios) it was decided to experimentally confirm the absorption correlation. Using a Viskin V-7 membrane to solution ratio of 0.3/1, and an initial concentration of 8.97 m, the equilibrium concentration of KOH in the solution was found to be 7.12 m, compared to the calculated equilibrium concentration of 6.82. It therefore appears that the mathematical correlation of absorption is reasonably accurate.

B. Transport Numbers

Another area of effort important to the definition of electrolyte-membrane relationship is the measurement of cation and anion transport numbers through membranes, together with the apparent transport number of solvent. One cannot strictly define the transport of solvent per faraday as a transport number, since the solvent is an uncharged material not directly entering into the current carrying process. It has become common practice, however, to designate the change in the number of moles of solvent associated with the anolyte or catholyte per faraday as the solvent transport number. We will follow this convention. Furthermore, since the direction of solvent movement is not defined by the stoichiometry of a reaction, we shall consider that a positive value of the solvent transport number corresponds to the direction of cation movement.

The method used to determine the transport numbers corresponded to that used by Kressman (Ref. 2). This method differs from the usual Hittorf method in that not only is the change of concentration after

electrolysis measured, but also the total weight of material remaining in the electrode compartment. In this manner, both the cation transport number, t_+, and the water transport number, t_w, could be determined. Since

$$t_+ + t_- = 1 \tag{11}$$

the anion transport number is also determinable. In the usual Hittorf cell, a compartment separating the anolyte and catholyte is used. Since the net transport in this compartment is zero, no concentration change should occur. Any measured change in this compartment may then be attributed to diffusion, due to the electrolytically created gradient. In addition, the Hittorf method usually involves direct measurement of t_+ and t_-. The accuracy of the method can then be verified by use of equation (11).

In the study of KOH transport through membranes, certain modifications of the Hittorf method were made by Kressman in order to facilitate the experimental procedure. The middle compartment was eliminated, and the anolyte compartment was made much larger than the catholyte compartment. The latter modification was made since it had been found that t_+ was dependent on the concentration in the receiving compartment. The effects of diffusion and concentration polarization were eliminated by determining a range of time and current density in which t_+ remained constant.

Similar precautions were used in our experiments. However, we unfortunately chose a range of conditions in which errors due to diffusion were sufficiently similar so as to give apparent consistency to our earlier experimental data. Therefore, the data which was presented in

previous reports is in error. The error was noted when several layers of membrane were used in the transference cell, as opposed to the single layer used in the initial experiments. Under these conditions, the effect of back-diffusion should be minimized, whereas no effect on the real value of the transport numbers should be seen. It was found that t_+ markedly increased under the new conditions. The corrected values of t_+ and t_w for PUDO-600 and Visking V-7 are presented in Table VIII. It was noted that the greatest change in t_+ occurred at those concentrations where the diffusion constant was greatest, lending some measure of veracity to the present experimental method.

Cation transport numbers in KOH solution have been previously determined (Ref. 3). The values of t_+ decrease from 0.26 at 1.0 m to 0.22 m at 3.0 m, remaining constant at 0.22 until 12.0 m and then increase to 0.26 at 17.0 m. It thus appears that the values of t_+ in the membranes are slightly higher than in free solution. That is, the apparent mobility of the potassium ion, relative to the hydroxide ion, is slightly greater in the membranes. Whether this increased mobility is due to change of ionic hydration, ion aggregation, or environmental effects (direct membrane-ion interaction) cannot be decided at this time. Similarly, the effect of concentration on t_+ within a given membrane appears to be too subtle to be related to any single factor.

TABLE VIII TRANSPORT NUMBERS, 30°C

PUDO-600

m	2.6	5.7	7.6	11.2	15.0
t_+	0.32	0.29	0.26	0.31	0.24
t_w	2.39	1.38	1.10	0.68	0.56

Visking V-7

m	2.6	5.71	7.6	11.2	15.0
t_+	0.28	0.29	0.3	0.26	0.24
t_w	2.34	1.38	1.21	0.74	0.51

III. FUTURE WORK

A. Derivation of differential equations relating change of electrolyte concentration with time.

B. Integration of these equations using the previously determined absorption, transport, and diffusion parameters.

C. Experimental verification of the integrated expressions under typical battery conditions.

IV. REFERENCES

1. Whittaker Corporation, Narmco R and D Division, Second Quarterly Report, Delco-Remy PO. DR108650 (Contract No. AF 33(615)3487)

2. T. R. E. Kressman, P. A. Stanbridge, and F. L. Tye, Trans. Far. Soc., 59 2129 (1963)

3. S. Lengyel, J. Giber, Gy. Beke, and A. Vertes, Acta Chim. Hung. 39 357 (1963)

APPENDIX V

DEVELOPMENT OF IMPROVED SEPARATOR MATERIALS FOR THE ALKALINE SILVER OXIDE-ZINC BATTERY

RAI RESEARCH Corporation

RAI 381

DEVELOPMENT OF IMPROVED SEPARATOR MATERIALS FOR THE ALKALINE SILVER OXIDE-ZINC BATTERY

RAI Sub-Contract D-R164719
Contract No. AF33-615-3487

with

Delco-Remy
Division of General Motors
Anderson, Indiana 46011

Prepared by

Vincent F. D'Agostino, Project Director

FIRST QUARTERLY REPORT

April-July, 1967

July 14, 1967

36-40 37th Street
Long Island City, N. Y. 11101
212 Empire 1-2170

ACKNOWLEDGMENT

We wish to express our appreciation to Dr. Warren Winsches for having made Dr. Donald Metz, Supervisor of Radiation Research Section of the Brookhaven National Laboratories, available for consultation during this research. Dr. Metz has been of significant help in guiding our thinking for setting up procedure and methods, particularly in the use of machine irradiation of polyethylene film. He has also been most helpful in the determination of procedures for the investigation of M_c values.

TABLE OF CONTENTS

LIST OF ILLUSTRATIONS

LIST OF TABLES

INTRODUCTION

During his first quarter, emphasis has been placed on the development of methods to insure the uniformity of the dose received by samples irradiated in our source, and to determine the effect of a non-aromatic solvent and a chain transfer agent on grafting. The proposed program requires a detailed study of grafting procedures during Phase III of this contract. This initial study was undertaken only to determine if gross effects on cycle life could be attributed to the use of chlorinated solvents. These solvents afford certain advantages in grafting over using benzene and a small percentage of carbontetrachloride in the grafting solution.

A detailed study was also undertaken on the crosslinking of three basic films to accurately determine the dose received by the samples irradiated with 1 MeV electrons. These crosslinked films were then extracted to determine the gel content. The irradiated films will also be evaluated to determine the number of crosslinks as a function of dose. A recent report by M. Dole, et al.,* indicates that the initial slope of the

$(S+S^{\frac{1}{2}})$ vs. $\frac{rg}{r}$ curve, where s is the fraction of soluble

component at dose r and rg is the dose at the incipient gel point, and is strongly dependent on the initial molecular weight distribution. Thus, from gel-dose measurements and a knowledge of the molecular weight distribution the number of crosslinks in the irradiated samples can be determined.

The implication of this finding is that different base polymers with differing molecular weight distributions could be more or less efficiently crosslinked. This area of investigation has not been completed during this first quarter. Work is continuing in this area.

Phase I of this program requires the investigation of three base films, two monomers, and three levels of crosslinking plus evaluation of control films (i.e., uncrosslinked films). This is outlined in Table I. To date, samples Nos. 1, 9 and 17 have been completed, Nos. 4, 12 and 20 are now being grafted and will subsequently be evaluated. The crosslinking dose received by

* H.Y. Kang, O. Saito, and M. Dole, Journal of American Chemical Society, 89:9, April 26, 1967 p. 1980

these samples is approximately 90 Mrads, rather than 70 Mrads as indicated in the table. This change was made because:

1. Investigations prior to the start of this program indicated improved cycle life with increased irradiation of the base polymer; and

2. The irradiation of a "package" of one mil film to 70 Mrads (i.e., a surface dose of 70 Mrads) affords film with a dose varying from 70 to 90 Mrads depending on the depth of the film in the package and the energy of the electron source. The selection of film having the desired extent of irradiation is simply made by choosing film at the desired depth in the "package". The maximum dose received by individual film in the package irradiated here was about 90 Mrads.

Table I Evaluation of Film Type, Crosslinking and Monomer Type on Cycle Life

	Film Type	Monomer Type	Crosslinking Dose (Mrads)	Remarks
1	USI-280 (222 BMI)	Acrylic	0	1. The base film is material currently used in 2.2XH
2	USI-280 (222 BMI)	"	30	
3	USI-280 (222 BMI)	"	50	
4	USI-280 (222 BMI)	"	70	
5	USI-280 (222 BMI)	Methacrylic	0	
6	USI-280 (222 BMI)	"	30	
7	USI-280 (222 BMI)	"	50	
8	USI-280 (222 BMI)	"	70	
9	Bakelite LFD-0602	Acrylic	0	1. The base film is material used in 2.2XH prior to 1965. This material was dropped by resin supplier in favor of 222 BMI
10	Bakelite DFD-0602	"	30	
11	Bakelite DFD-0602	"	50	
12	Bakelite DFD-0602	"	70	
13	Bakelite DFD-0602	Methacrylic	0	
14	Bakelite DFD-0602	"	30	
15	Bakelite DFD-0602	"	50	
16	Bakelite DFD-0602	"	70	
17	Phillips 1712	Acrylic	0	
18	Phillips 1712	"	30	
19	Phillips 1712	"	50	
20	Phillips 1712	"	70	
21	Phillips 1712	Methacrylic	0	
22	Phillips 1712	"	30	
23	Phillips 1712	"	70	
24	Phillips 1712	"	100	

EXPERIMENTAL

The experimental program followed during the first quarter can be divided into a number of areas:

1. Development of procedures to assure uniform radiation of test samples.
2. Evaluation on new grafting solutions.
3. Radiation crosslinking of films to be evaluated during Phase I.
4. Grafting of crosslinked films.
5. Evaluation of grafted films.

Development of Procedures to Assure Uniform Radiation of Test Samples

To assure absolute control of radiation grafting special motor mounts have been designed and constructed which can be placed into positions around the radiation source. The motor placed in these mounts carries an aluminum tube into which the test tube, containing the sample to be irradiated, is placed. Using this technique insures that:

1. The distance from the center of the source to the center of the tube is constant for all samples.
2. The test tube is parallel to the source.
3. A horizontal line passing through the center of the source also passes through the center of the samples.
4. By rotating both the sample and the source, maximum uniformity of the radiation dose will be received by the sample.

Evaluation of New Grafting Solutions

Table II lists a series of grafting experiments in which various grafting solutions were used. The first series of grafts, i.e., Nos. 211-6-1 through 211-6-7 compared grafts made with solutions A, B and C. The rationale behind these grafting solutions was to compare the substitution of methylene chloride for the aromatic component of the grafting solutions and also to determine the effect of the chain transfer agent, carbontetrachloride. The second series, Nos. 211-8-1 through 211-8-4, was set to note the effect of total dose on the graft level and thereby the variation of resistance with graft level. The last series, Nos. 211-18-1 through 211-18-6, was undertaken

to determine the effect of varying the chain transfer agent through a wide range (from 0 to 30%).

Tests are continuing to determine the cycle life of all these samples. No firm conclusions can be drawn from the results to date. There is a strong indication, however, that the resistance of grafted films is asymptotic with the graft level. Sample No. 211-8-1 with a graft of only 23% has a resistance value of 11/10/15 millichms (i.e., for left-center-right) while other samples grafted to much higher levels showed no significant improvement with increase in the graft level.

Crosslinking Studies

Three base polymers, designated U-280, P-1712, and B-0602 were crosslinked during this period. These films were irradiated to:

1. Establish a procedure which would permit ready determination of the dose received by the irradiated film.

2. Establish a procedure for irradiation of large quantities of film.

3. Determine if significant differences in gel content and M_c values at equivalent irradiation are a function of the films under investigation.

4. Obtain sufficient quantities of film for this research program.

Crosslinking of Polyethylene Film

An approach has been undertaken so as to obtain known and controlled doses by beta radiation of polyethylene film. Stacked sheets of polyethylene film (135 sheets, 25 ft. in length, each having a one mil nominal thickness) were irradiated to 70 Mrads (i.e., the surface dose was 70 Mrads). Since the dose a material receives is non-uniform with depth due to the variation of the percent ionization occurring in the material with depth, cellophane dosimeters were used to determine dose-depth relationship in the stacked films. The results of the dosimetry can be seen in Figure 1, curve A. Curve A gives the actual dosimetry on the experimental run. Curve B, which is similar to curve A is an independent run performed by Radiation Dynamics, Inc. Curve C, shows the theoretical dose-depth relationship for 1 MeV electrons. It can be seen that neither experimental curve approaches the theoretical curve in overall dose or spread with depth, which is mainly due to practical limitations in the electron accelerator used. In this study the fact that the experimental curve does not match up to the theoretical curve is of minor importance, since the main aim of the run was to produce film which was irradiated

Table II Evaluation of Grafted Samples

Sample No.	Base Film	Dose Rate (r./hr.)	Dose (Mr.)	% Graft	Resistance L-C-R (Milliohms)	Hull Test (Mins.)	Cycle Life*	Crosslink Dose (Mr.)	Gel Content
211-6-1(A)	P-1712	14,000	1.02	78.6	12/8/13	25	13	0	0
211-6-2	P-1712	14,000	1.35	109.0	Not tested, poor Uniformity				
211-6-3(B)	P-1712	14,000	1.69	97.4	7/12/11	25	10	0	0
211-6-4(C)	P-1712	14,000	1.02	102.0	18/17/10	21	23	0	0
211-6-5(C)	P-1712	14,000	1.35	83.0	14/14/12	25	40	0	0
211-6-6(B)	P-1712	14,000	1.02	63.0	11/13/11	38	30	0	0
211-6-7(B)	P-1712	14,000	2.37	103.3	10/9/11	30	35	0	0
211-8-1(C)	P-1712	10,600	0.51	23.0	11/10/15	73	57	0	0
211-8-2(C)	P-1712	10,600	0.59	74.0	14/12/13	25	16	0	0
211-8-3(C)	P-1712	10,600	0.76	81.0	11/10/16	25	13	0	0
211-8-4(C)	P-1712	10,600	1.02	110.2	14/14/12	25	15	0	0
211-18-1(D-3.6)	P-1712	10,600	0.76	103.0	15/12/12	75	-	0	0
211-18-2(D-5)	P-1712	10,600	0.76	90.0	13/13/13	50	-	0	0
211-18-3(D-10)	P-1712	10,600	0.76	95.0	43/25/16	62	-	0	0
211-18-4(D-20)	P-1712	10,600	0.76	149.0	11/18/14	78	-	0	0
211-18-5(D-30)	P-1712	10,600	0.76	80.0	17/18/21	60	-	0	0
211-18-6(C)	P-1712	10,600	0.76	75.0	21/23/19	72	-	0	0
211-32-1(E)	U-280	10,400	1.00	-	-	-	-	90	88
211-32-2(E)	P-1712	10,400	1.00	-	-	-	-	90	80.8
211-32-3(E)	B-0602	10,400	1.00	-	-	-	-	90	90.3
VISKING-7 (CONTROL)		-	-	-	-	-	113	-	-

*40% depth of discharge on three plate cell (2 silver, one zinc) using one layer of separator.

LEGEND TO TABLE II

Solution Components	Grafting Solution (%)				
	A	B	C	D	E
Benzene	33.5	67.0	35.0	(5-35)	66.4
Methylene chloride	33.5	-	35.0	35	-
Acrylic acid	30.0	30.0	30.0	30	30
Carbontetrachloride	3.0	3.0	-	(30-0)	3.6

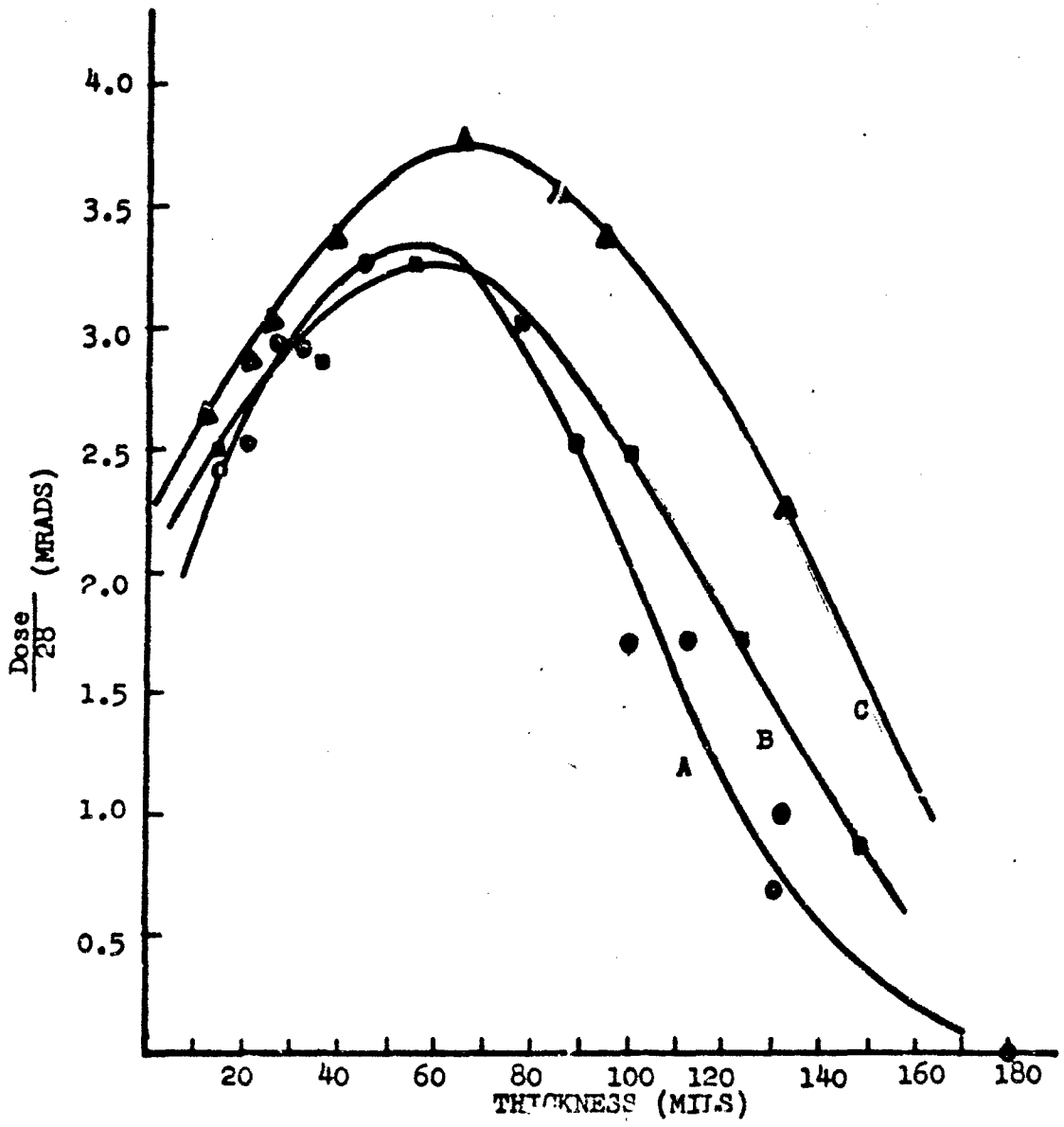

Figure 1 THEORETICAL AND ACTUAL DOSE-DEPTH CURVES FOR 1 MeV ELECTRONS ON POLYETHYLENE

to a known dose. Significantly, this experiment shows that it will be necessary during all future irradiations to use dosimeters as a quality control procedure to insure obtaining accurate readings of the irradiation dose.

For further verification of the effect of dose on crosslinking, a gel study was conducted on the irradiated films by determining the variation in gel content with depth or since this is a function of dose, with dose. The results for P-1712, B-0602 and U-280 film, plotted in Figure 2, shows that the minimum dose to achieve significant gelation is about 30 Mrads. This result indicates the minimum allowable dose on all future studies with these films should be 30 Mrads. The slope of the curve above the 30 Mrad dose indicates that the gel content does not significantly increase with increase in dose for this material. It is expected that this maximum gel content will vary from polymer to polymer depending on initial molecular weight distribution and perhaps antioxidant content. It is interesting to note that the gel content for the B-0602 film is higher than that of the P-1712 or U-280. The possible explanation for the lower gel content of the P-1712, when compared to the U-280, can be due to the higher antioxidant content of this film.

Grafting of Crosslinked Films

Samples Nos. 4, 12 and 20, as shown in Table I, are currently being grafted. The films used to graft these materials were all irradiated to approximately 90 Mrads. The results of the grafting will be reported in the next quarterly report.

Evaluation of Grafted Samples

The samples prepared during this quarter have not been completely evaluated. Only resistance, cycle life and zinc penetration, as determined by Hull Test, have been determined to date. This data was given in Table II.

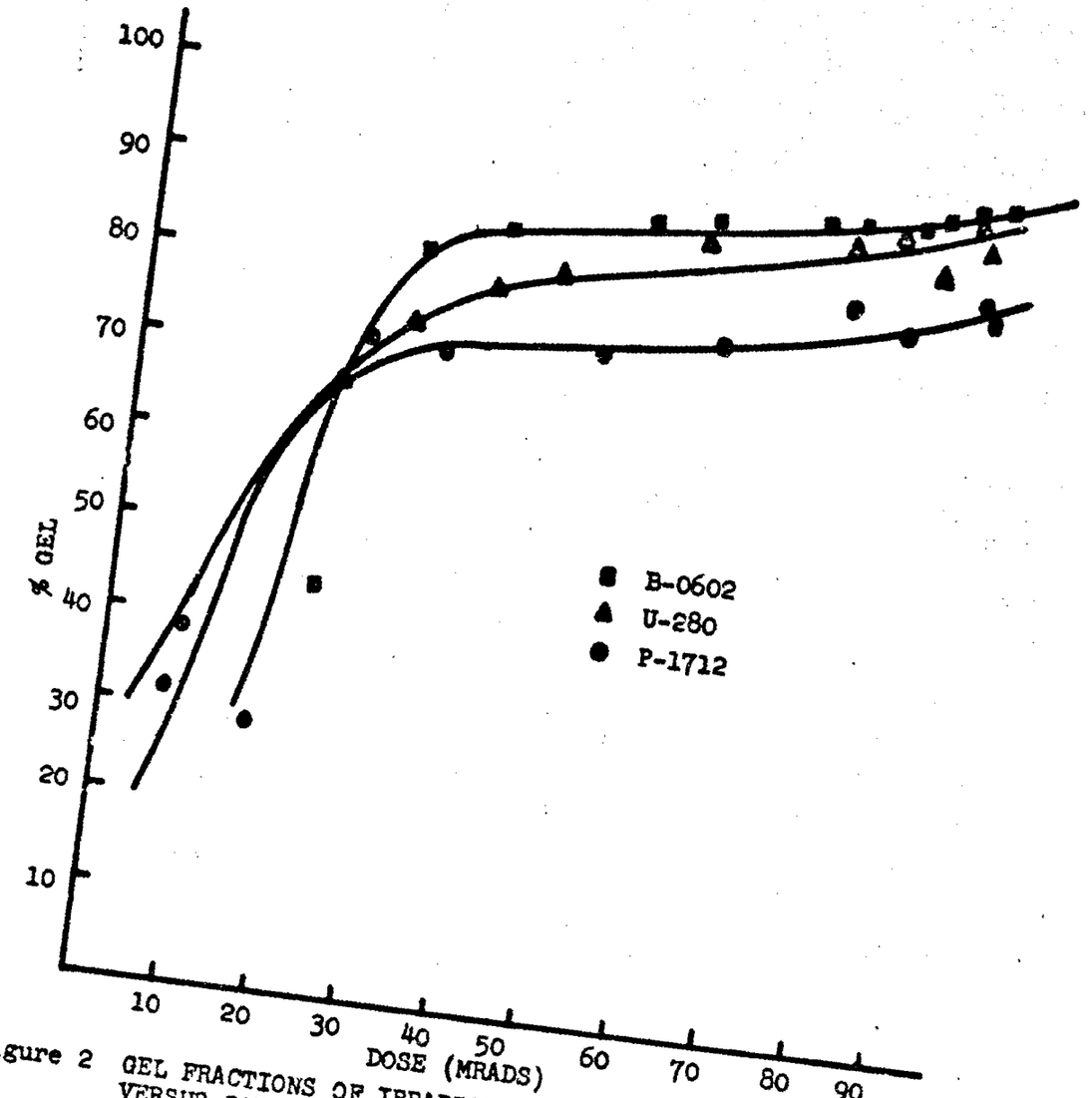

Figure 2 GEL FRACTIONS OF IRRADIATED POLYETHYLENE FILMS VERSUS RADIATION DOSE
(Samples extracted in xylene with 0.1% n-beta-phenylnaphthylamine at 105°C. for 48 hrs.)

RESULTS AND DISCUSSION

The results of the grafting experiments and crosslinking studies in general are in line with our basic concepts as proposed. Naturally, the data obtained to date is incomplete, therefore, we cannot form absolute conclusions. It is of interest to note, however, that the resistance values of the grafted films appear, within the limits tested, to be independent of the percent graft. Also, within the 211-8-1 through 211-8-4 series it appears that the Hull Test and cycle life values are some inverse functions of the percent graft. This particular observation must be used cautiously in developing a relationship because the percent graft is determined on the weight change of 25 feet of film while the resistance value is taken on a one-inch piece. If the graft is not uniform, then it is possible to select a small section with a higher than average graft. We are currently reviewing various methods for determining the percent graft over the entire film area so that we might plot a grart density. In addition, different grafting solvents are being evaluated to insure uniform grafting.

Cycle life on the grafted sample has all been done on three plate cells. These cells were constructed using two silver and one zinc plate. The plates were wrapped with one layer of membrane, and cycled at 40% depth using 350 ma charge for 85 minutes and 800 ma discharge for 30 minutes. All data during cycling is recorded.

The crosslinking of the control films indicates that the U-280 film has a higher gel content than the P-1712 base polymer. Based on the melt index this is not what would have been expected. The possible explanation for this result could be due to the apparent high concentration of antioxidant in the P-1712 film. The B-0602 film gave the high gel content as expected and should also yield the highest crosslink density. These three films have all been crosslinked from 30 to approximately 93 Mrads. The exact dose of individual films have been determined via use of the dose-depth curve. Table III shows the variation in dose with depth. It should be noted that from the 19th to the 37th layer, the dose variation is only 2.2/92.4 or less than 2.5%. Each of these represents 25 feet of film or a total of over 400 feet. This should be sufficient material to complete the requirements of Phase I of the contract.

Table III Crosslinked U-280 Film

Layer No.	Depth Thickness[a] (mil)	Depth of First Film[b] (mil)	Total Dose 28	Total Dose (Mrads)	Gel Content
1	1.13	23.89	2.64	73.4	72.1
10	11.30	34.06	3.00	84.0	88.9
19	21.47	44.23	3.22	90.2	90.1
28	31.64	54.40	3.35	93.8	90.7
37	41.81	64.57	3.30	92.4	88.1
46	51.98	74.74	3.10	86.8	84.2
55	62.15	84.91	2.74	76.7	87.3
67	75.71	48.47	2.20	61.6	86.2
79	89.27	112.03	1.66	46.5	81.2
85	96.05	118.81	1.35	37.8	77.9
91	102.83	125.59	1.08	30.2	74.0
97	109.61	132.37	0.84	23.5	66.0

[a]The average film thickness was found to be 1.13 mils.

[b]The electron prior to impinging on the film penetrates:
1. 2 mils of titanium
2. 6 inches of air and a 6 mil polyethylene bag.

This is equivalent to:

22.76 mils of unit density. depth of film = layer number x average thickness + 22.76.

FUTURE WORK

During the second quarter, the following work is scheduled:

1. Preparation of all membranes shown in Table I.
2. Evaluation of membranes Nos. 1-24.
3. Preparation of three membranes in 100 ft. quantities by August 15th. These will be submitted for testing to Delco-Remy.
4. Preparation of three additional membranes in 100 ft. quantities by October 15th. These will be submitted to Delco-Remy for testing.
5. Determination of M_c values of crosslinked films.
6. Selection of new base polymers to be evaluated during Phase II of this investigation.

UNCLASSIFIED
Security Classification

DOCUMENT CONTROL DATA - R&D

(Security classification of title, body of abstract and indexing annotation must be entered when the overall report is classified)

1. ORIGINATING ACTIVITY (Corporate author)
General Motors Corporation
Delco-Remy Division
Anderson, Indiana

2a. REPORT SECURITY CLASSIFICATION
Unclassified

2b. GROUP

3. REPORT TITLE
Silver-Zinc Electrodes and Separator Research

4. DESCRIPTIVE NOTES (Type of report and inclusive dates)
Technical Report, First Annual 31 August 1967

5. AUTHOR(S) (Last name, first name, initial)
J. J. Lander and J. A. Keralla

6. REPORT DATE	7a. TOTAL NO. OF PAGES	7b. NO. OF REFS
31 August 1967		

8a. CONTRACT OR GRANT NO.	9a. ORIGINATOR'S REPORT NUMBER(S)
AF33(615)-3487 b. PROJECT NO. 3145 c. Task No. 314522 d.	9b. OTHER REPORT NO(S) (Any other numbers that may be assigned this report) AFAPL-TR-67-107

10. AVAILABILITY/LIMITATION NOTICES
Foreign announcement and dissemination of this report by DDC is not authorized.

11. SUPPLEMENTARY NOTES	12. SPONSORING MILITARY ACTIVITY
	Aero Propulsion Laboratory, Wright-Patterson Air Force Base, Ohio

13. ABSTRACT

Additions of 1.2% to 2% lignosulfonic acid in the negative mix is helpful to negative plate cycle life. The use of cotton fibers helps to maintain the negative plate active material in place during cycle life. The surfactant BC-610 is the best choice for use in the zinc negative material found to date. However, at cold temperatures, surfactants appear to inhibit cycle life. The use of .1% Ethanol in the negative material helps cell cycle life as well as surfactant FC-95. Small percentages of acicular ZnO mixed with Kadox-15 appear to help negative plate cycle life. The use of 2% to 5% $ZnSO_4$ aids the negative plate cycle life at room temperature but is detrimental to cold (30-40°F.) operation. The best electrolyte to date at 60% depth-of-discharge is 50% KOH yielding 220 cycles.

DD FORM 1 JAN 64 1473

UNCLASSIFIED
Security Classification

14 KEY WORDS	LINK A		LINK B		LINK C	
	ROLE	WT	ROLE	WT	ROLE	WT

INSTRUCTIONS

1. ORIGINATING ACTIVITY: Enter the name and address of the contractor, subcontractor, grantee, Department of Defense activity or other organization *(corporate author)* issuing the report.

2a. REPORT SECURITY CLASSIFICATION: Enter the overall security classification of the report. Indicate whether "Restricted Data" is included. Marking is to be in accordance with appropriate security regulations.

2b. GROUP: Automatic downgrading is specified in DoD Directive 5200.10 and Armed Forces Industrial Manual. Enter the group number. Also, when applicable, show that optional markings have been used for Group 3 and Group 4 as authorized.

3. REPORT TITLE: Enter the complete report title in all capital letters. Titles in all cases should be unclassified. If a meaningful title cannot be selected without classification, show title classification in all capitals in parenthesis immediately following the title.

4. DESCRIPTIVE NOTES: If appropriate, enter the type of report, e.g., interim, progress, summary, annual, or final. Give the inclusive dates when a specific reporting period is covered.

5. AUTHOR(S): Enter the name(s) of author(s) as shown on or in the report. Enter last name, first name, middle initial. If military, show rank and branch of service. The name of the principal author is an absolute minimum requirement.

6. REPORT DATE: Enter the date of the report as day, month, year; or month, year. If more than one date appears on the report, use date of publication.

7a. TOTAL NUMBER OF PAGES: The total page count should follow normal pagination procedures, i.e., enter the number of pages containing information.

7b. NUMBER OF REFERENCES: Enter the total number of references cited in the report.

8a. CONTRACT OR GRANT NUMBER: If appropriate, enter the applicable number of the contract or grant under which the report was written.

8b, 8c, & 8d. PROJECT NUMBER: Enter the appropriate military department identification, such as project number, subproject number, system numbers, task number, etc.

9a. ORIGINATOR'S REPORT NUMBER(S): Enter the official report number by which the document will be identified and controlled by the originating activity. This number must be unique to this report.

9b. OTHER REPORT NUMBER(S): If the report has been assigned any other report numbers *(either by the originator or by the sponsor)*, also enter this number(s).

10. AVAILABILITY/LIMITATION NOTICES: Enter any limitations on further dissemination of the report, other than those imposed by security classification, using standard statements such as:

(1) "Qualified requesters may obtain copies of this report from DDC."

(2) "Foreign announcement and dissemination of this report by DDC is not authorized."

(3) "U. S. Government agencies may obtain copies of this report directly from DDC. Other qualified DDC users shall request through _____."

(4) "U. S. military agencies may obtain copies of this report directly from DDC. Other qualified users shall request through _____."

(5) "All distribution of this report is controlled. Qualified DDC users shall request through _____."

If the report has been furnished to the Office of Technical Services, Department of Commerce, for sale to the public, indicate this fact and enter the price, if known.

11. SUPPLEMENTARY NOTES: Use for additional explanatory notes.

12. SPONSORING MILITARY ACTIVITY: Enter the name of the departmental project office or laboratory sponsoring *(paying for)* the research and development. Include address.

13. ABSTRACT: Enter an abstract giving a brief and factual summary of the document indicative of the report, even though it may also appear elsewhere in the body of the technical report. If additional space is required, a continuation sheet shall be attached.

It is highly desirable that the abstract of classified reports be unclassified. Each paragraph of the abstract shall end with an indication of the military security classification of the information in the paragraph, represented as *(TS), (S), (C), or (U)*.

There is no limitation on the length of the abstract. However, the suggested length is from 150 to 225 words.

14. KEY WORDS: Key words are technically meaningful terms or short phrases that characterize a report and may be used as index entries for cataloging the report. Key words must be selected so that no security classification is required. Identifiers, such as equipment model designation, trade name, military project code name, geographic location, may be used as key words but will be followed by an indication of technical context. The assignment of links, rules, and weights is optional.

DD 1 JAN 64 1473 (BACK) (PAGE 2)